UNIVERSITY OF CAPE TOWN

EXOTIC $(Q\bar{Q})^N$–MESONS IN PERTURBATIVE CAVITY QCD USING A MODIFIED BOUNDARY CONDITION

By

Remus F[illegible]retea

A THESIS

[illegible]ed to the Faculty of Science
[illegible]he University of Cape Town
[illegible]tial fulfillment of the requirements for
the degree of Doctor of Philosophy

Department of Physics
August 1999

Abstract

Cavity QCD has been used for more than two decades to describe the properties of ordinary hadrons in terms of interacting quarks and gluons. In the framework of perturbative Cavity QCD, a variety of non-diverging and diverging, but renormalizable Feynman diagrams have been evaluated to order α_S and α_S^2.

The purpose of this thesis is to explore the properties of exotic mesons of the type $q^2\bar{q}^2$ and $q^3\bar{q}^3$ to order α_S. In the past, $q^2\bar{q}^2$ mass spectra have been calculated using the linear M.I.T. bag boundary condition for quarks of masses $m_q \geq 0$. The present work extends these calculations to include a new boundary condition which is equivalent to introducing negative quark masses $m_q < 0$. This new boundary condition is then applied to the well-studied case of $q^2\bar{q}^2$ states, and to $q^3\bar{q}^3$ states which have not been investigated before.

In principle, the sign of the mass in the Dirac equation can be rotated away trivially with a γ_5 transformation. However, once the quark boundary condition is chosen, the sign of the quark mass matters. As the quark mass varies from positive to negative values, the results smoothly interpolate between the M.I.T. ($m_q \geq 0$) and the S.L.A.C. bag ($m_q \to -\infty$) boundary conditions.

For simplicity, the calculations have been done for equal mass up and down quarks residing in the lowest cavity mode. The many-body wave functions of the exotic mesons are calculated taking into account the colour, spin and isospin degrees of freedom of the quarks and the Pauli principle. The P-, C- and G-parities are determined for each state, and the technique of coefficients of fractional parentage is used to evaluate the two-particle interaction matrix elements at the tree level, in the framework of perturbative Cavity QCD. The results are compared with the experimental hadron spectrum.

Contents

List of Figures

Chapter 1

Introduction

Today there is little doubt that QCD ([1], [2], [3]) is the correct theory of the strongly interacting of quarks and gluons, even though there are still many open issues where our understanding of this relativistic quantum field theory is not complete. One of these areas is the low-energy domain, where perturbative expansion of the theory is not expected to yield meaningful results, as the strong "fine structure constant" α_S is large and the number of Feynman diagrams to be calculated increases rapidly with the order of the perturbation expansion. These are the main reasons why QCD is performing so poorly compared to QED, where the perturbative expansion converges asymptotically. In fact, in some particular cases, QED corrections calculated perturbatively agree with the experimental data to even 9 digits, as for the case of the anomalous magnetic moment of the electron. However, achieving similar accuracy in the calculation of QCD seems hopeless at present.

Today it is believed that quark confinement, which plays an important role in hadronic physics, is an inherently non-perturbative phenomenon which cannot be handled analytically at present. Even if one expects that confinement is contained within the framework of QCD, at this stage it is unknown how to derive it from the fundamental theory. Thus, at present, we are forced to use a model that incorporates confinement phenomenologically. This will of course, lead to results that depend on the chosen confinement mechanism. However, we are confident that at least some general features will be independent of the confinement mechanism on which this work is based.

The framework used here is perturbative Cavity QCD where confinement is introduced by imposing the linear boundary conditions of the M.I.T. bag model [6] on the field operators describing the particles of the theory. It has been shown that perturbative Cavity QCD can be calculated [7], and the $\overline{MS}$ renormalization technique for evaluating diverging graphs within cavity field theories has been developed ([8], [9], [10], [11]). Predictions of quantities calculated in perturbative Cavity QCD as e.g. the weak vector and axial current coupling, the anomalous magnetic moment of the nucleon, the general electroweak properties of the nucleon have been compared to the experimental data with success.

The main drawback of Cavity QCD is that the rigid boundary condition breaks both translational and Lorentz invariance. Also chiral symmetry is lost due to the boundary condition. These disadvantages are largely compensated by the fact that nearly all interesting processes and quantities can be calculated in Cavity QCD and a good phenomenological understanding of subhadronic physics is achieved in this way. This is perhaps more satisfactory than trying to solve QCD non-perturbatively that usually leads to insurmountable mathematical problems. The results obtained in perturbative Cavity QCD, so far, describe the experimental data well, so that one may be confident that this framework could capture the essential features of exotic states. Thus, we do not claim that perturbative Cavity QCD is the full answer to low-energy hadron physics, but it is perhaps a reasonable starting point.

Hadrons are generally assumed to be a combination of either three quarks or a quark-antiquark pair. These are the simplest sets of quarks and antiquarks that can be combined to colour singlet states. But in the realm of QCD, there are other possibilities to combine quarks, antiquarks and gluons so that the final hadron is a colour singlet and the constituent particles obey the correct statistics. The most general state satisfying these requirements is $\left|q^{3B}(q\overline{q})^M g^N\right\rangle$ with $B, M, N = 0, 1, 2, ...$ These states are in principle allowed by the theory, but convincing evidence for their existence is still lacking. There are, however, some recent indications that exotic states may exist, as e.g. the isovector $J^{PC} = 1^{-+}$ exotic resonance at 1593 ± 8MeV (E852 Collab., [4]) and 1620 ± 20MeV (VES Collab., [5]) which have been observed recently.

There are in principle three possible attitudes towards tackling the puzzle of exotic hadrons:

(*i*)either exotic states do not exist, but then a mechanism should be found that forbids the existence of these states or

(*ii*)the exotic states exist, but as many other particles in physics, they have not been discovered yet, or

(*iii*) as there are lots of these perhaps short-lived states, they might merely contribute to a continuous hadronic background in scattering or decay processes.

We will explore in this work the second scenario and calculate the mass spectrum for general exotic states of the form $q^2\bar{q}^2$ [6] and $q^3\bar{q}^3$ for both the original and the new boundary condition. The mass spectrum of $q^3\bar{q}^3$ states has not been reported in the literature to our knowledge.

The properties of exotic states of the form $q^2\bar{q}^2$, $q\bar{q}g$, q^3g, $q\bar{q}g^2$, q^3g^2, $q\bar{q}g^3$ and q^3g^3 have been studied in the context of Cavity QCD by Zimak [21] and Viollier *et al.* [16]. Similar techniques are used in this work for calculating the mass spectrum of $q^2\bar{q}^2$ and $q^3\bar{q}^3$ states.

In the second chapter we present the main results developed in Cavity QCD to order α_S. The field operators are expanded into cavity modes that obey eigenvalue equations. The energy shift of the interacting states is calculated to order α_S while including two-particle interactions via one-gluon exchange and one-gluon annihilation.

In chapter three, the wave function of an exotic state is constructed and the general theory is presented. Subsequently, the transformation matrices between two different choices of many-particle wave functions are calculated. We then briefly discuss how the P-, C- and G-parities are defined for exotic states.

In the following chapter, we describe the results of our calculations. The spectrum for $q^2\bar{q}^2$ and $q^3\bar{q}^3$ states are presented for $m_q = 0$.

In chapter five, the model is extended to include a new linear boundary condition. This boundary condition [28], is equivalent to the standard linear boundary condition of the M.I.T. bag where the mass of the quark is taken to be negative. This interpretation helps to make a smooth connection between the M.I.T. bag boundary condition ($m_q \geq 0$) and the S.L.A.C. bag [37] boundary condition ($m_q = -\infty$). The

spectra are then recalculated for the new boundary condition and non-zero quark masses. The final results are plotted for positive and negative values of m_q in the case of standard boundary condition.

In chapter six we present the results in terms of graphs. The mass spectra for $q^2\bar{q}^2$ and $q^3\bar{q}^3$ states calculated for $m_q \in [-10...10]$ in natural mass units, are presented and analyzed.

Finally, in chapter seven, conclusions are drawn.

Chapter 2

Cavity Quantum Chromodynamics

In this chapter, we present the foundations of Cavity QCD. The notation and description of the theory follows closely the theory developed in the mid-eighties by Buser, Viollier and Zimak [16]. We first review the Free-space QCD. In order to quantize this theory, the gauge should be fixed, which breaks local gauge invariance. However, introducing the Faddeev-Popov [17] ghost term, a modified local gauge symmetry is recovered and the modified theory is now invariant under the so-called Becchi-Rouet-Stora transformation ([18],[19]). Based on the Gell-Mann and Low theorem in the symmetric form due to Sucher [24], and Dyson's expansion, the eigenvectors and eigenvalues of the full Hamiltonian operator can be obtained as a perturbative expansion of the time-evolution operator in terms of Feynman diagrams. The difference between Cavity QCD and Free-space QCD is merely that the field operators are expanded in terms of the cavity modes of a spherically symmetric and static cavity instead of plane-wave states. Restricting ourselves to tree graphs, the $qq, \bar{q}\bar{q}$ and $q\bar{q}$ interaction via one-gluon exchange and the $q\bar{q}$ interaction through one-gluon annihilation are calculated to order α_S.

2.1 QCD Lagrange and Hamilton Densities

The QCD Lagrange density is given by

$$\begin{aligned} \mathcal{L} &= \bar{\psi}(i\gamma_\mu D^\mu - m_f)\psi - \frac{1}{2}i\partial_\mu(\bar{\psi}\gamma^\mu\psi) - \frac{1}{4}\mathbf{F}_{\mu\nu}\cdot\mathbf{F}^{\mu\nu} \\ &\quad -\frac{1}{2}\lambda\partial_\mu\mathbf{A}^\mu\cdot\partial_\nu\mathbf{A}^\nu - i\partial_\mu\boldsymbol{\chi}\cdot\mathcal{D}^\mu\boldsymbol{\omega}, \end{aligned} \tag{2.1}$$

where ψ is the quark field, m_f is the mass of the quark, $\mathbf{A}^\mu$ is the gauge field describing the gluon and χ and ω are the Faddeev-Popov ghost fields. The first term of the Lagrangian density (2.1) describes the locally gauge-invariant interaction of the quarks and gluons. The second and third terms are kinetic terms for the quarks and gluons. The fourth term, which contains the gauge parameter λ, is a covariant gauge-fixing term which is globally gauge-invariant. The last term is the Faddeev-Popov ghost term which make the Lagrangian density invariant under (local) Becchi-Rouet-Stora (BRS) transformation.

The covariant derivative D^μ is defined as

$$D^\mu\psi = (\partial^\mu - \frac{1}{2}ig\boldsymbol{\lambda}\cdot\mathbf{A}^\mu) \tag{2.2}$$

and the covariant derivative in the adjoint representation of the gauge group $\mathcal{D}^\mu$ is given by

$$\mathcal{D}^\mu\boldsymbol{\omega} = \partial^\mu\boldsymbol{\omega} + g\mathbf{A}^\mu\times\boldsymbol{\omega}. \tag{2.3}$$

For the Lagrange density, the eight-dimensional scalar and vector products operating in the color space of the gluons have been used

$$\mathbf{A}\cdot\mathbf{B} = \sum_{a=1}^{8} A_a B_a \qquad ; \qquad (\mathbf{A}\times\mathbf{B})_a = \sum_{b,c=1}^{8} f_{abc}A_bB_c. \tag{2.4}$$

The $\boldsymbol{\lambda}$'s are the eight Gell-Mann matrices, the f_{abc} are the structure constants of $SU(3)_{colour}$ and λ parametrizes the gauge.

The Hamilton density is derived from the Lagrange density by using the Euler-Lagrange equations [16]. The Hamilton density obtained in this manner, can be written as

$$\mathcal{H} = \mathcal{H}_0 + \mathcal{H}_{int}, \tag{2.5}$$

where $\mathcal{H}$ is the total Hamiltonian, $\mathcal{H}_0$ contains the free fields which are independent on the strong coupling constant g,

$$\begin{aligned}\mathcal{H}_0 &= \bar{\psi}\left(-\frac{1}{2}i\gamma_k\overleftrightarrow{\partial^k} + M\right)\psi + \frac{1}{4}\left(\partial_k\mathbf{A}^l - \partial_l\mathbf{A}^k\right)\cdot\left(\partial_k\mathbf{A}^l - \partial_l\mathbf{A}^k\right) + \frac{1}{2}\boldsymbol{\Pi}^k\cdot\boldsymbol{\Pi}^k \\ &\quad -\frac{1}{2\lambda}\boldsymbol{\Pi}^0\cdot\boldsymbol{\Pi}^0 + \boldsymbol{\Pi}^k\cdot\partial_k\mathbf{A}^0 - \boldsymbol{\Pi}^0\cdot\partial_k\mathbf{A}^k - i\boldsymbol{\Omega}\cdot\mathbf{X} - i\partial_k\boldsymbol{\chi}\cdot\partial_k\boldsymbol{\omega},\end{aligned} \tag{2.6}$$

and $\mathcal{H}_{int}$ is the interaction term that depends linearly and quadratically on the coupling constant g

$$\mathcal{H}_{int} = -\frac{1}{2}g\bar{\psi}\gamma_\mu\boldsymbol{\lambda}\psi\cdot\mathbf{A}^\mu - \frac{1}{2}g\left(\partial_k\mathbf{A}^l - \partial_l\mathbf{A}^k\right)\cdot\left(\mathbf{A}^k\times\mathbf{A}^l\right) - g\boldsymbol{\Pi}^k\cdot\left(\mathbf{A}^k\times\mathbf{A}^0\right) +$$

$$+g\mathbf{\Omega}\cdot\left(\mathbf{A}^k\times\boldsymbol{\omega}\right)+ig\partial_k\boldsymbol{\chi}\cdot\left(\mathbf{A}^k\times\boldsymbol{\omega}\right)+\frac{1}{4}g^2\left(\mathbf{A}^k\times\mathbf{A}^l\right)\cdot\left(\mathbf{A}^k\times\mathbf{A}^l\right). \quad (2.7)$$

For the free Hamiltonian $\mathcal{H}_0$, the canonically conjugate momenta of the gluon and two ghost fields are $\mathbf{\Pi}^k$, $\mathbf{\Omega}$ and $\mathbf{X}$, respectively. The various terms of the interaction Hamilton density, describe the quark-gluon, three-gluon, ghost-gluon and the four-gluon interactions.

The Hamilton densities eqs. (2.6, 2.7) are quantized by interpreting the classical fields as field operators and imposing equal-time anticommutation or commutation relations for the field operators. For the quarks and gluons these relations are

$$\begin{aligned}\left\{\psi_{cf\alpha}(\mathbf{x},t),\psi^\dagger_{c'f'\alpha'}(\mathbf{y},t)\right\} &= \delta_{cc'}\delta_{ff'}\delta_{\alpha\alpha'}\delta^{(3)}(\mathbf{x}-\mathbf{y})\\ [A^\mu_a(\mathbf{x},t),\Pi^\nu_b(\mathbf{y},t)] &= ig^{\mu\nu}\delta_{ab}\delta^{(3)}(\mathbf{x}-\mathbf{y}),\end{aligned} \quad (2.8)$$

where the quark field subscripts denote the colour, flavour and Dirac indices.

Although the ghost fields have integer spin, they satisfy anti-commutation relations given by

$$\begin{aligned}\{\omega_a(\mathbf{x},t),\Omega_b(\mathbf{y},t)\} &= -i\delta_{ab}\delta^{(3)}(\mathbf{x}-\mathbf{y})\\ \{\chi_a(\mathbf{x},t),X_b(\mathbf{y},t)\} &= -i\delta_{ab}\delta^{(3)}(\mathbf{x}-\mathbf{y}).\end{aligned} \quad (2.9)$$

All other commutators or anti-commutators between field operators, which do not appear here explicitly, are understood to vanish.

With the quantization, the fields have become operators in the Heisenberg picture. It is useful for further calculation to transform all the field operators into the interaction or Dirac picture. This is realized by using a unitary transformation $U(t)$ which satisfies the differential equation

$$i\frac{\partial}{\partial t}U(t)=U(t)H_{int}(t). \quad (2.10)$$

Therefore, a Heisenberg state $|\psi\rangle$ transforms into a Dirac state $\left|\hat{\psi}(t)\right\rangle$ under $U(t)$ as

$$\left|\hat{\psi}(t)\right\rangle=U(t)\left|\psi\right\rangle. \quad (2.11)$$

The anti-commutation and commutations relations (2.8) and (2.9) remain unchanged in the Dirac picture. The field operators satisfy the non-interacting field equations

[16]

$$(i\gamma_\mu \partial^\mu - m)\,\hat{\psi} = \hat{\psi}\left(i\gamma_\mu \overleftarrow{\partial^\mu} - m\right) = 0 \tag{2.12}$$

$$\Box \hat{\mathbf{A}}^\mu + (\lambda - 1)\partial^\mu \partial_\nu \hat{\mathbf{A}}^\nu = 0 \tag{2.13}$$

$$\Box \hat{\omega} = \Box \hat{\chi} = 0. \tag{2.14}$$

The properties of QCD which have been discussed so far are quite general; no boundary conditions have been imposed yet. As we are interested in analyzing the properties of the mesons, we will introduce a finite volume of space in which the colour carrying particles are confined, i.e. we will develop Cavity QCD.

2.2 Boundary Conditions

Confinement of the colour-carrying particles is achieved by imposing boundary conditions on a static sphere of surface S. The boundary conditions must be compatible with the field equations. They are chosen by requiring that no colour charge escapes through the surface S. In the case of a static and spherical cavity, these boundary conditions are simply those of the M.I.T. bag model [6] which are linear in the field operators and independent of the strong coupling constant

$$\left(in_k\gamma^k - 1\right)\hat{\psi}\Big|_S = i\hat{\psi}\left(in_k\gamma^k + 1\right)\Big|_S = 0 \tag{2.15}$$

$$n_k\left(\partial^k \hat{\mathbf{A}}^\nu - \partial_\nu \hat{\mathbf{A}}_k\right)\Big|_S = n_k \hat{\mathbf{A}}^k\Big|_S = n_k \partial^k\left(\partial_\nu \hat{\mathbf{A}}^\nu\right)\Big|_S = 0 \tag{2.16}$$

$$n_k \partial^k \hat{\omega}\Big|_S = n_k \partial^k \hat{\chi}\Big|_S = 0. \tag{2.17}$$

The vector $n^\mu = (n^0, \vec{n})$ denotes a spacelike unit vector

$$n^\mu n_\mu = -1, \tag{2.18}$$

where $\vec{n}$ is perpendicular to the cavity surface S and pointing outward. By imposing the boundary conditions (A.2) to (A.4) to the non-interacting field equations (2.12) to (2.14), we obtain the quark and gluon cavity modes (see Appendix A).

2.3 The Quark Propagator

The quark-field operator can be expanded in terms of the cavity modes as

$$\hat{\psi}_{cf} = \sum_{\substack{\kappa,\mu \\ \nu>0}} \left(\hat{a}_{cfn} u_n \left(\vec{x}\right) e^{-i\varepsilon_n t} + \hat{b}^{\dagger}_{cfn} u_{-n} \left(\vec{x}\right) e^{i\varepsilon_n t} \right), \tag{2.19}$$

where n denotes the set of quantum numbers $n = \{\nu, \kappa, \mu\}$, which characterize the radial, angular momentum and magnetic quantum numbers of the quark, respectively, with $-n = \{-\nu, -\kappa, -\mu\}$. The expansion coefficients $\hat{a}$ and $\hat{b}^{\dagger}$ are quark annihilation and antiquark creation operators. The spinors $u_n\left(\vec{x}\right)$ are the cavity modes given in Appendix A, and ε_n being the energy of the mode.

The quark propagator is defined as the vacuum expectation value of the time-ordered product of the fields

$$iS\left(x_1, x_2\right) = \left\langle \hat{0} \middle| T\left[\hat{\psi}_{cf}\left(x_1\right) \hat{\psi}_{c'f'}\left(x_2\right)\right] \middle| \hat{0} \right\rangle \tag{2.20}$$

$$= \delta_{cc'}\delta_{ff'} \sum_{\substack{\kappa,\mu \\ \nu>0}} \left[u_n\left(\vec{x_1}\right) \bar{u}_n\left(\vec{x_2}\right) \Theta(t_1 - t_2) - u_{-n}\left(\vec{x_1}\right) \bar{u}_{-n}\left(\vec{x_2}\right) \Theta(t_2 - t_1) \right] e^{-i\varepsilon_n |t_1 - t_2|},$$

where the spinor indices have been suppressed. It can be written as

$$iS(x_1, x_2) = i\delta_{cc'}\delta_{ff'} \sum_n u_n\left(\vec{x_1}\right) \bar{u}_n\left(\vec{x_2}\right) \int \frac{d\omega}{2\pi} \frac{e^{-i\varepsilon_n |t_1 - t_2|}}{\omega - \varepsilon_n \pm i0} \tag{2.21}$$

by using the integral representation of the theta function

$$\Theta(t) = \lim_{\varepsilon \to 0} \frac{-1}{2\pi i} \int_{-\infty}^{\infty} d\omega \frac{e^{-i\omega t}}{\omega + i\varepsilon}. \tag{2.22}$$

The sum over n now includes both positive and negative radial quantum numbers. The usual Feynman prescription for the poles should be employed when performing the contour integral, i.e. the poles with positive (negative) energy acquire a small, imaginary negative (positive) part. The quark propagator is a Green's function of the Dirac equation

$$\left(i\partial_x - m\right) S\left(x, y\right) = \delta^{(4)}(x, y). \tag{2.23}$$

2.4 The Gluon Propagator

The gluon-field operator can be expanded in a way similar to the quark-field operator in terms of the gluon cavity modes as

$$\hat{A}^{\mu}_{a}(x) = \sum_{m\Sigma} \frac{1}{\sqrt{2\Omega^{\Sigma}_{m}}} \left[\hat{c}^{\Sigma}_{am} a^{\mu}_{m\Sigma}(\vec{x}) e^{-i\Omega^{\Sigma}_{m} t} + \hat{c}^{\Sigma\dagger}_{am} a^{\mu *}_{m\Sigma}(\vec{x}) e^{-i\Omega^{\Sigma}_{m} t} \right]. \tag{2.24}$$

The functions $a^{\mu}_{m\Sigma}(\vec{x})$ are the gluon cavity modes (see Appendix A), the operators $\hat{c}^{\Sigma\dagger}_{am}$ and $\hat{c}^{\Sigma}_{am}$ are the gluon creation and annihilation operators, $m = \{N, J, M\}$ denotes the radial, angular momentum and magnetic quantum numbers, and the label Σ denotes the scalar $\mathcal{S}$, longitudinal $\mathcal{L}$, transverse magnetic $\mathcal{M}$ and transverse electric $\mathcal{E}$ polarizations of the gluon, respectively. The propagator of the gluon is defined as the vacuum expectation value of the time-ordered product of the gluon field operators

$$\begin{aligned} iD^{\mu\nu}_{ab}(x_1, x_2) &= \left\langle \hat{0} \middle| T\left\{ \hat{A}^{\mu}_{a}(x_1) \hat{A}^{\nu}_{b}(x_2) \right\} \middle| \hat{0} \right\rangle \\ &= -\delta_{ab} \sum_{m\Sigma} \frac{g^{\Sigma\Sigma}}{\sqrt{2\Omega^{\Sigma}_{m}}} a^{\mu}_{m\Sigma}(\vec{x}_1) a^{\nu *}_{m\Sigma}(\vec{x}_2) e^{-i\Omega^{\Sigma}_{m}|t_1 - t_2|}, \end{aligned} \tag{2.25}$$

where the metric tensor in polarization space $g^{\Sigma\Sigma}$ is defined in Appendix A. By using the integral representation of the theta function (2.22), the gluon propagator can be written as

$$iD^{\mu\nu}_{ab}(x_1, x_2) = -\delta_{ab} \sum_{m\Sigma} g^{\Sigma\Sigma} a^{\mu}_{m\Sigma}(\vec{x}_1) a^{\nu *}_{m\Sigma}(\vec{x}_2) \int \frac{d\omega}{2\pi} \frac{e^{-i\omega(t_1 - t_2)}}{\omega^2 - \left(\Omega^{\Sigma}_{m}\right)^2 + i0}, \tag{2.26}$$

in the Feynman gauge. The gluon propagator satisfies the inhomogeneous d'Alembert equation

$$\Box D^{\mu\nu}_{ab}(x, y) = \delta_{ab} g^{\mu\nu} \delta^{(4)}(x, y). \tag{2.27}$$

2.5 The Gell-Mann and Low Theorem

Assuming that perturbation theory is valid, Cavity QCD can be expanded as a power series in the strong coupling constant g. In Cavity QCD, the interactions, e.g. the one-gluon exchange between two quarks may be expressed in terms of the shift in energy produced by the interaction. The usual way of calculating energy shifts is via the Gell-Mann and Low theorem [22], in the form given by Fetter and Walecka [23].

The Gell-Mann and Low theorem may be expressed in terms of the time-evolution operator $U(t,t_0)$ which is related to the unitary transformation $U(t)$ of section 2.1 by

$$U(t,t_0) = U(t)U^{-1}(t_0). \tag{2.28}$$

The time-evolution operator satisfies the same differential equation as $U(t)$

$$i\frac{\partial U(t,t_0)}{\partial t} = \hat{H}_{int}(t)U(t,t_0), \tag{2.29}$$

subject to the initial condition $U(t_0,t_0) = 1$. The time-evolution operator $U(t,t_0)$ transforms a state at time t_0 into a state at time t,

$$\left|\hat{\psi}(t)\right\rangle = U(t,t_0)\left|\hat{\psi}\,(t_0)\right\rangle. \tag{2.30}$$

The solution of the differential equation (2.29), with the specified initial condition, is given by Dyson's expansion in terms of the Hamiltonian in the interaction picture $\hat{H}^{\epsilon}_{int}(t)$

$$U^{\epsilon}(t,t_0) = \sum_{n=0}^{\infty}\frac{(-i)^n}{n!}\int_{t_0}^{t} dt_1 ... \int_{t_0}^{t} dt_n T\left(\hat{H}^{\epsilon}_{int}(t_1)...\hat{H}^{\epsilon}_{int}(t_n)\right), \tag{2.31}$$

where T is the time-ordering operator. We have also introduced adiabatic switching on of the interaction by

$$\hat{H}^{\epsilon}_{int}(t) = e^{-\epsilon|t|}\hat{H}_{int}(t), \tag{2.32}$$

with ϵ being a small positive number.

There is a link between Dyson's expansion and the energy shift due to the interaction. The total Hamiltonian can be written as $\hat{H}(0) = \hat{H}_0 + \hat{H}_{int}(0)$. Let $\left|\hat{\phi}_k\right\rangle$ be a complete and orthonormal set of eigenvectors of the non-interacting Hamiltonian and E^0_k the eigenvalues of the same Hamiltonian, then

$$\hat{H}_0\left|\hat{\phi}_k\right\rangle = E^0_k\left|\hat{\phi}_k\right\rangle. \tag{2.33}$$

The Gell-Mann and Low theorem states that if a state vector $\left|\hat{\psi}_k\right\rangle$ is given by

$$\left|\hat{\psi}_k\right\rangle = \lim_{\epsilon\to 0_+}\frac{U^{\epsilon}(0,-\infty)\left|\hat{\phi}_k\right\rangle}{\left\langle\hat{\phi}_k\right| U^{\epsilon}(0,-\infty)\left|\hat{\phi}_k\right\rangle} \tag{2.34}$$

and exists to all orders, then it is an eigenstate of the full Hamiltonian with the energy E_k given by

$$\hat{H}(0)\left|\hat{\psi}_k\right\rangle = E_k\left|\hat{\psi}_k\right\rangle. \tag{2.35}$$

The energy shift between the interacting and non-interacting systems can be written as

$$E_k - E_k^0 = \lim_{\epsilon \to 0_+} \frac{\left\langle \hat{\phi}_k \right| \hat{H}_{int}^{\epsilon}(t) U^{\epsilon}(0, -\infty) \left| \hat{\phi}_k \right\rangle}{\left\langle \hat{\phi}_k \right| U^{\epsilon}(0, -\infty) \left| \hat{\phi}_k \right\rangle}. \tag{2.36}$$

There is an alternative form of the Gell-Mann and Low theorem, given by Sucher [24] which makes use of the $S-$ matrix that is symmetric in the time integrations. In this formulation, the energy shift becomes

$$E_k - E_k^0 = \lim_{\substack{\eta \to 1 \\ \epsilon \to 0}} \frac{i\epsilon}{2} \frac{\partial \left\langle \hat{\phi}_k \right| S_{\eta}^{\epsilon} \left| \hat{\phi}_k \right\rangle_c / \partial \eta}{\left\langle \hat{\phi}_k \right| S_{\eta}^{\epsilon} \left| \hat{\phi}_k \right\rangle}, \tag{2.37}$$

where the subscript c implies including connected diagrams only. The adiabatic S -matrix S_{η}^{ϵ}, can be written as

$$S_{\eta}^{\epsilon} = 1 + \sum_{n=1}^{\infty} S_{\eta}^{\epsilon(n)} \tag{2.38}$$

with

$$S_{\eta}^{\epsilon(n)} = \frac{(-i\eta)^n}{n!} \int_{-\infty}^{\infty} dt_1 ... \int_{-\infty}^{\infty} dt_n e^{-\epsilon(|t_1| + ... + |t_n|)} T \left[\hat{H}_{int}^{\epsilon}(t_1) ... \hat{H}_{int}^{\epsilon}(t_n) \right]. \tag{2.39}$$

Taking the limit $\eta \to 1$ in eq. (2.37) and substituting eq. (2.38), one finds

$$\Delta E = \lim_{\epsilon \to 0} \frac{i\epsilon}{2} \frac{\left\langle S_{\epsilon}^{(1)} \right\rangle + 2 \left\langle S_{\epsilon}^{(2)} \right\rangle + 3 \left\langle S_{\epsilon}^{(3)} \right\rangle + ...}{1 + \left\langle S_{\epsilon}^{(1)} \right\rangle + \left\langle S_{\epsilon}^{(2)} \right\rangle + \left\langle S_{\epsilon}^{(3)} \right\rangle + ...}. \tag{2.40}$$

Expanding the denominator in a Taylor series, a more workable expression is obtained for the energy shift, i.e.

$$\begin{aligned} \Delta E \;=\; & \lim_{\epsilon \to 0} \frac{i\epsilon}{2} \left[\left\langle S_{\epsilon}^{(1)} \right\rangle + 2 \left\langle S_{\epsilon}^{(2)} \right\rangle + 3 \left\langle S_{\epsilon}^{(3)} \right\rangle \right. \\ & \left. - \left\langle S_{\epsilon}^{(1)} \right\rangle^2 + \left\langle S_{\epsilon}^{(1)} \right\rangle^3 - 3 \left\langle S_{\epsilon}^{(1)} \right\rangle \left\langle S_{\epsilon}^{(2)} \right\rangle \right]. \end{aligned} \tag{2.41}$$

If only the terms which connect to the asymptotic state of the mesons are taken, one is left, up to the order $O(g^2)$, with

$$\Delta E = \lim_{\epsilon \to 0} \frac{i\epsilon}{2} \left[2 \left\langle S_{\epsilon}^{(2)} \right\rangle - \left\langle S_{\epsilon}^{(1)} \right\rangle^2 \right]. \tag{2.42}$$

The first term produces the one-gluon exchange and annihilation diagrams and the second is responsible for cancelling the poles in the Feynman diagrams. We are interested in calculating the interaction between two quarks up to second order in g. Therefore, the following calculations will take into consideration only the $\left\langle S_{\epsilon}^{(2)} \right\rangle$ term.

2.6 Two-Particle Interactions

In this section we present the energy shifts due to one-gluon exchange and one-gluon annihilitation contributions to the quark-antiquark interaction. The part of $H_{int}(t)$ that describes the quark-gluon vertex is given by the first term of the Hamiltonian density (2.7) integrated over the volume

$$\hat{H}_{int}(t) = -g \int d^3x \hat{\psi}(x) \gamma_\mu \frac{\lambda_a}{2} \hat{A}^\mu_a \hat{\psi}(x), \tag{2.43}$$

since all other terms are either of different order or not connected to the asymptotic states considered in this work.

The quark self-energy is also contained in this term of the interaction Hamiltonian, but we will not discuss it here. The calculation has been described in detail in ref. [28]. If the relevant interaction Hamiltonian (2.43) is inserted into the $\left\langle S^{(2)}_\epsilon \right\rangle$ term, one obtains

$$\begin{aligned} \Delta E &= \lim_{\varepsilon \to 0_+} i\varepsilon \frac{(-i)^2}{2!} \int d^4x_1 \int d^4x_2 e^{-\varepsilon(|t_1|+|t_2|)} \\ &\quad \times \left\langle \hat{X} \right| T \left[\left(g\hat{\psi}\gamma_\mu \frac{\lambda_a}{2} \hat{A}^\mu_a \hat{\psi} \right)_{x_1} \left(g\hat{\psi}\gamma_\mu \frac{\lambda_a}{2} \hat{A}^\mu_a \hat{\psi} \right)_{x_2} \right] \left| \hat{X} \right\rangle, \end{aligned} \tag{2.44}$$

where $\left|\hat{X}\right\rangle$ is an asymptotic quark-antiquark state. This eigenstate of the non-interacting Hamiltonian can be written as a linear combination of quark-antiquark creation operators acting on the vacuum

$$\left|\hat{X}\right\rangle = \hat{a}^\dagger_{c_1 f_1 n_1} \hat{b}^\dagger_{c_2 f_2 n_2} \left|\hat{0}\right\rangle. \tag{2.45}$$

Using Wick's theorem, the time-ordered product may be expanded in terms of normal-ordered products. Because we are interested here in the one-gluon exchange or annihilation diagrams, only the gluon fields are contracted, yielding

$$\begin{aligned} \Delta E &= \lim_{\varepsilon \to 0_+} i\varepsilon \frac{(-i)^2}{2!} \int d^4x_1 \int d^4x_2 e^{-\varepsilon(|t_1|+|t_2|)} \\ &\quad \times \left\langle \hat{X} \right| T \left[\left(g\hat{\psi}\gamma_\mu \frac{\lambda_a}{2} \overset{|}{\hat{A}^\mu_a} \hat{\psi} \right)_{x_1} \left(g\hat{\psi}\gamma_\mu \frac{\lambda_a}{2} \overset{|}{\hat{A}^\mu_a} \hat{\psi} \right)_{x_2} \right] \left| \hat{X} \right\rangle. \end{aligned} \tag{2.46}$$

Substituting in eq. (2.46) the cavity-mode expansion of the quark fields and the gluon propagator, one gets for one-gluon exchange case

$$\Delta E = \lim_{\varepsilon \to 0_+} \frac{i\varepsilon}{2} g^2 \delta_{f'f} \delta_{g'g} \left\langle \hat{X} \right| a^\dagger_{c'f'\alpha'} b^\dagger_{d'g'\beta'} \left(\frac{\lambda_a}{2} \right)_{c'c} \left(-\frac{\lambda_a}{2} \right)_{d'd} a_{cf\alpha} b_{dg\beta} \left| \hat{X} \right\rangle \tag{2.47}$$

$$\sum_{m\Sigma} \frac{g^{\Sigma\Sigma}}{2\Omega_m^{\Sigma}} Q_{fi}^{m\Sigma} \tilde{Q}_{-f'-i'}^{m\Sigma} \iint dt_1 dt_2 e^{-\varepsilon(|t_1|+|t_2|)} e^{it_1(\varepsilon_f - \varepsilon_i)} e^{it_2(\varepsilon_{f'} - \varepsilon_{i'})} e^{-i\Omega_m^{\Sigma}|t_1-t_2|},$$

and for one-gluon annihilation case

$$\Delta E = \lim_{\varepsilon \to 0_+} \frac{i\varepsilon}{2} g^2 \delta_{f'g'} \delta_{fg} \left\langle \hat{X} \right| a_{c'f'\alpha'}^{\dagger} b_{d'g'\beta'}^{\dagger} \left(\frac{\lambda_a}{2}\right)_{c'd'} \left(\frac{\lambda_a}{2}\right)_{cd} a_{cf\alpha} b_{dg\beta} \left| \hat{X} \right\rangle \tag{2.48}$$

$$\sum_{m\Sigma} \frac{g^{\Sigma\Sigma}}{2\Omega_m^{\Sigma}} Q_{n'-\bar{n}'}^{m\Sigma} \tilde{Q}_{-\bar{n}n}^{m\Sigma} \iint dt_1 dt_2 e^{-\varepsilon(|t_1|+|t_2|)} e^{it_1(\varepsilon_n + \varepsilon_{\bar{n}})} e^{it_2(\varepsilon_{n'} + \varepsilon_{\bar{n}'})} e^{-i\Omega_m^{\Sigma}|t_1-t_2|}.$$

The quantities $Q_{fi}^{m\Sigma}$ denote the quark-gluon vertex integrals as defined in Appendix A and the subscripts n ($\bar{n}$) and n' ($\bar{n}'$) describe the initial quark (antiquark) and the final quark (antiquark) quantum numbers.

Solving the integrals and interpreting the shift energy ΔE as a two-body operator $\hat{V}$ sandwiched between the states $\left|\hat{X}\right\rangle$, the final expression for the two processes are

$$\hat{V}_{ex} = -g^2 \left(\frac{\lambda_a}{2}\right)_{c'c} \left(-\frac{\lambda_a}{2}\right)_{dd'} \delta_{f'f} \delta_{g'g} \frac{g^{\Sigma\Sigma}}{(\Omega_m^{\Sigma})^2} Q_{n'n}^{m\Sigma} \tilde{Q}_{-\bar{n}'-\bar{n}}^{m\Sigma} a_{c'f'\alpha'}^{\dagger} b_{d'g'\beta'}^{\dagger} a_{cf\alpha} b_{dg\beta}, \tag{2.49}$$

and

$$\hat{V}_{an} = -g^2 \left(\frac{\lambda_a}{2}\right)_{c'd'} \left(\frac{\lambda_a}{2}\right)_{cd} \delta_{f'g'} \delta_{fg} \frac{g^{\Sigma\Sigma}}{(\Omega_m^{\Sigma})^2} Q_{n'-\bar{n}'}^{m\Sigma} \tilde{Q}_{-\bar{n}n}^{m\Sigma} a_{c'f'\alpha'}^{\dagger} b_{d'g'\beta'}^{\dagger} a_{cf\alpha} b_{dg\beta}. \tag{2.50}$$

As we are calculating the interaction energy for many-quark systems, it is convenient to have a two-body operator (eqs.(2.38) and (2.50)) expressed in first instead of second quantization. The two-body operator which corresponds to $\hat{V}$ can be written as

$$V_{12} = \frac{\alpha_S}{R} \mathbf{F}_1 \cdot \mathbf{F}_2 \sum_J \mu_{12}(J) K_{12}(J), \tag{2.51}$$

where R is the radius of the cavity, $\mathbf{F}_i$ is the $SU(3)_c$ generator of the i-th quark, μ_{12} and K_{12} are two-body operators that act on the radial and angular part of the two-body wave function and J is the total angular momentum of the corresponding state. K_{12} can be expanded in terms of angular momentum as

$$\langle n', \bar{n}' | K_{12}(J) | n, \bar{n} \rangle = (2J+1) \sum_M (-1)^M F_{JM}(n', n) F_{J-M}(\bar{n}', \bar{n}), \tag{2.52}$$

where n ($\bar{n}$) is a generic label for all the quantum numbers carried by the quark (antiquark) and F is a factor which arises from the angular integration i.e.

$$F_{JM}(n', n) = (-1)^{\mu'+1/2} \hat{j}' \hat{j} \begin{pmatrix} j' & J & j \\ \frac{1}{2} & 0 & -\frac{1}{2} \end{pmatrix} \begin{pmatrix} j' & J & j \\ -\mu' & M & \mu \end{pmatrix}. \tag{2.53}$$

The matrix element of the operator μ_{12} arises from the radial integration (see Appendix B) and for one-gluon exchange it has the form

$$\begin{aligned}\langle n', \bar{n}' | \mu_{12}(J) | n, \bar{n}' \rangle &= -\sum_{\substack{N>0 \\ \Sigma}} \frac{2}{3} \frac{g^{\Sigma\Sigma}\eta_\Sigma}{2J+1} S^{\Sigma m}_{n'n} S^{\Sigma m}_{-\bar{n}-\bar{n}'} \frac{1}{R^2 \Omega^\Sigma_m} \\ &\quad \times \left(\frac{1}{\Omega^\Sigma_m + \varepsilon_{n'} - \varepsilon_n} + \frac{1}{\Omega^\Sigma_m + \varepsilon_{\bar{n}'} - \varepsilon_{\bar{n}}} \right), \end{aligned} \tag{2.54}$$

while for the one-gluon annihilation we obtain the expression

$$\begin{aligned}\left\langle n', \bar{n}' \right| \mu_{12}(J) | n, \bar{n} \rangle &= -\sum_{\substack{N>0 \\ \Sigma}} \frac{2}{3} \frac{g^{\Sigma\Sigma}\eta_\Sigma}{2J+1} S^{\Sigma m}_{-\bar{n}n} S^{\Sigma m}_{n'-\bar{n}'} \frac{1}{R^2 \Omega^\Sigma_m} \\ &\quad \times \left(\frac{1}{\Omega^\Sigma_m - \varepsilon_n - \varepsilon_{\bar{n}}} + \frac{1}{\Omega^\Sigma_m + \varepsilon_{n'} + \varepsilon_{\bar{n}'}} \right). \end{aligned} \tag{2.55}$$

For convenience we also introduce a dimensionless form of the interaction operator

$$\Delta_{12} = \frac{R}{\alpha} V_{12}. \tag{2.56}$$

The operators Δ_{12} for quark-quark interaction through one-gluon exchange and through one-gluon annihilation are then given by

one-gluon exchange	$F_{12}[\mu_{12}(0) + 4\mu_{12}(1) S_{12}]$
one-gluon annihilation	$(\frac{1}{4} - T_{12})(F_{12} + \frac{4}{3})[\mu_{12}(0)(\frac{1}{4} - S_{12}) + \mu_{12}(1)(\frac{3}{4} + S_{12})]$

, (2.57)

where we have used the abbreviation $X_{12} = \mathbf{X}_1 \cdot \mathbf{X}_2$ to denote the product of two generators of colour, spin or isospin. Note that the two operators (2.57) do not exhaust all the possible interaction operators to order α_S. For a detailed treatment of all the possible interactions at the tree-diagram level, the reader is referred to [7].

The separation of the angular and radial part brings a simplification into the calculation for two reasons. First, by splitting the two-body operator in two parts, the effective calculations become easier to follow and various checks can be done to verify the accuracy of the method. Second, in pursuing the goal of this work, the angular part is not affected by the mass of the quark (eqs. (2.52), (2.53)) and therefore it remains unchanged and no extra calculations are required. Instead, the radial part (eq. (2.54)) is sensitive to the mass of the quarks (both S function and the eigenenergy ε depend on m_q).

Chapter 3

The wave function of exotic states

The quarks and antiquarks of the exotic meson are carrying the quantum numbers of colour, flavour and the orbital. Considering only equal-mass up and down quarks, flavour degenerates to isospin symmetry. As the exotic meson must be colourless, the overall colour wave function will be a sum of products of colour triplet (or antitriplet) wave functions transforming as a colour singlet under $SU(3)_c$. As the quarks and antiquarks are assumed to reside in the lowest-energy $1s_{1/2}$ cavity mode, the overall orbital wave function will be a sum of products of spin 1/2 wave functions. Finally the overall flavour wave function will be a sum of products of isospin 1/2 wave functions. As quarks and antiquarks are fermions, the colour, isospin and spin parts of the wave function is antisymmetric with respect to interchange of any two quarks or any two antiquarks. This chapter illustrates how the wave function is calculated for exotic mesons of the form $q^2\bar{q}^2$ and $q^3\bar{q}^3$.

3.1 SU(3) Colour Wave Function

The colour degree of freedom of the quarks, antiquarks and gluons is described by the group $SU(3)_c$. A quark will be represented by a tensor [20] with one index

$$c^i, \qquad i = 1, 2, 3, \tag{3.1}$$

where the index i labels different colours of the quarks ($i = R$ red, G green, and B blue). An upper index is used to denote a quark and a lower index denotes an antiquark. Under a general $SU(3)$ transformation c^i and c_i transform as the components

of a contravariant and a covariant tensor respectively. Thus c^i is a vector in the fundamental representation $\{3\}$ of $SU(3)$ and c_i is a vector in the adjoint fundamental representation $\{\overline{3}\}$. For completeness, the gluon is described in its tensorial form as

$$G^i_j, \qquad i,j = 1,2,3. \qquad\qquad G^i_i = 0. \tag{3.2}$$

The gluon carries two indices because, unlike the quark $\{3\}$ and the antiquark $\{\overline{3}\}$, the gluon resides in the $\{8\}$ representation of $SU(3)$. Using Einstein's summation convention, the condition $G^i_i = 0$ projects out the colour singlet $\{1\}$ part of the tensor. This condition implies that gluons cannot be colourless and it ensures that only eight gluons exist.

In summary, the tensor representation of the $SU(3)$ group constitutes the framework for constructing the colour wave function and the building blocks used to obtain the exotic states are c^i, c_i and G^i_j.

3.1.1 Two-Quark (or Two-Antiquark) System

Having the tensor form for one quark c^i, the tensor form of two quarks can be constructed by combining c^i with c^j. But the tensor product c^ic^j is reducible to a symmetric and antisymmetric combination

$$c^ic^j + c^jc^i \qquad \text{and} \qquad c^ic^j - c^jc^i \tag{3.3}$$

in accordance with the Young Diagrams for the $SU(3)$ group

$$\{3\} \otimes \{3\} = \{\overline{3}\} \oplus \{6\}, \tag{3.4}$$

where the $\{\overline{3}\}$ representation is antisymmetric and the $\{6\}$ is symmetric. Antisymmetric combination found above describing two quarks has two upper indices and corresponds to a $\{\overline{3}\}$ representation of $SU(3)$. As was mentioned before, the $\{\overline{3}\}$ representation is bearing a lower index. Using the Levi-Civita's tensor ε^{ijk} or ε_{ijk}, the antisymmetric form can be rewritten as

$$c^ic^j - c^jc^i \sim \varepsilon_{kij}c^ic^j, \tag{3.5}$$

leaving only one lower index.

Therefore, for the system of two quarks, two colour wave functions

$$\{qq\}^{ij} \;=\; c^ic^j + c^jc^i$$

$$[qq]_k = \varepsilon_{kij} c^i c^j. \tag{3.6}$$

are possible. In order to normalize these, the product $\langle \{qq\}^{ij}, \{qq\}^{i'j'} \rangle$ must be evaluated. Using the identity $\sum_n \varepsilon_{ijn}\varepsilon_{nkl} = \delta_{ik}\delta_{jl} - \delta_{il}\delta_{jk}$, we arrive at

$$\begin{aligned} \langle \{qq\}^{ij}, \{qq\}^{i'j'} \rangle &= 2(\delta^{ii'}\delta^{jj'} + \delta^{ij'}\delta^{ji'}) \\ \langle \{qq\}^{ij}, [qq]_k \rangle &= 0 \\ \langle [qq]_i, [qq]_{i'} \rangle &= 2\delta_{ii'}. \end{aligned} \tag{3.7}$$

For the case of two antiquarks, the wave functions are obtained simply from those of the two quarks by exchanging the upper and lower indices. The symmetric and antisymmetric combinations for antiquarks are $\{\overline{qq}\}_{ij}$ and $[\overline{qq}]^i$, respectively.

3.1.2 Quark-Antiquark System

The combination of a quark $\{3\}$ with an antiquark $\{\overline{3}\}$, according to the Young diagrams for the $SU(3)$ group, results in a singlet and an octet

$$\{3\} \otimes \{\overline{3}\} = \{1\} \oplus \{8\}. \tag{3.8}$$

The product $c^i c_j$ is reducible and can be split in a scalar trace and a traceless tensor

$$\begin{aligned} [q\overline{q}] &= c^i c_i \\ [q\overline{q}]^i_j &= c^i c_j - \frac{1}{3}\delta^i_j c^k c_k \end{aligned} \tag{3.9}$$

corresponding to the $\{1\}$ and $\{8\}$ representations of $SU(3)$. The normalization coefficients are calculated, as in the previous section for two quarks yielding

$$\begin{aligned} \langle [q\overline{q}], [q\overline{q}] \rangle &= 3 \\ \langle [q\overline{q}], [q\overline{q}]^i_j \rangle &= 0 \\ \langle [q\overline{q}]^i_j, [q\overline{q}]^{i'}_{j'} \rangle &= \delta^{ii'}\delta_{jj'} - \frac{1}{3}\delta^i_j\delta^{i'}_{j'}. \end{aligned} \tag{3.10}$$

In an analogous way, the gluon can be introduced and coupled with the quark, antiquark or another gluon. Because, in this work the exotic states studied do not contain explicitly the gluon, the treatment of the gluon will be omitted. It would be necessary to study the tensor form of the gluon-quark and gluon-gluon systems for glueballs and hybrid exotic states only.

3.1.3 Two Quark-Two Antiquark System

The next step in constructing the colour part of the wave function for the $q^3\overline{q}^3$ system is to construct the $q^2\overline{q}^2$ system. One is faced now with two possibilities, to build a two quark-two antiquark state because (i) it is possible to assemble two quarks, then two antiquarks and finally combining the two or (ii) it is possible to assemble a quark with an antiquark, another quark-antiquark state and at the end to couple them together.

Both combinations are used to calculate the energy of the exotic states. For the study of the quark-quark and antiquark-antiquark interaction, the first combination is important, i.e. $(q^2)(\overline{q}^2\ )$ while for the quark-antiquark interaction we need the second combination, i.e. $(q\overline{q})(q\overline{q})$.

Following the first option, two quarks (q^2, $\{\overline{3}\}\oplus\{6\}$) are combined with two antiquarks ($\overline{q}^2, \{3\}\oplus\{\overline{6}\}$). There are four possibilities to combine two quarks with two antiquarks. According to the Young diagrams these are

$$\begin{aligned}
\{\overline{3}\}\otimes\{3\} &= \{1\}\oplus\{8\} \\
\{6\}\otimes\{\overline{6}\} &= \{1\}\oplus\{8\}+\{27\} \\
\{\overline{3}\}\otimes\{\overline{6}\} &= \{8\}\oplus\{\overline{10}\} \\
\{6\}\otimes\{3\} &= \{8\}\oplus\{10\}.
\end{aligned} \tag{3.11}$$

Combining two pairs of quarks and antiquarks ($q\overline{q}$, $\{1\}\oplus\{8\}$) to the final state $q^2\overline{q}^2$, the following representations are possible

$$\begin{aligned}
\{1\}\otimes\{1\} &= \{1\} \\
\{1\}\otimes\{8\} &= \{8\} \\
\{8\}\otimes\{1\} &= \{8\} \\
\{8\}\otimes\{8\} &= \{1\}\oplus\{8\}_s\oplus\{8\}_a\oplus\{\overline{10}\}\oplus\{10\}\oplus\{27\},
\end{aligned} \tag{3.12}$$

where the indices s and a stand for symmetric and antisymmetric.

In order to get the colour wave functions for the exotic state $q^2\overline{q}^2$ those combinations which reside in colour singlet state are picked up. These states are

$\lvert q^2,\overline{q}^2\rangle$	$\lvert q\overline{q},q\overline{q}\rangle$
$\lvert\{\overline{3}\},\{3\};\{1\}\rangle$	$\lvert\{1\},\{1\};\{1\}\rangle$
$\lvert\{6\},\{\overline{6}\};\{1\}\rangle$	$\lvert\{8\},\{8\};\{1\}\rangle$

(3.13)

Here the notation for the state vectors for the two columns $|q^2,\overline{q}^2\rangle$ and $|q\overline{q},q\overline{q}\rangle$ is $\left|\{N_{q^2}\},\{N_{\overline{q}^2}\};\{N_{q^2\overline{q}^2}\}\right\rangle$ and $\left|\{N_{q\overline{q}}\},\{N_{q\overline{q}}\};\{N_{q^2\overline{q}^2}\}\right\rangle$. In terms of the tensors, these normalized colour singlet states are described by

$$(q^2)(\overline{q}^2)\begin{cases}\left|\{\overline{3}\},\{3\};\{1\}\right\rangle=\frac{1}{\sqrt{12}}[qq]_i[\overline{q}\overline{q}]^i\\ \left|\{6\},\{\overline{6}\};\{1\}\right\rangle=\frac{1}{4\sqrt{3}}\{qq\}^{ij}\{\overline{q}\overline{q}\}_{ij}\end{cases}\tag{3.14}$$

$$(q\overline{q})(q\overline{q})\begin{cases}|\{1\},\{1\};\{1\}\rangle=\frac{1}{3}[q\overline{q}][q\overline{q}]\\ |\{8\},\{8\};\{1\}\rangle=\frac{1}{\sqrt{8}}[q\overline{q}]^i_j[q\overline{q}]^j_i.\end{cases}\tag{3.15}$$

Of course there is a linear transformation between the complete and orthonormal base $(q^2)(\overline{q}^2)$ and the overcomplete base $(q\overline{q})(q\overline{q})$ ([21] [16]).

The transition between the two basis is given by

$$\begin{pmatrix}\left|\{\overline{3}\},\{3\};\{1\}\right\rangle\\ \left|\{6\},\{\overline{6}\};\{1\}\right\rangle\end{pmatrix}=\frac{1}{\sqrt{3}}\begin{pmatrix}1&-\sqrt{2}\\ \sqrt{2}&1\end{pmatrix}\cdot\begin{pmatrix}|\{1\},\{1\};\{1\}\rangle\\ |\{8\},\{8\};\{1\}\rangle\end{pmatrix}.\tag{3.16}$$

The above colour information is sufficient if one wants to describe $q^2\overline{q}^2$ exotic states. However, for $q^3\overline{q}^3$ exotic states, it is necessary to consider the octet state $q^2\overline{q}^2$ as well.

3.1.4 Three Quark-Three Antiquark System

In this section we calculate the colour wave functions for an exotic $q^3\overline{q}^3$ system. Due to the fact that the state should be physical, it is necessary that its representation is a singlet $\{1\}$ of colour $SU(3)$. Because later the $q-q$ and $q-\overline{q}$ interaction will be needed, we express the wave function in both the $(q^3)(\overline{q}^3)$ and the $(q^2\overline{q}^2)(q\overline{q})$ bases. For the first base a quark (antiquark) is added to the two quark (two antiquark) system presented in section 2.1.1. Because the $q-\overline{q}$ can reside in a $\{1\}$ or $\{8\}$ representation, the corresponding $\{1\}$ and $\{8\}$ representations for $q^2\overline{q}^2$ system are needed. Details of the calculations for the $q^3\overline{q}^3$ system can be found in Appendix B1. The main results for the complete and orthonormal base are

$$(q^3)(\overline{q}^3)\begin{cases} \left|\{\overline{3}\},1,\{3\},1;1\right\rangle = \frac{1}{6}[qqq][\overline{qqq}] \\ \left|\{\overline{3}\},8_a,\{3\},8_a;1\right\rangle = \frac{1}{4\sqrt{2}}[qqq]^i_j[\overline{qqq}]^j_i \\ \left|\{6\},8_s,\{\overline{6}\},8_s;1\right\rangle = \frac{1}{12\sqrt{2}}\{qqq\}^i_j\{\overline{qqq}\}^j_i \\ \left|\{\overline{3}\},8_a,\{\overline{6}\},8_s;1\right\rangle = \frac{1}{4\sqrt{6}}[qqq]^i_j\{\overline{qqq}\}^j_i \\ |\{6\},8_s,\{3\},8_a;1\rangle = \frac{1}{4\sqrt{6}}\{qqq\}^i_j[\overline{qqq}]^j_i \\ \left|\{6\},10,\{\overline{6}\},\overline{10};1\right\rangle = \frac{1}{36\sqrt{10}}\{qqq\}^{ijk}\{\overline{qqq}\}_{ijk}. \end{cases} \tag{3.17}$$

The notation used here is $\left|\{N_{q^2}\},N_{q^3},\{N_{\overline{q}^2}\},N_{\overline{q}^3};N_{q^3\overline{q}^3}\right\rangle$ and all five numbers denote a representation . The curly bracket is reserved for diquark states. The overcomplete base has the following basis vectors

$$(q^2\overline{q}^2)(q\overline{q})\begin{cases} \left|\{\overline{3}\},\{3\},1,1;1\right\rangle = \frac{1}{6}[qq]_i[\overline{qq}]^i[q\overline{q}] \\ \left|\{\overline{3}\},\{3\},8,8;1\right\rangle = \frac{1}{4\sqrt{2}}[qq]_i[\overline{qq}]^j[q\overline{q}]^i_j \\ \left|\{6\},\{\overline{6}\},8,8;1\right\rangle = \frac{1}{4\sqrt{10}}\{qq\}^{ij}\{\overline{qq}\}_{aj}[q\overline{q}]^a_i \\ \left|\{\overline{3}\},\{\overline{6}\},8,8;1\right\rangle = \frac{1}{4\sqrt{6}}\varepsilon^{ibm}[qq]_i\{\overline{qq}\}_{ab}[q\overline{q}]^a_m \\ |\{6\},\{3\},8,8;1\rangle = \frac{1}{4\sqrt{6}}\varepsilon_{ibm}\{qq\}^{jb}[\overline{qq}]^m[q\overline{q}]^i_j \\ \left|\{6\},\{\overline{6}\},1,1;1\right\rangle = \frac{1}{12\sqrt{2}}\{qq\}^{ij}\{\overline{qq}\}_{ij}[q\overline{q}]. \end{cases} \tag{3.18}$$

The notation used here is $\left|\{N_{q^2}\},\{N_{\overline{q}^2}\},N_{q^2\overline{q}^2},N_{q\overline{q}};N_{q^3\overline{q}^3}\right\rangle$. As seen from the above table, the original states $\{N_{q^2}\},\{N_{\overline{q}^2}\}$ must be specified in each base element in order to distinguish among $q^3\overline{q}^3$ singlets obtained from $q^2\overline{q}^2$ and $q\overline{q}$ states.

The matrix transformation between the two bases is given by

$$\begin{pmatrix} \left|\{\overline{3}\},1,\{3\},1;1\right\rangle \\ \left|\{\overline{3}\},8_a,\{3\},8_a;1\right\rangle \\ \left|\{6\},8_s,\{\overline{6}\},8_s;1\right\rangle \\ \left|\{6\},10,\{\overline{6}\},\overline{10};1\right\rangle \\ \left|\{\overline{3}\},8_a,\{\overline{6}\},8_s;1\right\rangle \\ |\{6\},8_s,\{3\},8_a;1\rangle \end{pmatrix} = \begin{pmatrix} \frac{1}{3} & \frac{2\sqrt{2}}{3} & 0 & 0 & 0 & 0 \\ \frac{2\sqrt{2}}{3} & -\frac{1}{3} & 0 & 0 & 0 & 0 \\ 0 & 0 & -\frac{\sqrt{5}}{3} & \frac{2}{3} & 0 & 0 \\ 0 & 0 & \frac{2}{3} & \frac{\sqrt{5}}{3} & 0 & 0 \\ 0 & 0 & 0 & 0 & 1 & 0 \\ 0 & 0 & 0 & 0 & 0 & -1 \end{pmatrix} \begin{pmatrix} \left|\{\overline{3}\},\{3\},1,1;1\right\rangle \\ \left|\{\overline{3}\},\{3\},8,8;1\right\rangle \\ \left|\{6\},\{\overline{6}\},8,8;1\right\rangle \\ \left|\{6\},\{\overline{6}\},1,1;1\right\rangle \\ \left|\{\overline{3}\},\{\overline{6}\},8,8;1\right\rangle \\ |\{6\},\{3\},8,8;1\rangle \end{pmatrix} \tag{3.19}$$

We have now calculated the colour wave functions for the exotic states $q^3\overline{q}^3$ and $q^2\overline{q}^2$ and the transformation matrices between the overcomplete and the complete and orthonormal bases. The next step is to construct in a similar way - using the group $SU(2)$ this time - the spin and isospin wave functions for the exotic states and then to combine all of them in a single wave function.

3.2 SU(2) Spin and Isospin

In this section we construct the $SU(2)_{spin}$ and $SU(2)_{isospin}$ wave functions in analogy to the previous section. The qq, $\overline{q}\overline{q}$ and $q\overline{q}$ systems are discussed first, and then these will be coupled to $q^2\overline{q}^2$ and $q^3\overline{q}^3$ states in various ways.

Since the isospin symmetry group is identical to that of the spin group, the isospin wave functions are essentially the same as those of the spin. Only the latter will be considered here. All the constructions are valid for the up and down quarks, having spin 1/2 and isospin 1/2.

3.2.1 Two Quark-Two Antiquark System

The combination of two spins 1/2 will produce a total spin of 0 or 1 where the first combination is symmetric and the second antisymmetric [12] . For the two quark-two antiquark system, the total spin is $0, 1$ or 2. As in the colour case two bases are used. These are denoted by $\left|J_{q^2}, J_{\overline{q}^2}; J, j\right\rangle$ and $\left|J_{q\overline{q}}, J'_{q\overline{q}}; J, j\right\rangle$, where J_{q^2} and $J_{\overline{q}^2}$ stand for the spin of the two quarks and two antiquarks respectively, $J_{q\overline{q}}$ ($J'_{q\overline{q}}$) denote the spins of the quark-antiquark pairs and J and j are the spin of the exotic state and its projection. Recoupling the four spins of the four quarks, we obtain the well known 9-j symbols [21], [16]

$$\left|J_{q^2}, J'_{\overline{q}^2}; J, j\right\rangle = \sum_{J_{q\overline{q}} J'_{q\overline{q}}} \hat{J}_{q^2}\hat{J}_{\overline{q}^2}\hat{J}_{q\overline{q}}\hat{J}'_{q\overline{q}} \begin{pmatrix} 1/2 & 1/2 & J_{q^2} \\ 1/2 & 1/2 & J_{\overline{q}^2} \\ J_{q\overline{q}} & J'_{q\overline{q}} & J \end{pmatrix} \left|J_{q\overline{q}}, J'_{q\overline{q}}; J, j\right\rangle, \qquad (3.20)$$

where $\hat{J} = \sqrt{2J+1}$.

3.2.2 Three Quark-Three Antiquark System

The spin wave function of this exotic state can be obtained from the $q^2\overline{q}^2$ and $q\overline{q}$ spin wave functions or from the q^3 and $\overline{q}^3$ spin wave functions, as in the case of colour. The relationship between the two bases can be established by recoupling the spin $J_{q^2}, J_{\overline{q}^2}, J_q$ and $J_{\overline{q}}$. The results are given in Appendix B where all the elements of the two bases are listed.

As explained above, the situation for the isospin is identical to that of the spin,

so all the results obtained for the spin are valid for isospin too. This means that for the exotic state ($q^3\bar{q}^3$) there are 6 possible wave functions for colour, 20 for spin and 20 for isospin. Therefore all combinations of colour, spin and isospin which obey the Pauli principle and are colourless, are possible exotic states.

3.3 P-, C- and G-parities

Before gathering all the information obtained for the colour, spin and isospin parts of the wave function, a short discussion concerning the parities of the final states is necessary. It turns out that it is important to identify the states not only by their J and I quantum numbers but also by their P-, C- and G-parities.

Parity is defined as a transformation which changes the sign of all the spatial components of a wave function and nothing else. For the present $q^3\bar{q}^3$case, it is interesting to study the parity of a quark-antiquark pair. As it is known [13] [14], the intrinsic parity of a fermion is opposite to that of an antifermion. When a system of two particles is investigated, its parity is a product of the intrinsic parities times a factor which depends on orbital quantum number l

$$P = (-1)^l \times \text{intrinsic parity of components},$$

where l is the relative orbital quantum number of the components. For a meson consisting of a "n" quark-antiquark pairs in the lowest-energy state, the parity is

$$P = (-1)^n \tag{3.21}$$

so that for all two quark-two antiquark states, the parity is positive while for all three quark-three antiquark states the parity is negative.

For the C or charge conjugation parity, the problem is not so simple as it was for parity. By definition, the charge conjugation operator C changes particles into antiparticles and vice versa. The charge conjugation operator changes the sign for additive quantum numbers (e.g. charge, strangeness) and leaves momentum and spin unaffected. Moreover, not all the states are eigenstates of the charge conjugation operator further complicating the matter. In order to understand how the charge conjugation quantum number is related to colour, spin and isospin, we will look at

each quantum number separately. In general the charge conjugation operator looks like

$$C = C^C \cdot C^J \cdot C^I \cdot C^{SS} \tag{3.22}$$

where different terms describe the action on the colour, spin, isospin and a factor related to the spin-statistics of the state. The following explanations will refer to a general state $q^N\bar{q}^N$.

For the colour wave function, the action of C on any number of quark-antiquark pairs is $+1$. This can be easily shown by considering eq. (C.1). After the charge conjugation operator having changed each particle into its antiparticle, we obtain back by simple permutation, the quarks and antiquarks in their original state, and the colour gives no contribution. Taking the quark-antiquark system in its $\{8\}$ colour representation as an example, the colour state is described by

$$[q\bar{q}]^i_j = c^i c_j - \frac{1}{3}\delta^i_j c^n c_n. \tag{3.23}$$

Acting with the charge conjugation operator C^C on this state, the result is

$$\begin{aligned} C^C c^i &= c_i \qquad\qquad C^C c_j = c^j \\ C^C [q\bar{q}]^i_j &= C^C(c^i c_j - \frac{1}{3}\delta^i_j c^n c_n) = c_i c^j - \frac{1}{3}\delta^i_j c_n c^n \\ &= c^j c_i - \frac{1}{3}\delta^i_j c^n c_n. \end{aligned} \tag{3.24}$$

In the last equality the quark wave function was interchanged with that of the antiquark without affecting the colour wave function. Note that a factor $C^{SS}(=-1)$ should be considered due to the Fermi-Dirac statistics.

Interchanging the quarks in the spin wave function yields a factor of $(-1)^{j_1+j_2-J}$, where j_1 and j_2 are the spins of the quarks and the antiquarks respectively, and J is the total spin of the exotic state. The above factor is a result of a rearrangement of two spins. Using from [12] the relation

$$|j_1, j_2; Jm\rangle = (-1)^{j_1+j_2-J} |j_2, j_1; Jm\rangle , \tag{3.25}$$

the action of C on spin is

$$C^J |j_1, j_2; Jm\rangle = |j_2, j_1; Jm\rangle = (-1)^{j_1+j_2-J} |j_2, j_1; Jm\rangle . \tag{3.26}$$

A permutation was applied on the $|j_2, j_1; Jm\rangle$ factor to get the initial spin order, which produced the rearrangement of the spins and an extra factor due to relation (3.25) .

For the isospin, the same rearrangement in eq. (3.25) is necessary and further care should be taken due to the fact that the charge conjugation changes the third component of the isospin ($Q = 1/2\, Y + I_3$). We thus arrive at

$$C^I\, |i_1, i_2; Im_i\rangle = (-1)^{i_1 - i_2 + m_i}\, |i_2, i_1; I - m_i\rangle\,. \tag{3.27}$$

Eq. (3.27) shows that not all the vectors are eigenstates of C due to the different spins of the constituents. Two cases can be described. First, if $i_1 = i_2$ and $m_i = 0$, the vector is well defined and applying C on it yields

$$C^I\, |i, i; I0\rangle = |i, i; I0\rangle\,. \tag{3.28}$$

Thus the state is an eigenvector for the charge conjugation operator. For the second case, when $i_1 \neq i_2$ and $m_i = 0$, the vector is an eigenvector for C if it is chosen to be

$$|i_1, i_2; Im_i\rangle_\pm = \frac{1}{\sqrt{2}} \left(|i_1, i_2; Im_i\rangle \pm |i_2, i_1; Im_i\rangle \right). \tag{3.29}$$

The action of C on eq. (3.29) yields

$$C^I\, |i_1, i_2; I0\rangle_\pm = \pm (-1)^{i_1 - i_2}\, |i_2, i_1; I0\rangle_\pm\,. \tag{3.30}$$

The last factor in eq. (3.22) which plays a role in the overall charge conjugation is the spin-statistics factor. Because the particles composing the exotic state are fermions, they should be permuted back to their original position, so that a factor $(-1)^N$ arises.

The third discrete operation, the G-parity, arises as a consequence of the fact that not all members of an isospin multiplet are eigenstates of C operator. In order to rectify the problem, G parity is defined as a product of C parity and the second projection of the total spin operator, I_2. The exact mathematical relationship is

$$G = e^{i\pi I_2} C. \tag{3.31}$$

The application of the second projection of the total isospin I_2 has the property

of restoring the sign of the I_3 after C has changed its sign, obtaining in this way the original vector. Having this property, G leaves all the members of the isospin multiplet in their original form and in this manner all the members of the multiplet are eigenvectors for G and their eigenvalues are given by the relation

$$G = C\,(-1)^I\,. \tag{3.32}$$

3.4 The Total Wave Function

The total wave function for the $q^2\bar{q}^2$ system was calculated by Zimak *et al.* [15], [16]. We follow a similar path to construct the wave function of the $q^3\bar{q}^3$ system. In order to get all the allowed combinations, we use the fact that the three-quark system was studied in detail (see Appendix B). The starting point is the q^3 system which was built to obey the Pauli principle, and no restrictions were imposed on the total colour. If one wants to have the $\bar{q}^3$ built in the same way, by simply applying a C transformation on q^3, all the results can be translated to the three-antiquark system. The total wave function for $\bar{q}^3$ is identical with that of the q^3 system if all the colour indices are flipped (lower $\Leftrightarrow$ upper), the spin is unchanged, the total isospin remains the same, only its third component changes the sign. Now, if one brings together the wave functions for three-quark and three-antiquark system and demands that the final colour is in the singlet representation, we obtain the exotic state. The Pauli principle is built in for quarks and antiquarks separately (see appendix B). Quarks and antiquarks are distinguishable particles so they do not obey the Pauli principle, the colour is $\{1\}$, therefore all the conditions are fulfilled to get the correct total wave function.

In the table below the states $(q^3)(\bar{q}^3)$ with $J = 0$ are shown:

$I=0$	$N^{10}_{\frac{1}{2}}\bar{N}^{10}_{\frac{1}{2}}$	$\Delta^{8}_{\frac{1}{2}}\bar{\Delta}^{8}_{\frac{1}{2}}$	$N^{1}_{\frac{1}{2}}\bar{N}^{1}_{\frac{1}{2}}$	$N^{8}_{\frac{1}{2}}\bar{N}^{8}_{\frac{1}{2}}$	$\Delta^{1}_{\frac{3}{2}}\bar{\Delta}^{1}_{\frac{3}{2}}$	$N^{8}_{\frac{3}{2}}\bar{N}^{8}_{\frac{3}{2}}$		
$I=1$	$N^{10}_{\frac{1}{2}}\bar{N}^{10}_{\frac{1}{2}}$	$\Delta^{8}_{\frac{1}{2}}\bar{\Delta}^{8}_{\frac{1}{2}}$	$\Delta^{8}_{\frac{1}{2}}\bar{N}^{8}_{\frac{1}{2}}{}^{-}$	$N^{8}_{\frac{1}{2}}\bar{\Delta}^{8}_{\frac{1}{2}}{}^{+}$	$N^{1}_{\frac{1}{2}}\bar{N}^{1}_{\frac{1}{2}}$	$N^{8}_{\frac{1}{2}}\bar{N}^{8}_{\frac{1}{2}}$	$\Delta^{1}_{\frac{3}{2}}\bar{\Delta}^{1}_{\frac{3}{2}}$	$N^{8}_{\frac{3}{2}}\bar{N}^{8}_{\frac{3}{2}}$
$I=2$	$\Delta^{8}_{\frac{1}{2}}\bar{\Delta}^{8}_{\frac{1}{2}}$	$\Delta^{8}_{\frac{1}{2}}\bar{N}^{8}_{\frac{1}{2}}{}^{-}$	$N^{8}_{\frac{1}{2}}\bar{\Delta}^{8}_{\frac{1}{2}}{}^{+}$	$\Delta^{1}_{\frac{3}{2}}\bar{\Delta}^{1}_{\frac{3}{2}}$				
$I=3$	$\Delta^{8}_{\frac{1}{2}}\bar{\Delta}^{8}_{\frac{1}{2}}$	$\Delta^{1}_{\frac{3}{2}}\bar{\Delta}^{1}_{\frac{3}{2}}$						

(3.33)

For $J = 1$ the following states are possible

$I = 0$	$N^{10}_{\frac{1}{2}}\bar{N}^{10}_{\frac{1}{2}}$	$\Delta^{8}_{\frac{1}{2}}\bar{\Delta}^{8}_{\frac{1}{2}}$	$N^{1}_{\frac{1}{2}}\bar{N}^{1}_{\frac{1}{2}}$	$N^{8}_{\frac{1}{2}}\bar{N}^{8}_{\frac{1}{2}}$
	$N^{8}_{\frac{1}{2}}\bar{N}^{8}_{\frac{3}{2}}$	$\Delta^{1}_{\frac{3}{2}}\bar{\Delta}^{1}_{\frac{3}{2}}$	$N^{8}_{\frac{3}{2}}\bar{N}^{8}_{\frac{1}{2}}$	$N^{8}_{\frac{3}{2}}\bar{N}^{8}_{\frac{3}{2}}$
$I = 1$	$N^{10}_{\frac{1}{2}}\bar{N}^{10}_{\frac{1}{2}}$	$\Delta^{8}_{\frac{1}{2}}\bar{\Delta}^{8}_{\frac{1}{2}}$	$\Delta^{8}_{\frac{1}{2}}\bar{N}^{8}_{\frac{1}{2}}$ -	$\Delta^{8}_{\frac{1}{2}}\bar{N}^{8}_{\frac{3}{2}}$ -
	$N^{8}_{\frac{1}{2}}\bar{\Delta}^{8}_{\frac{1}{2}}$ +	$N^{1}_{\frac{1}{2}}\bar{N}^{1}_{\frac{1}{2}}$	$N^{8}_{\frac{1}{2}}\bar{N}^{8}_{\frac{1}{2}}$	$N^{1}_{\frac{1}{2}}\bar{\Delta}^{1}_{\frac{3}{2}}$ +
	$N^{8}_{\frac{1}{2}}\bar{N}^{8}_{\frac{3}{2}}$	$\Delta^{1}_{\frac{3}{2}}\bar{N}^{1}_{\frac{1}{2}}$ -	$\Delta^{1}_{\frac{3}{2}}\bar{\Delta}^{1}_{\frac{3}{2}}$	$N^{8}_{\frac{3}{2}}\bar{\Delta}^{8}_{\frac{1}{2}}$ -
	$N^{8}_{\frac{3}{2}}\bar{N}^{8}_{\frac{1}{2}}$	$N^{8}_{\frac{3}{2}}\bar{N}^{8}_{\frac{3}{2}}$		
$I = 2$	$\Delta^{8}_{\frac{1}{2}}\bar{\Delta}^{8}_{\frac{1}{2}}$	$\Delta^{8}_{\frac{1}{2}}\bar{N}^{8}_{\frac{1}{2}}$ +	$\Delta^{8}_{\frac{1}{2}}\bar{N}^{8}_{\frac{3}{2}}$ -	$N^{8}_{\frac{1}{2}}\bar{\Delta}^{8}_{\frac{1}{2}}$ -
	$N^{1}_{\frac{1}{2}}\bar{\Delta}^{1}_{\frac{3}{2}}$ +	$\Delta^{1}_{\frac{3}{2}}\bar{N}^{1}_{\frac{1}{2}}$ -	$\Delta^{1}_{\frac{3}{2}}\bar{\Delta}^{1}_{\frac{3}{2}}$	$N^{8}_{\frac{3}{2}}\bar{\Delta}^{8}_{\frac{1}{2}}$ +
$I = 3$	$\Delta^{8}_{\frac{1}{2}}\bar{\Delta}^{8}_{\frac{1}{2}}$	$\Delta^{1}_{\frac{3}{2}}\bar{\Delta}^{1}_{\frac{3}{2}}$		

(3.34)

For $J = 2$ the states are

$I = 0$	$N^{8}_{\frac{1}{2}}\bar{N}^{8}_{\frac{3}{2}}$	$\Delta^{1}_{\frac{3}{2}}\bar{\Delta}^{1}_{\frac{3}{2}}$	$N^{8}_{\frac{3}{2}}\bar{N}^{8}_{\frac{1}{2}}$	$N^{8}_{\frac{3}{2}}\bar{N}^{8}_{\frac{3}{2}}$				
$I = 1$	$\Delta^{8}_{\frac{1}{2}}\bar{N}^{8}_{\frac{3}{2}}$ -	$N^{1}_{\frac{1}{2}}\bar{\Delta}^{1}_{\frac{3}{2}}$ +	$N^{8}_{\frac{1}{2}}\bar{N}^{8}_{\frac{3}{2}}$	$\Delta^{1}_{\frac{3}{2}}\bar{N}^{1}_{\frac{1}{2}}$ -	$\Delta^{1}_{\frac{3}{2}}\bar{\Delta}^{1}_{\frac{3}{2}}$	$N^{8}_{\frac{3}{2}}\bar{\Delta}^{8}_{\frac{1}{2}}$ +	$N^{8}_{\frac{3}{2}}\bar{N}^{8}_{\frac{1}{2}}$	$N^{8}_{\frac{3}{2}}\bar{N}^{8}_{\frac{3}{2}}$
$I = 2$	$\Delta^{8}_{\frac{1}{2}}\bar{N}^{8}_{\frac{3}{2}}$ -	$N^{1}_{\frac{1}{2}}\bar{\Delta}^{1}_{\frac{3}{2}}$ +	$\Delta^{1}_{\frac{3}{2}}\bar{N}^{1}_{\frac{1}{2}}$ -	$\Delta^{1}_{\frac{3}{2}}\bar{\Delta}^{1}_{\frac{3}{2}}$	$N^{8}_{\frac{3}{2}}\bar{\Delta}^{8}_{\frac{1}{2}}$ +			
$I = 3$	$\Delta^{1}_{\frac{3}{2}}\bar{\Delta}^{1}_{\frac{3}{2}}$							

and for $J = 3$ the states are

$I = 0$	$\Delta^{1}_{\frac{3}{2}}\bar{\Delta}^{1}_{\frac{3}{2}}$	$N^{8}_{\frac{3}{2}}\bar{N}^{8}_{\frac{3}{2}}$
$I = 1$	$\Delta^{1}_{\frac{3}{2}}\bar{\Delta}^{1}_{\frac{3}{2}}$	$N^{8}_{\frac{3}{2}}\bar{N}^{8}_{\frac{3}{2}}$
$I = 2$	$\Delta^{1}_{\frac{3}{2}}\bar{\Delta}^{1}_{\frac{3}{2}}$	
$I = 3$	$\Delta^{1}_{\frac{3}{2}}\bar{\Delta}^{1}_{\frac{3}{2}}$	

(3.35) .

where the label " $\pm$ " refers to a state $|ab\rangle = 1/\sqrt{2}\,(|ab\rangle \pm |ba\rangle)$.

There are 76 states listed in the tables above. It is not worthwhile to list all the states $(q^2\bar{q}^2)(q\bar{q})$ because they can be easily obtained by considering their colour, spin and isospin in a identical manner as for the $(q^3)(\bar{q}^3)$ states.

The relationship between the two bases yields a large matrix, and its elements represent the coefficients of fractional parentage. Some elements in the $(q^3)(\bar{q}^3)$ base transform to the $(q^2\bar{q}^2)(q\bar{q})$ base in up to 92 elements, a fact that makes difficult to reproduce here all the coefficients. In Appendix C two examples are presented in

detail. Using the rules determined in this chapter for colour (eqs. 2.17-2.19), spin (eqs. B.20-24) and isospin (eqs. B.20-24), these coefficients of fractional parentage are calculated numerically.

Chapter 4

Results for $q^3\bar{q}^3$ states for massless quarks

In this chapter we discuss the $q^3\bar{q}^3$ mass spectrum for massless up and down quarks. For completeness the $q^2\bar{q}^2$ mass spectrum which has been obtained in earlier calculations [16] is included. The M.I.T. mass formula is introduced. We calculate the wave function for all the states of various quantum numbers. Then the mass spectrum is calculated based on various two-particle interaction operators. Using the $(q^3)(\bar{q}^3)$ base, the one-gluon exchange interaction is obtained, while the overcomplete $(q^2\bar{q}^2)(q\bar{q})$ base is used to evaluate the one-gluon annihilation interaction. These interactions, together with the coefficients of fractional parentage make the calculation of the energy of the non-interacting system possible. The energy of the real system is obtained by diagonalizing the Hamilton matrix. Finally we plot the mass spectrum.

4.1 The M.I.T. Mass Formula

We denote a multiquark-antiquark state by $q^N\bar{q}^N$. The effective Hamiltonian operator of the interacting system in a cavity is

$$\mathcal{H} = \mathcal{H}^0 + \mathcal{V}^{qq} + \mathcal{V}^{q\bar{q}}, \tag{4.1}$$

where the first term in the right hand side is the non-interacting Hamiltonian, $\mathcal{V}^{qq}$ represents the quark-quark (or antiquark-antiquark) interaction and $\mathcal{V}^{q\bar{q}}$ represents the quark-antiquark interaction. When $\mathcal{H}^0$ acts on a non-interacting state $|\phi_A\rangle$, its

eigenvalue is $N\frac{\omega}{R}$, where ω is the non-interacting quark energy in dimensionless units (see Appendix B). The lower index "A"of the wave function, denotes any state. Later, two different states will be involved in calculation and for the second state, the lower index "B" is used. To order α_S one would have to consider the quark self-energy [25], [26], [27], [8], [28] as well, but for the purpose of this calculation, this term is ignored. The self-energy will be introduced later when the complete spectrum is calculated.

A general state can be written in terms of the $(q^N)(\bar{q}^N)$ base as a linear combination

$$|\phi_A\rangle = \sum_{\substack{K_a,k_a \\ K_{\bar{a}},k_{\bar{a}}}} \langle K_a, k_a K_{\bar{a}}, k_{\bar{a}} \,|K_A, k_A\rangle \,|\phi_a\rangle \,|\phi_{\bar{a}}\rangle \tag{4.2}$$

or in terms of the $(q\bar{q})^{N-1}(q\bar{q})$ base as

$$|\phi_A\rangle = \sum_{\substack{K_{b^*},k_{b^*} \\ K_b,k_b}} \langle K_{b^*}, k_{b^*} K_b, k_b \,|K_A, k_A\rangle \, C_{b^*b} \,|\phi_{b^*}\rangle \,|\phi_b\rangle \,, \tag{4.3}$$

where C_{b^*b} are the coefficients of fractional parentage introduced in Chapter 3. The following notation has been used for different states

$$a \equiv q^N; \bar{a} \equiv \bar{q}^N; b \equiv q\bar{q} \text{ and } b^* \equiv (q\bar{q})^{N-1} \,. \tag{4.4}$$

The elements of $\mathcal{H}$ can be now expressed as

$$\langle\phi_A|\,\mathcal{H}\,|\phi_B\rangle = N\frac{\omega}{R}\delta_{AB} + V^{qq}_{AA}\cdot\delta_{AB} + V^{q\bar{q}}_{AB}, \tag{4.5}$$

where $\mathcal{H}^0$ and $\mathcal{V}^{qq}$ are diagonal in the $(q^N)(\bar{q}^N)$ base (eq. (4.2))

$$V^{qq}_{AA} = \langle\phi_A|\,\mathcal{V}^{qq}\,|\phi_A\rangle = \sum_{a\bar{a}} \langle\phi_a\phi_{\bar{a}}|\,\mathcal{V}^{qq}\,|\phi_a\phi_{\bar{a}}\rangle \,. \tag{4.6}$$

The $\mathcal{V}^{q\bar{q}}$ interaction matrix is not diagonal, but it can be calculated easily by using the $(q\bar{q})^{N-1}(q\bar{q})$ base (eq. (4.3))

$$V^{q\bar{q}}_{AB} = \langle\phi_A|\,\mathcal{V}^{q\bar{q}}\,|\phi_B\rangle = \sum_{b^*b} \langle\phi_{b^*}\phi_b|\,\mathcal{V}^{q\bar{q}}\,|\phi_{b^*}\phi_b\rangle \,. \tag{4.7}$$

The two bases used to express the Hamiltonian are non-interacting bases. The aim of these calculation is to evaluate the energy of the interacting system in terms of the energy of the particles involved (ω) and the dimensionless interaction operator (Δ_{12},

eq.(2.56)). This is achieved by diagonalizing the Hamiltonian (eq.(4.5)). The result is

$$E_A = \frac{N \cdot \omega}{R} + \frac{\alpha_S}{R}\Delta_{12}. \tag{4.8}$$

Here we have assumed a fixed cavity by taking into account the linear boundary condition of the M.I.T. bag model only. However, considering the quadratic boundary condition, the particles in the cavity will exert a pressure on the surface which must be matched by the exterior pressure B [6] of the nonperturbative vacuum. By introducing the new parameter B, the radii of all hadron bags can be calculated. This pressure contributes to the total energy with a volume energy $\frac{4\pi}{3}R^3B$.

The total energy in the M.I.T. bag model should be corrected with the zero point energy E_0

$$E_0 = -\frac{Z}{R}, \tag{4.9}$$

which scales the mass and radius for mesons and baryons. Physically, the term describes the C.M. motion and the Casimir effect [29] due to the fields.

With all these corrections, the total energy in the cavity is

$$E_A(R) = \frac{4\pi}{3}R^3B + \frac{N \cdot \omega}{R} + -\frac{Z}{R} + \frac{\alpha_S}{R}\Delta_{12}. \tag{4.10}$$

The energy of the bag [6], [32], [33] given by the eq. (4.10), can be rewritten as

$$\begin{aligned} E(R) &= \frac{N\omega_q}{R} - \frac{Z_0}{R} + \frac{\alpha_S\Delta}{R} + \frac{4\pi}{3}R^3B \\ &= \frac{A}{R} + \frac{4\pi}{3}R^3B \\ \text{with } A &= N\omega_q - Z_0 + \alpha_S\Delta. \end{aligned} \tag{4.11}$$

The last term containing the bag pressure B, ensures that at the surface of the bag there is a balance between the spherical internal quark pressure and external vacuum pressure. The balance of the pressures at the surface of the bag is equivalent to the fact that an infinitesimal displacement of the of the surface requires no energy. Translated into mathematics, the condition is

$$\frac{\partial E}{\partial R} = 0 \tag{4.12}$$

from which we obtain

$$-\frac{A}{R_0^2} + 4\pi R_0^2 B = 0, \tag{4.13}$$

if the masses of the up and down quarks are taken to be zero. For the case of massive quarks the method has to be changed (see Chapter 6). Using eq. (4.13), the radius of the bag is $R_0 = \frac{A^{1/4}}{(4\pi B)^{1/4}}$. The mass thus takes the form

$$M = E(R_0) = \frac{4}{3}(4\pi B)^{1/4}(N\omega_q - Z_0 + \alpha_S\Delta)^{3/4}. \tag{4.14}$$

Making use of the mass of a few well-known states (the nucleon, the delta and the rho), the three parameters B, Z_0 and α_S are determined. The set used in this work to calculate the mass spectrum when $m_q = 0$ is [34]

$$\alpha_S = 2.2, \qquad B^{1/4} = 146MeV, \qquad Z_0 = 1.84. \tag{4.15}$$

Having calculated the single particle energy ω_q within the M.I.T. bag model, the parameters of the model and the energy interaction Δ (eq. (2.57)), the mass spectrum can be now easily evaluated.

4.2 The $q^3\bar{q}^3$ Wave Function

Due to the fact that the wave function for the $q^3\bar{q}^3$ system is quite complicated, we present here only one example of how the wave function has been constructed. For the other states, the wave function is calculated in a similar manner.

The state with the quantum numbers singlet colour representation $\{1\}$, total spin $J = 0$ and total isospin $I = 3$ is taken as an example. The state is obtained from the combination of three quarks in the state $\Delta^1_{3/2}$ and three antiquarks in the state $\bar{\Delta}^1_{3/2}$ (3.33).

4.2.1 Colour Wave Function

In terms of colour, both the q^3 and $\bar{q}^3$ systems are in the colour singlet representation $\{1\}$. The wave function for the three quarks system is presented in Appendix A. The same wave function is valid for the three antiquark system if the indices are flipped around. Combining the two expressions, 36 different terms emerge

$$\begin{aligned} |colour\ \{1\}\rangle \;=\; & \frac{1}{6} rgb\bar{r}\bar{g}\bar{b} - rgb\bar{r}\bar{b}\bar{g} - rgb\bar{g}\bar{r}\bar{b} + rgb\bar{g}\bar{b}\bar{r} + rgb\bar{b}\bar{r}\bar{g} - rgb\bar{b}\bar{g}\bar{r} \\ & -rbg\bar{r}\bar{g}\bar{b} + rbg\bar{r}\bar{b}\bar{g} + rbg\bar{g}\bar{r}\bar{b} - rbg\bar{g}\bar{b}\bar{r} - rbg\bar{b}\bar{r}\bar{g} + rbg\bar{b}\bar{g}\bar{r} \end{aligned}$$

$$
\begin{aligned}
&-grb\bar{r}\bar{g}\bar{b} + grb\bar{r}\bar{b}\bar{g} + grb\bar{g}\bar{r}\bar{b} - grb\bar{g}\bar{b}\bar{r} - grb\bar{b}\bar{r}\bar{g} + grb\bar{b}\bar{g}\bar{r} \\
&+brg\bar{r}\bar{g}\bar{b} - brg\bar{r}\bar{b}\bar{g} - brg\bar{g}\bar{r}\bar{b} + brg\bar{g}\bar{b}\bar{r} + brg\bar{b}\bar{r}\bar{g} - brg\bar{b}\bar{g}\bar{r} \\
&-bgr\bar{r}\bar{g}\bar{b} + bgr\bar{r}\bar{b}\bar{g} + bgr\bar{g}\bar{r}\bar{b} - bgr\bar{g}\bar{b}\bar{r} - bgr\bar{b}\bar{r}\bar{g} + bgr\bar{b}\bar{g}\bar{r} \\
&+gbr\bar{r}\bar{g}\bar{b} - gbr\bar{r}\bar{b}\bar{g} - gbr\bar{g}\bar{r}\bar{b} + gbr\bar{g}\bar{b}\bar{r} + gbr\bar{b}\bar{r}\bar{g} - gbr\bar{b}\bar{g}\bar{r}) \qquad (4.16)
\end{aligned}
$$

where r, g and b represent the colours red, green and blue. Note that the colour $\{1\}$ representation does not allow any two-(anti)quarks to have the same colour. However, this will be possible for the octet or decuplet representations.

4.2.2 Spin and Isospin Wave Function

The spins of the two three-particle systems are both 3/2 . Using the Clebsch-Gordan coefficients [31] to couple 3/2 with 3/2 to $|\ 0,0\rangle$, we obtain the spin wave function

$$
\begin{aligned}
|0,0\rangle \;=\; & \frac{1}{2}\,|3/2,3/2\rangle\,|3/2,-3/2\rangle - \frac{1}{2}\,|3/2,1/2\rangle\,|3/2,-1/2\rangle \\
& + \frac{1}{2}\,|3/2,-1/2\rangle\,|3/2,1/2\rangle - \frac{1}{2}\,|3/2,-3/2\rangle\,|3/2,3/2\rangle\,. \qquad (4.17)
\end{aligned}
$$

For the isospin wave function, the two systems have each $I_{1,2} = 3/2$, and they are combined to a total isospin $I = 3$. Using also the Clebsch-Gordan coefficients [31], we arrive at the total isospin wave function

$$
\begin{aligned}
|3,0\rangle \;=\; & \frac{1}{\sqrt{20}}\,|3/2,3/2\rangle\,|3/2,-3/2\rangle + \frac{3}{\sqrt{20}}\,|3/2,1/2\rangle\,|3/2,-1/2\rangle \\
& + \frac{3}{\sqrt{20}}\,|3/2,-1/2\rangle\,|3/2,1/2\rangle + \frac{1}{\sqrt{20}}\,|3/2,-3/2\rangle\,|3/2,3/2\rangle\,. \qquad (4.18)
\end{aligned}
$$

By combining the expressions (4.16), (4.17) and (4.18), we obtain the total wave function for $q^3\bar{q}^3$. For all the other combinations of colour, spin and isospin (allowed by the Pauli principle for quarks and antiquarks taken separately and requiring that the physical state does not carry colour), the path to be followed to get the total wave function is identical to the one described above.

It is worthwhile to have the wave function of any state written in the $(q^2\bar{q}^2)(q\bar{q})$ overcomplete base to study the quark-antiquark interaction. This is achieved by using the expressions (3.19), (B.23), (B.24) and (B.25) derived in the sections 3.1.4 and B.2 respectively. Using the above example with the quantum numbers $\{1\}$ for colour, 0

for spin and 3 for isospin, the transformation to the $(q^2\bar{q}^2)(q\bar{q})$ base reads

$$\begin{aligned}
|\{1\},0,3\rangle &= |\{1\},\{1\};1\rangle_{colour}\,|3/2,3/2;0\rangle_{spin}\,|3/2,3/2;3\rangle_{isospin} \qquad (4.19)\\
&= \left[\frac{1}{3}|\{1\},\{1\};1\rangle + \frac{2\sqrt{2}}{3}|\{8\},\{8\};1\rangle\right]_{colour}\\
&\quad \times \left[\frac{\sqrt{6}}{3}|0,0;0\rangle - \frac{1}{\sqrt{3}}|1,1;0\rangle\right]_{spin} |2,1;3\rangle_{isospin}\\
&= \frac{1}{3}\frac{\sqrt{6}}{3}|\{1\},0,2\rangle\,|\{1\},0,1\rangle - \frac{1}{3}\frac{1}{\sqrt{3}}|\{1\},1,2\rangle\,|\{1\},1,1\rangle\\
&\quad + \frac{2\sqrt{2}}{3}\frac{\sqrt{6}}{3}|\{8\},0,2\rangle\,|\{8\},0,1\rangle - \frac{2\sqrt{2}}{3}\frac{1}{\sqrt{3}}|\{8\},1,2\rangle\,|\{8\},1,1\rangle\,,
\end{aligned}$$

where the notations $(q^3)-(\bar{q}^3)-(q^3\bar{q}^3)$ for the first three lines and $(q^2\bar{q}^2)-(q\bar{q})-(q^3\bar{q}^3)$ for the last two lines were used. Since in this base the wave functions may contain as many as 92 components, the coefficients of fractional parentage have not been listed here. In Appendix C a detailed example is presented. The remaining coefficients are calculated in a similar way.

What it is left, is to evaluate the P, C and G parities. The P parity for three pairs of quarks is (-1) because each pair contributes with a (-1) factor and it is assumed the relative orbital angular moment is 0. The C parity for the above state is according to eq. (3.22), $(-1)^{J-J_1-J_2}(-1)^{I_1-I_2}(-1)^N = +1$ and the G parity is given by eq. (3.32) and it is -1.

With these informations, the particular state treated in the above section can be labeled as $3^-(0^{-+})$, where the standard notation [31] $I^G(J^{PC})$ has been used.

4.3 The Mass Spectrum of Exotic States for $m_q = 0$

The quarks and antiquarks are assumed to be in the lowest cavity mode $\kappa = -1$ and $\nu = 1$ (Appendix A). Using the formalism presented in Chapter 2 and 3 and Appendix A, the values of the number μ are calculated for the interaction via one-gluon exchange and via annihilation into a gluon. These values are

$$\begin{aligned}
\mu_{q\bar{q}}(0) &= 0.0098\\
\mu_{q\bar{q}}(1) &= -0.1770 \qquad (4.20)
\end{aligned}$$

for the first kind of interaction and

$$\begin{aligned} \mu_{q\bar{q}}(0) &= 0 \\ \mu_{q\bar{q}}(1) &= -0.0124 \end{aligned} \tag{4.21}$$

for the second. These results agree with those calculated by Buser *et al.* [7]. When the final results are presented, the quark self energy is added to the single particle energy. With the relations (4.20) and (4.21) the Δ operator (eq. (2.57)) is calculated. Its value is used in eq. (4.14) together with the parameters defined in eq. (4.15) and the mass spectrum is obtained.

For completeness, the spectrum of $q^2\bar{q}^2$ state is reproduced here but it was calculated previously [16]. The figure 4.1 shows the mass spectrum of the $q^2\bar{q}^2$ state.

A discussion on the exotic states will be deferred to the end of the paper because the states presented in this chapter turn out to be a particular case of the final exotic states presented in Chapter 6.

For the case of $q^3\bar{q}^3$ system, the next graphs exhibit the states with $J = 0, 1, 2$ and 3 (figures 4.2, 4.3, 4.4 and 4.5). It is expected that the lowest state for the $q^3\bar{q}^3$ exotic mesons to be the state with $J = 0$ and $I = 0$ and its mass should be approximately 1000 MeV, taking into account that the $q^3\bar{q}^3$ state can be written as a product of a $q^2\bar{q}^2$ and a $q\bar{q}$ pair. The lowest $q^3\bar{q}^3$ state with $J = I = 0$ has a mass of 700 MeV and a quark-antiquark pair has a mass of $\simeq$ 300 MeV. From our figure 4.2, we can see that the lowest exotic meson has indeed the spin and isospin zero but its mass is much higher than the estimated values. The explanation is that in reality the $q^3\bar{q}^3$ meson is predominantly a $q^2\bar{q}^2$ core with $J = I = 0$ combined with a $q\bar{q}$ pair, but rather in a linear combination of all possible states. In table 4.1 the six states with the quantum numbers of $J = I = 0$ are listed. It can be seen that in reality the combination mentioned above (with masses 700MeV and 300MeV, respectively) contributes only 5% to the total mass of the $q^3\bar{q}^3$ state. Other heavier states weight much more in the linear combination of $q^3\bar{q}^3$ state and therefore determine the increase in mass of the lowest state.

$N^{10}_{1/2}\overline{N}^{10}_{1/2}$	$\Delta^{10}_{1/2}\overline{\Delta}^{0}_{1/2}$	$N^{1}_{1/2}\overline{N}^{1}_{1/2}$	$N^{8}_{1/2}\overline{N}^{8}_{1/2}$	$\Delta^{1}_{3/2}\overline{\Delta}^{1}_{3/2}$	$N^{8}_{3/2}\overline{N}^{8}_{3/2}$	C	J	I	J	I	C	J	I	C	J	I
0.0000	0.0000	-0.2121	-0.1442	0.0000	0.0000	1	0	0	0	0	3	0	0	3	0	0
0.0000	0.0000	-0.4360	0.1919	0.0000	0.0000	8	0	0	0	0	3	0	0	3	0	0
0.0000	0.0000	-0.1090	0.2327	0.0000	0.0000	1	1	1	1	1	3	0	0	3	1	1
0.0000	0.0000	-0.4725	0.0587	0.0000	0.0000	8	1	1	1	1	3	0	0	3	1	1
0.0000	0.0000	-0.0547	-0.1999	0.0000	0.0000	8	0	1	0	1	3	0	0	6	0	1
0.0000	0.0000	-0.0547	-0.1999	0.0000	0.0000	8	1	0	1	0	3	0	0	6	1	0
0.0000	0.0000	-0.2390	0.2327	0.0000	0.0000	1	1	1	1	1	3	1	1	3	0	0
0.0000	0.0000	-0.4725	0.0587	0.0000	0.0000	8	1	1	1	1	3	1	1	3	0	0
0.0000	0.0000	-0.1156	-0.1767	0.2837	-0.1633	1	0	0	0	0	3	1	1	3	1	1
0.0000	0.0000	-0.1306	-0.1921	-0.2505	-0.1930	1	0	1	0	1	3	1	1	3	1	1
0.0000	-0.3435	-0.0846	-0.0179	0.0567	0.1926	1	1	0	1	0	3	1	1	3	1	1
0.0000	0.2501	-0.1083	0.0210	-0.4865	0.2694	1	1	1	1	1	3	1	1	3	1	1
0.0000	0.4211	-0.1543	0.0849	0.4728	0.0196	8	0	0	0	0	3	1	1	3	1	1
0.0000	-0.3031	-0.1772	0.1519	-0.3265	0.0978	8	0	1	0	1	3	1	1	3	1	1
0.0000	-0.1657	-0.1935	0.0902	-0.4351	-0.0388	8	1	0	1	0	3	1	1	3	1	1
0.0000	0.1118	-0.3148	0.0743	0.2994	-0.1128	8	1	1	1	1	3	1	1	3	1	1
0.0000	0.3401	0.0000	-0.0800	0.0000	0.0000	8	1	0	1	0	3	1	1	6	0	1
0.0000	-0.2273	0.0000	-0.1883	0.0000	0.0000	8	1	1	1	1	3	1	1	6	0	1
0.0000	0.0000	0.0000	0.0712	0.0000	0.4198	8	0	1	0	1	3	1	1	6	1	0
0.0000	0.0000	0.0000	-0.2952	0.0000	-0.1364	8	1	1	1	1	3	1	1	6	1	0
0.0000	0.0000	0.0000	-0.1999	0.0000	0.0000	8	0	1	0	1	6	0	1	3	0	0
0.0000	0.3481	0.0000	-0.0800	0.0000	0.0000	8	1	0	1	0	6	0	1	3	1	1
0.0000	-0.2273	0.0000	-0.1883	0.0000	0.0000	8	1	1	1	1	6	0	1	3	1	1
-0.1901	0.2532	0.0000	0.0608	0.0000	0.0000	8	0	0	0	0	6	0	1	6	0	1
-0.2971	-0.1699	0.0000	0.0299	0.0000	0.0000	8	0	1	0	1	6	0	1	6	0	1
-0.1991	-0.2085	0.0000	-0.1583	0.0000	0.0000	1	0	0	0	0	6	0	1	6	0	1
-0.2562	0.1775	0.0000	-0.1737	0.0000	0.0000	1	0	1	0	1	6	0	1	6	0	1
-0.2830	0.0000	0.0000	-0.2384	0.0000	0.0000	8	1	1	1	1	6	0	1	6	1	0
-0.3861	0.0000	0.0000	0.0333	0.0000	0.0000	1	1	1	1	1	6	0	1	6	1	0
0.0000	0.0000	0.0000	-0.1999	0.0000	0.0000	8	1	0	1	0	6	1	0	3	0	0
0.0000	0.0000	0.0000	0.0712	0.0000	0.4198	8	0	1	0	1	6	1	0	3	1	1
0.0000	0.0000	0.0000	-0.2952	0.0000	-0.2464	8	1	1	1	1	6	1	0	3	1	1
-0.2830	0.0000	0.0000	-0.2384	0.0000	0.0000	8	1	1	1	1	6	1	0	6	0	1
-0.4671	0.0000	0.0000	0.0333	0.0000	0.0000	1	1	1	1	1	6	1	0	6	0	1
-0.2750	0.0000	0.0000	0.1735	0.0000	0.0180	8	0	0	0	0	6	1	0	6	1	0
-0.2370	0.0000	0.0000	-0.0498	0.0000	-0.2896	8	1	0	1	0	6	1	0	6	1	0
-0.1231	0.0000	0.0000	-0.2591	0.0000	-0.2015	1	0	0	0	0	6	1	0	6	1	0
-0.3099	0.0000	0.0000	-0.1024	0.0000	0.4617	1	1	0	1	0	6	1	0	6	1	0

Table 4.1 The linear combinations of $q^2\bar{q}^2$ and $q\bar{q}$ states that make up the $q^3\bar{q}^3$ state for $J = I = 0$. The first six columns indicate the coefficients of the $(q^2\bar{q}^2)(q\bar{q})$ combinations and the next columns indicate the colour, spin and isospin of the $q^2\bar{q}^2$, $q\bar{q}$, q^2 and $\bar{q}^2$ states in this order.

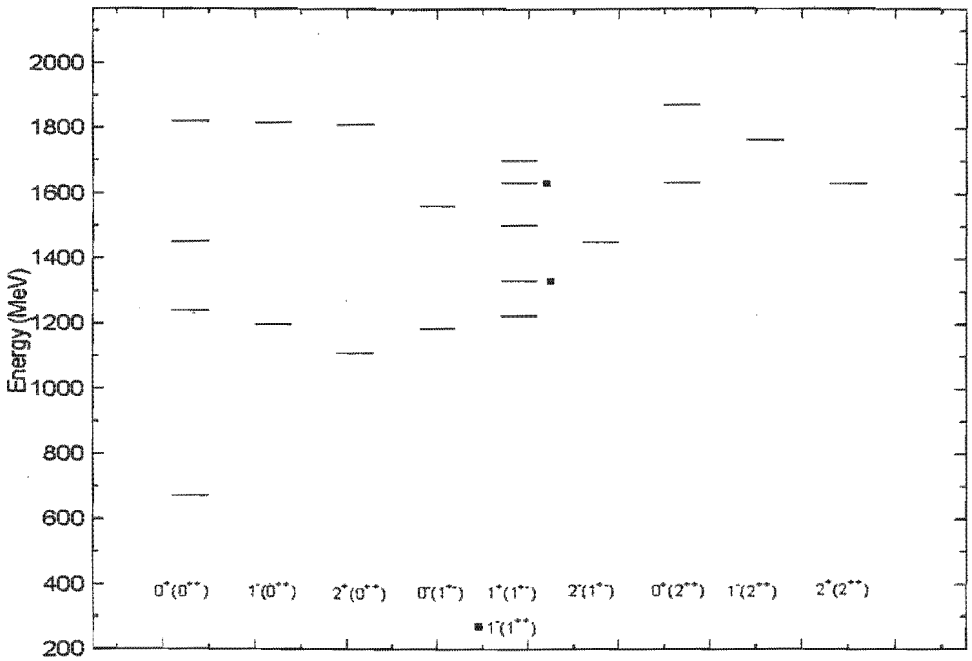

Figure 4.1: The mass spectrum for $q^2\bar{q}^2$ states with $m_q = 0$. The notation is $I^G(J^{PC})$.

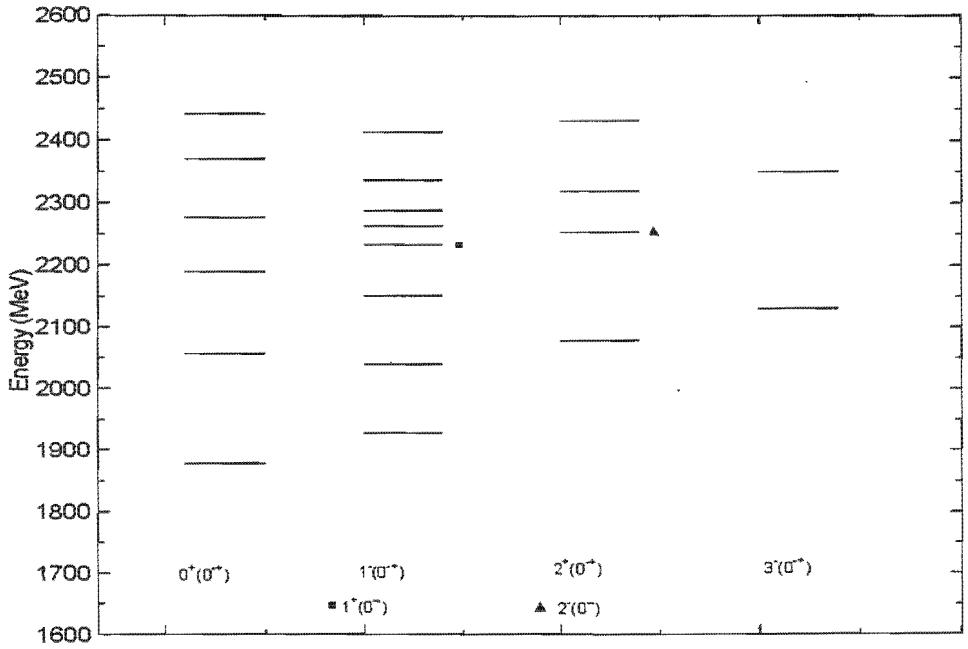

Figure 4.2: The mass spectrum of $q^3\bar{q}^3$ states with $m_q = 0$ for $J = 0$ and $I = 0, 1, 2, 3$.

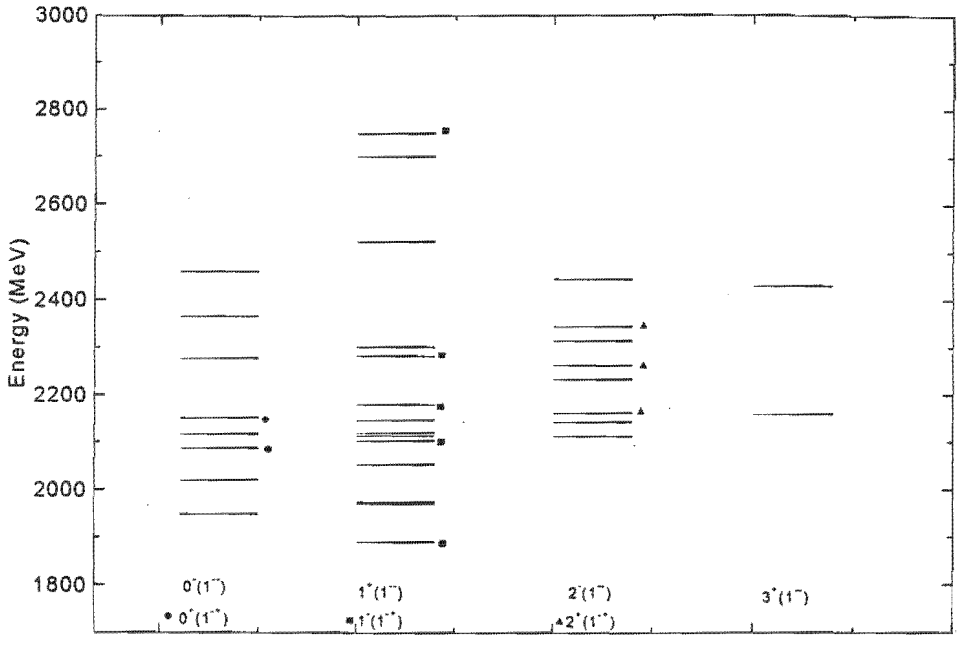

Figure 4.3: Mass spectrum of $q^3\bar{q}^3$ states with $m_q = 0$ for $J = 1$ and $I = 0, 1, 2, 3$.

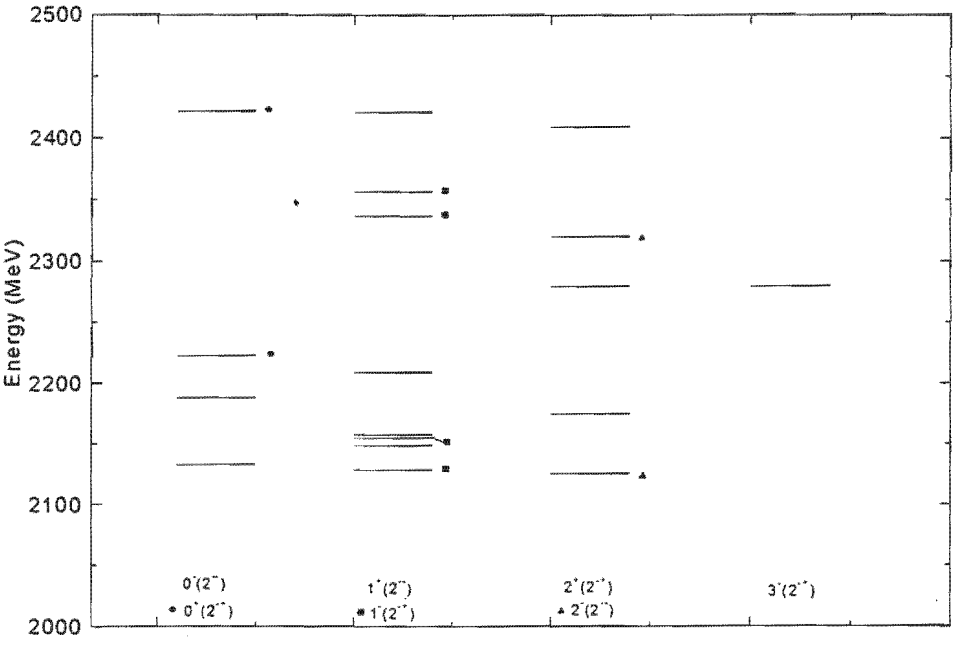

Figure 4.4: Mass spectrum of $q^3\bar{q}^3$ states with $m_q = 0$ for $J = 2$ and $I = 0, 1, 2, 3$.

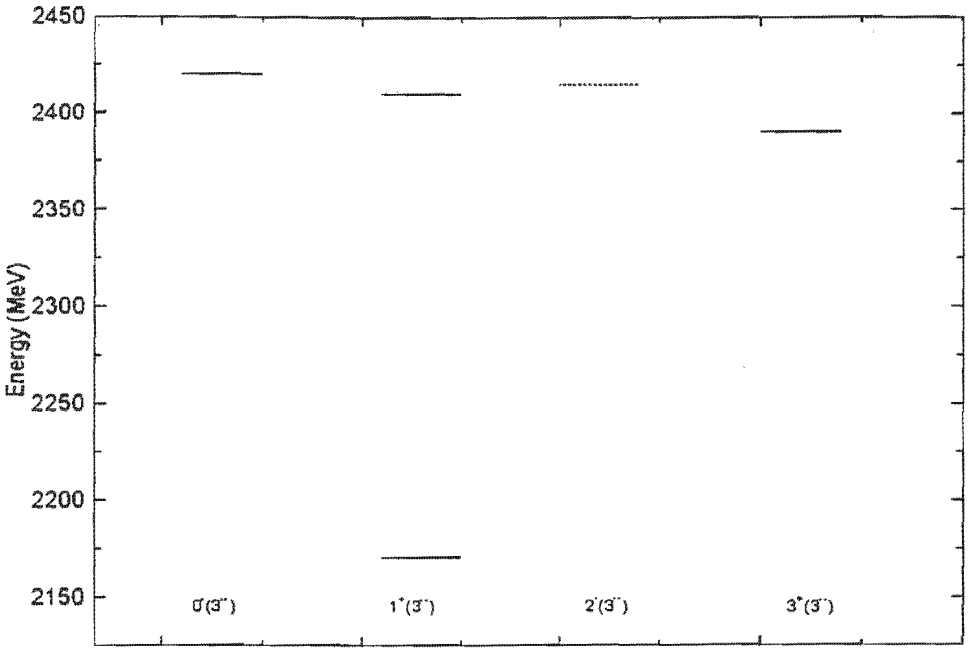

Figure 4.5: Mass spectrum of $q^3\bar{q}^3$ states with $m_q = 0$ for $J = 3$ and $I = 0, 1, 2, 3$.

Chapter 5

The Boundary Condition

The linear boundary condition for the quark fields has been introduced originally in the M.I.T. bag model, in order to confine the quarks in the interior of the cavity [6]. It is worth mentioning that this boundary condition is by no means the only one which is confining the quarks and is at the same time compatible with the field equations. In this chapter we will investigate another linear boundary condition for the quark fields which was considered long time ago by the creators of the M.I.T. bag model [6]. It was recently re-examined by Lindebaum [28], who showed that imposing this new boundary condition, is equivalent to introducing quarks with negative mass in the cavity. By varying the mass from positive to negative values, we obtain results that interpolate smoothly between the M.I.T. and the S.L.A.C. bag boundary conditions.

5.1 The New Boundary Condition

The standard boundary condition that was chosen for the M.I.T. bag model is

$$(in_\mu \gamma^\mu + 1)\, \psi(r)|_{surface} = 0, \tag{5.1}$$

where n_μ is a four-vector perpendicular to the surface of the cavity pointing outwards and obeying the normalization condition $n_\mu n^\mu = 1$. An equally acceptable linear boundary condition would be

$$(-in_\mu \gamma^\mu + 1)\, \psi(r)|_{surface} = 0, \tag{5.2}$$

the only difference to the standard boundary condition being the minus sign in front of the four-vector normal to the boundary.

Both boundary conditions are consistent with the field equations and confining the quarks. Confinement of the quarks requires that the current $j^\mu = \bar{\psi}\gamma^\mu\psi$ vanishes at the surface of the cavity, i.e.

$$n_\mu j^\mu|_{surface} = 0. \tag{5.3}$$

Multiplying eq. (5.2) with $\bar{\psi}$ to the left, taking the adjoint equation of (5.2) i.e.

$$\bar{\psi}(r)\,(in_\mu\gamma^\mu + 1)|_{surface} = 0 \tag{5.4}$$

and multiplying it with ψ from the right yields

$$-i\bar{\psi}\psi\Big|_{surface} = n_\mu\bar{\psi}\gamma^\mu\psi = i\bar{\psi}\psi\Big|_{surface}. \tag{5.5}$$

The fact that both equations (5.2) and (5.4) have a common term $in_\mu\gamma^\mu$ has been used to get condition (5.5). The scalar density thus vanishes at the surface

$$n_\mu\bar{\psi}\gamma^\mu\psi = \bar{\psi}\psi\Big|_{surface} = 0. \tag{5.6}$$

Therefore the new linear boundary condition takes care of the quark confinement and has many of the properties of the standard boundary condition.

It is necessary now to study how the quark field is behaving with the new boundary condition. Consider a field ϕ, a new letter is used for this field (ψ describes a quark under the standard boundary condition) which obeys the Dirac equation and the new boundary equation simultaneously

$$(i\gamma^\mu\partial_\mu - m)\,\phi(r) = 0 \tag{5.7}$$

$$(-in_\mu\gamma^\mu + 1)\,\phi(r)|_{surface} = 0. \tag{5.8}$$

Multiplying the two equations from the left by γ^5 and commuting the γ^5 to the right, the former boundary condition of the M.I.T. bag model is recovered

$$(i\gamma^\mu\partial_\mu + m)\,\gamma^5\phi(r) = 0 \tag{5.9}$$

$$(in_\mu\gamma^\mu + 1)\,\gamma^5\,\phi(r)|_{surface} = 0, \tag{5.10}$$

but the field that obeys these equations is now $\psi = \gamma^5\phi$. What it is more interesting, the Dirac equation has now a negative mass term.

A short discussion is necessary at this stage to try to clarify the meaning and implications of the Dirac equation with a negative mass term. It has been shown that a field that obeys the Dirac equation and the new boundary condition behaves identical to a field which obeys Dirac equation with a negative mass term and the standard boundary condition. This means that we can recalculate all the physical quantities for the new boundary condition by only replacing the quark mass m with $-m$ and using the standard boundary condition.

The quark field ψ which corresponds to the negative mass term has the upper and lower components flipped relative to those of ϕ. This means that, in order to keep the same meaning for the κ quantum number for the ψ field, it is necessary to use the substitution $\kappa \rightarrow -\kappa$. Thus the fundamental state $\kappa = -1$ which was used for the ϕ field becomes $\kappa = +1$ for the ψ field.

Another observation is that for the free space, the sign of the mass in the Dirac equation is meaningless, as it can be rotated away with a γ^5 transformation which flips the upper and lower components of the Dirac spinor. In the cavity the sign of the mass must always be seen in conjuction with the boundary condition.

5.2 The Cavity Modes with New Boundary Condition

In this section, the quark cavity modes and the renormalization constants are recalculated for the new boundary condition [28]. The gluon cavity modes are not recalculated here as they do not affect our calculations. A solution of equation (A.1) was calculated in Appendix A, eq.(A.2), with the upper and lower components given by the spherical Bessels functions (eq.(A.3) and eq.(A.4)). Instead of using the standard boundary condition eq. (A.8), we impose the new boundary on the quark field

$$(-in_\mu\gamma^\mu + 1)\,\phi(r)|_{surface} = 0$$

so that the eq. (A.9) reads now

$$j_l(x_n) - \frac{x_n \mathrm{sgn}\kappa}{\omega_n + \zeta_f} j_{\bar{l}}(x_n) = 0, \tag{5.11}$$

where the notation is that used in Appendix A, (eqs. (A.10)-(A.12)). The only difference is the "minus" sign between the two terms. As a consequence of the new boundary condition, the normalization constant $\mathcal{N}_n$ (eq. (A.15)) is given by the expression

$$\mathcal{N}_n^2 = \frac{1}{2\omega_n(\omega_n + \kappa) - |\zeta_f|} \left(\frac{x_n}{j_l(x_n)} \right)^2. \tag{5.12}$$

The absolute value of the mass ensures that the expression is also valid if one uses the negative mass interpretation.

As discussed in the previous section, the fundamental mode is obtained for $\kappa = +1$ instead of -1 as for the usual M.I.T. bag model. Using in eq. (5.11) the value $+1$ for the Dirac quantum number, the eigenvalue equation becomes

$$j_1(p_n R) - \frac{p_n R}{\varepsilon_n R + |m|} j_0(p_n R) = 0, \tag{5.13}$$

where again, the absolute value of the mass is used to accommodate the negative mass interpretation.

If one tries to solve this equation, it turns out that there are only real solutions for p_n when $|m| < 1.5$. For $|m| > 1.5$ only purely imaginary solutions exist for p_n. Imaginary values for momentum are not unusual in quantum mechanics. The best known example is the tunnel effect, where there are no classical solutions, but quantum mechanics provides a solution with an imaginary momentum.

As it is not pleasant to work with an imaginary momentum, the momentum is made real by redefining it. To redefine the momentum it is necessary to look at the Dirac equation, more specifically to its radial part. The equation can be written as a system of two equations where each component of the Dirac spinor eq. (A.2) satisfies one of the equations. For the upper component one gets

$$\frac{d^2}{dr^2} f(r) + \frac{2}{r} \frac{d}{dr} f(r) + \left(p^2 - \frac{\kappa(\kappa+1)}{r} \right) f(r) = 0, \tag{5.14}$$

and its solution is the Bessel function $j_l(pr)$. If a purely imaginary momentum is considered now, eq. (5.14) still holds but it can be rewritten taking into account the

complex nature of the momentum as

$$\frac{d^2}{dr^2}f(r)+\frac{2}{r}\frac{d}{dr}f(r)+\left(-p^2-\frac{\kappa(\kappa+1)}{r}\right)f(r)=0. \tag{5.15}$$

Note that p is now real. The solution of the new equation [35] is given by the modified Bessel function $k_j(pr)$. The modified Bessel function can be expressed in terms of the original Bessel function as

$$k_j(pr)=i^{-l}j_l(pr). \tag{5.16}$$

Because of the complex nature of the momentum, the energy-mass relation should be rewritten as $\varepsilon^2=-p^2+m^2$.

Finally, the normalization constant is recalculated for the complex momentum by using its definition given in eq. (A.14)

$$\mathcal{N}_n^2=\frac{1}{2\varepsilon_n(\kappa-\varepsilon_n)+|m|}\left(\frac{p_n}{j_l(p_nR)}\right)^2. \tag{5.17}$$

To summarize this section, the boundary conditions and the normalization constants are listed below for three regions and a figure 5.1 of the one particle energy and momentum is plotted for m_q in the range $[-10,10]$, expressed in natural units defined in Appendix D.

The three regions presented in table 5.1 are

region	I	II	III
mass	-10 to -1.5	-1.50 to 0	0 to 10
momentum	imaginary	real	real
energy	$\varepsilon^2=-p^2+m^2$	$\varepsilon^2=p^2+m^2$	$\varepsilon^2=p^2+m^2$
κ	$+1$	$+1$	-1

Table 5.1. The one particle mass, momentum and energy in the range $[-10,10]$.

Their boundary conditions and normalization constants are given in Table 5.2.

region	bound. cond. & norm. const.
I	$k_1(p_nR) - \frac{p_nR}{\varepsilon_nR+\lvert m\rvert} k_0(p_nR) = 0$
	$\mathcal{N}_n^2 = \frac{1}{2\varepsilon_n(\kappa-\varepsilon_n)+\lvert m\rvert}\left(\frac{p_n}{k_1(p_nR)}\right)^2$
II	$j_1(p_nR) - \frac{p_nR}{\varepsilon_nR+\lvert m\rvert} j_0(p_nR) = 0$
	$\mathcal{N}_n^2 = \frac{1}{2\varepsilon_n(\varepsilon_n-\kappa)-\lvert m\rvert}\left(\frac{p_n}{j_1(p_nR)}\right)^2$
III	$j_0(p_nR) - \frac{p_nR}{\varepsilon_nR+\lvert m\rvert} j_1(p_nR) = 0$
	$\mathcal{N}_n^2 = \frac{1}{2\varepsilon_n(\varepsilon_n+\kappa)+m}\left(\frac{p_n}{j_0(p_nR)}\right)^2$

Table 5.2. The boundary conditions and normalizations coefficients for different regions of mass.

region	bound. cond. & norm. const.
I	$k_1(p_nR) - \frac{p_nR}{\varepsilon_nR+\lvert m\rvert} k_0(p_nR) = 0$
	$\mathcal{N}_n^2 = \frac{1}{2\varepsilon_n(\kappa-\varepsilon_n)+\lvert m\rvert}\left(\frac{p_n}{k_1(p_nR)}\right)^2$
II	$j_1(p_nR) - \frac{p_nR}{\varepsilon_nR+\lvert m\rvert} j_0(p_nR) = 0$
	$\mathcal{N}_n^2 = \frac{1}{2\varepsilon_n(\varepsilon_n-\kappa)-\lvert m\rvert}\left(\frac{p_n}{j_1(p_nR)}\right)^2$
III	$j_0(p_nR) - \frac{p_nR}{\varepsilon_nR+\lvert m\rvert} j_1(p_nR) = 0$
	$\mathcal{N}_n^2 = \frac{1}{2\varepsilon_n(\varepsilon_n+\kappa)+m}\left(\frac{p_n}{j_0(p_nR)}\right)^2$

Table 5.3. The boundary conditions and normalizations coefficients for different regions of mass.

We now plot the single particle energy and momentum for the three regions described above versus the mass of the quark. Note that, in spite of the different equations describing the momentum and energy for the three regions, the wave functions and their derivatives are continuous.

With this understanding of the negative mass of the quark, we can now plot all the characteristics of a state for m_q from $-\infty$ to $+\infty$. For $m_q \to -\infty$, the characteristics of the wave function and the one particle energy approach those of the S.L.A.C. bag model [37]. In these calculations, the mass m_q of the quark has been chosen to be within the bounds $-10 \leqslant m_q \leqslant 10$.

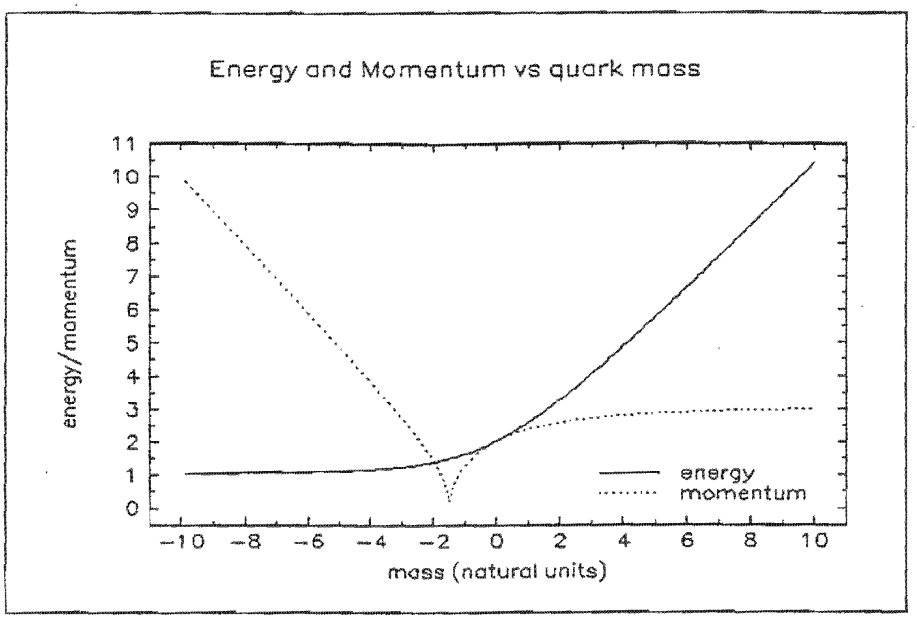

Figure 5.1: The one-particle energy and momentum of the state of lowest energy versus quark mass.

Chapter 6

Results and Discussion

The calculations presented here, produced some interesting results when the mass of the quark is allowed to vary from positive to negative values. In this chapter, the calculated mass spectra are analyzed and compared to both experimental data and theoretical results obtained using other models. A up to date discussion is presented to provide an overview of the situation in this field.

Conflicts still persist among experiments [39] performed at KEK, GAMS at CERN, VES and BNL - E852 in the search of exotic mesons. Unanswered questions remain between the accumulated experimental data and the predictions made by the theoretical models, even if the agreement between them is good in general.

This chapter is structured as follows: in the first section, our calculations are discussed. A few details involving the computer logistic are given and the tests performed to check the consistency of the calculations are presented. What is expected from the model, which are the results and what are the implications of changing the boundary condition are discussed. The second section presents the experimental facts, the possible candidates for exotic states and possible identification of our states with the experimental ones. The third section, which concludes this chapter, reviews the other theoretical models available and their predictions.

6.1 Our Calculations

A few computer codes have been used to calculate and check the coefficients of the 76 states presented in this work. As a partial test of the calculations, the orthogonality of the base $(q^3)(\bar{q}^3)$ is checked. The norm is found to be +1 for all the states. Another test for checking the correctness of the coefficients of fractional parentage, is to use the operator $\overrightarrow{\sigma}_i \cdot \overrightarrow{\sigma}_j$ (the spin-spin operator). The eigenvalues of the spin-spin operator are calculated in both bases, the $(q)^3(\bar{q})^3$ base and the $(q^2\bar{q}^2)(q\bar{q})$ base. The eigenvalues of the spin-spin operator should be the same in the two bases, if the coefficients of fractional parentage are calculated correctly. The test has been performed for each element of the base $(q)^3(\bar{q})^3$ and $(q^2\bar{q}^2)(q\bar{q})$ base and the values found were identical.

A challenge has been to recalculate the R and μ functions (defined in Appendix A and chapter 2) for the situation when m_q varies. The implication of changing m_q is that the one-particle energy ε_n for both quarks and anti-quarks is changing. Another consequence is that the normalization constant $\mathcal{N}_n$ (eq. (A.15)) is changing with the mass of the quark and had to be reevaluated. The new boundary condition also changes the value of the Dirac quantum number κ (the components of the spinor are flipped around) which is now +1 for the fundamental state. This change of κ is propagating to the orbital angular quantum numbers l and $\tilde{l}$. Even more, the complex momentum which appears in the mass range of $-10\ldots-1.5$ natural units, affects the Bessel functions by changing them into modified spherical Bessel functions (eq. (5.16)).

All these changes affect the calculation of $R's$ functions. Therefore, computer codes have been designed to tackle separately each of the three regions of $-10...10$ mass interval (table 5.1).

A few tests are employed to check the reliability of the results obtained. First, the one-particle energy and momentum of the quark were calculated and plotted against the mass and their graphs were found to be continuous (figure 5.1). Another test is to check the symmetry relation $\varepsilon_{-n} = -\varepsilon_n$ where n and $-n$ denote sets of quantum numbers defined as $n = \{f, \nu, \kappa, \mu\}$ and $-n = \{f, -\nu, -\kappa, -\mu\}$ (see Appendix A). This property is very important as it is a general symmetry relation for quarks irrespective of their quantum numbers or mass of the quark. Therefore, this symmetry relation

has been verified on each one of the three sectors.

Another indication that the calculations are reasonable is given by the plot of the radial interaction operator μ_{12} as a function of quark mass for one-gluon exchange and one-gluon annihilation with $J = 0$ and 1. The functions are continuous and their derivative are continuous too (figure 6.1) at the boundary of the sectors described in table 5.1.

The last test performed, was to compare the values for the interaction operator from figure 6.1 for $m_q = 0$ with the values already calculated by Viollier and Zimak [16]. The agreement for the case $m_q = 0$ is evident.

It is worthwhile saying that not all the polarizations of the gluons give a contribution to the two-particle interaction. The most significant case is the one-gluon annihilation with $J = 0$ where all the polarizations are prohibited to appear for the two quarks with $\kappa = -1$, and consequently this eigenvalue of the interaction operator is zero for any mass. This happens because the interaction operator (eq. (2.54)) has a built in parity selection factor (eq. (A.37)).

The connection of coefficients of fractional parentage, one-particle energy and energy shift due to two-particle interaction with the total energy of a multiparticle state is made in the framework of the M.I.T. bag model. The bag model provides an expression (eq. (4.11)) to calculate the total energy.

Few words are necessary to be said about the quark self-energy. Much effort has been put in the calculation of the quark self-energy. To order α_S, the self-energy has been calculated for $m_q = 0$ by [25], [26], [27], [8]. More recently, Lindebaum [28] has calculated the quark self-energy as a function of mass in the $\overline{MS}$ renormalization scheme. Therefore the graph of the quark self-energy (figure 6.2) is scheme dependent, but it is believed that any renormalization scheme would produce the same shape of the graph.

It was pointed out by Goldhaber *et al.* [27], that in the on-mass shell renormalization scheme, the second order corrections are larger that the first order corrections for m_q near zero. In the $\overline{MS}$ scheme this problem does not appear. It is interesting to observe that the self-energy of the quark has a maximum value around $m_q = 0$ and decreases for both $m_q \to \pm 10$. Moreover, the quark self-energy becomes negative as the mass of the quark approaches the value 2.5. Hence, the mass spectra of the exotic

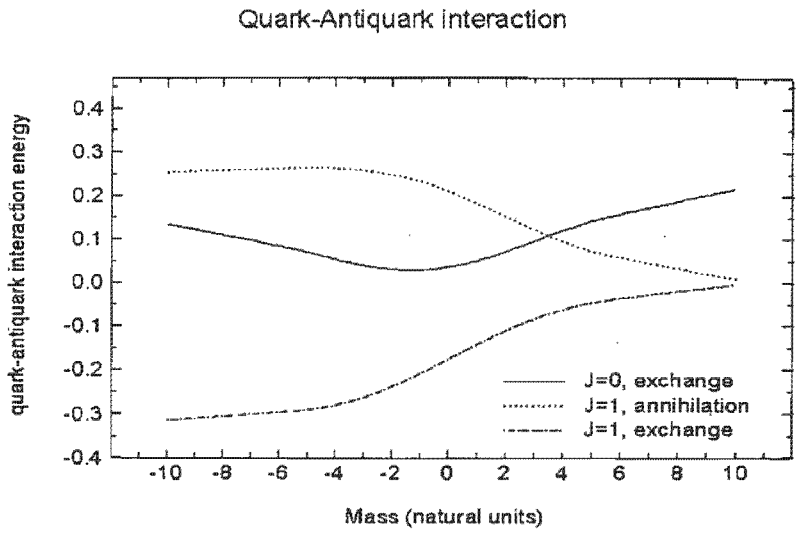

Figure 6.1: Two-particle interaction energy for one-gluon exchange and one-gluon annihilation diagrams.

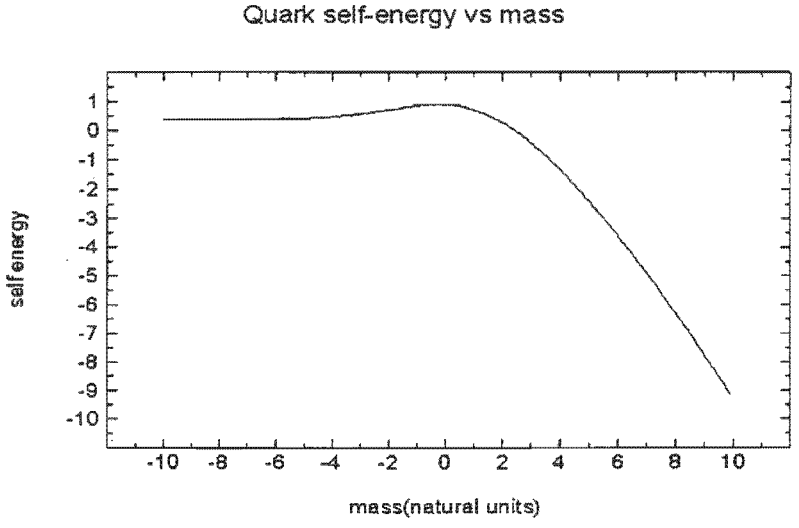

Figure 6.2: Graph of quark self-energy versus mass.

states include all first order Feynman diagrams.

Before discussing how the total energy formula is used to get the parameters of the model and the energy itself, the link between the radial integral and the interaction operator is discussed briefly.

For the $q\bar{q}$ interaction, the overcomplete base of $(q^2\bar{q}^2)(q\bar{q})$ has to be used. The Δ operator is sandwiched between two exotic states and then each state is decomposed in $q\bar{q}$ pairs. A lengthy sum results, sometimes having up to 92 terms. For a well-defined J and I, few exotic states can be constructed. It is necessary to sandwich the Δ operator between all the states with the same J and I so that a nondiagonal interaction matrix is obtained. For the qq and $\bar{q}\bar{q}$ case, the interaction matrix is diagonal while for the $q\bar{q}$ interaction the matrix has off diagonal terms. To obtain the total interaction matrix, the two matrices described above are summed up and the total matrix is diagonalized. The diagonal elements of the diagonalized matrix are the eigenvalues of the interaction operator Δ.

The process of calculating all the nondiagonal elements it is time consuming. In the case of $J = 1$ and $I = 1$ there are 14 states. For this specific case, approximately 300 hours were needed to perform the calculations as all the values are repeatedly calculated for different m_q, in total 200 times. Another technical problem is the way in which Turbo Pascal 6.0 allocates the memory for arrays of data. In order to handle correctly and completely the process, the computer has to read 200 times a 14×14 matrix, to diagonalize it and to calculate its eigenvalues. Trying to store all this data produced a conflict of memory. Luckily, the next generation of Turbo Pascal, the 7.0 version, came in time, with the memory limit extended, so that with one code all the states have been calculated and the problem of Δ operator solved. The Jacobi method is used to calculate the eigenvalues for a matrix. This is possible due to the fact that the interaction matrix is symmetric.

The calculation of the total energy (eq. (4.11)) of an exotic state has been described in Chapter 4 for massless quarks. For the massive quarks case, the calculations are different because the one-particle energy and the eigenvalues of the interaction operator Δ depend on ζ_n, the reduced mass (eq. (A.12)) of the quark. The parameters of the model α_S, B and Z_0 are calculated by fitting the energy of nucleon, Δ^{++} and ρ meson. Therefore, indirectly, the one-particle energy and Δ operator depend

on the radius of the cavity. For the case of massless up and down quarks, this indirect dependence on R does not exist and an analytic solution (eq. (4.14)) is found when the condition $\partial E/\partial R = 0$ (stability of the bag) is imposed.

For the massive quarks, when the derivative of the energy with radius R is performed, two extra terms arise in contrast with the massless case, namely a term proportional with the derivative of ω_n and another one proportional with the derivative of Δ. The experimental value of the masses of the three particles mentioned above ($m_p = 938$, $m_{\Delta^{++}} = 1232$ and $m_\rho = 770$ MeV) are set to be equal with the masses predicted by the M.I.T. bag model. A set of three equations are obtained. Another set of three equations results when the condition which reflects the stability of the bag is imposed for each particle. In total there are six equations and six unknown quantities, $\alpha_S, Z_0, B, R_p, R_{\Delta^{++}}$ and R_ρ. By substituting the radius of each state into its corresponding energy, the system of six equations is reduced to three. Using a root finder program code for a system of equations, the above parameters are calculated for all the values of m_q. The step between two consecutive masses has been chosen to be 0.1 in natural units and all the calculations and graphs involve 200 values of m_q from -10 to $+10$.

The figures 6.3, 6.4 and 6.5 show the values of α_S, B and Z_0.

In the first graph (figure 6.3), the strong coupling constant is plotted against the mass of the quark. The value of α_S for $m_q = 0$ is 3.04, higher than the standard value of 2.2 for the M.I.T. bag model. The reason for this is the quark self-energy, which is not incorporated in the original calculations of the M.I.T. bag model. As a test, the quark self-energy was set to zero and the strong coupling constant was recalculated using the same codes. The result is very close to the original values of the M.I.T. group. The same trend was obtained for the other two parameters, B and Z_0. The set of parameters does not coincide identically with the original set because of the two extra terms which appear when the derivative of the total energy is taken.

As the mass of the quark is increased, the coupling constant increases. The opposite is true when the mass of the quark takes negative values. Apparently, the coupling constant tends toward a limit as the $m_q \to \infty$. The smallest value of α_S in the graph presented corresponds to $m_q = -10$ and is 0.65.

Figure 6.4 shows the bag pressure constant B at power $1/4$ versus m_q. An ab-

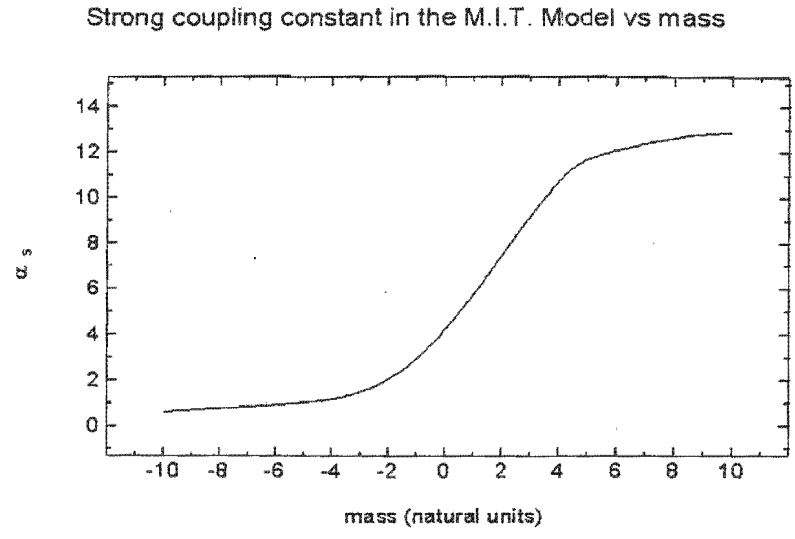

Figure 6.3: The strong coupling constant α_S versus mass, calculated in the M.I.T. bag model.

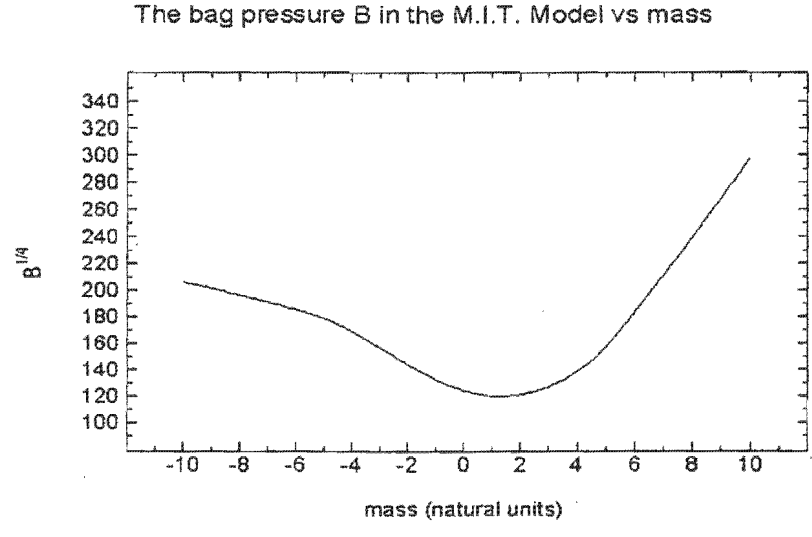

Figure 6.4: The bag pressure B calculated versus mass by fitting the proton, Δ^{++} and ρ

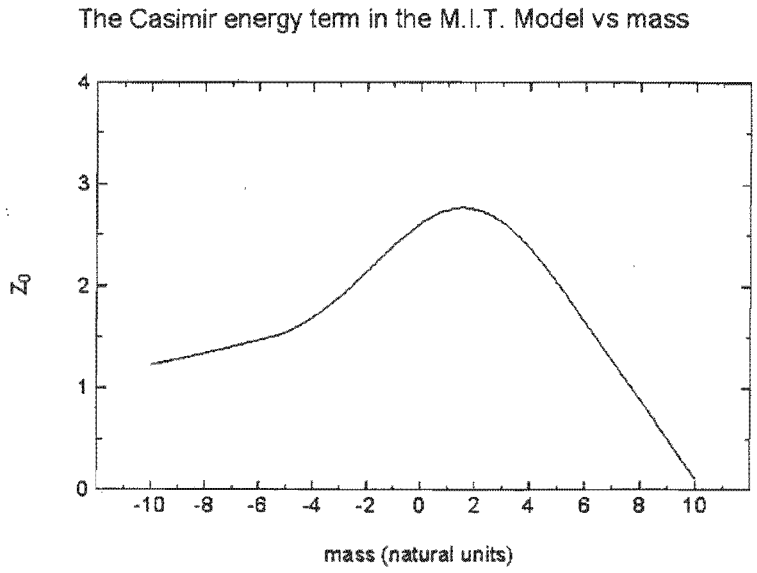

Figure 6.5: The Casimir energy, another parameter of the M.I.T. bag model versus mass

solute minimum is observed around $m_q = 1.0$ for which $B^{1/4} = 117.68$ MeV. For values of the quark mass bigger than 1.0 the value of $B^{1/4}$ is increasing linearly. For $m_q < 1.0$ the value of $B^{1/4}$ increases as well.

Finally, figure 6.5 shows the Casimir term Z_0. It exhibits an absolute maximum of 2.81 around $m_q = 1.5$ and decreases in both directions of m_q. When m_q becomes negative, the tendency of Z_0 is towards a constant value.

By substituting in eq. (4.11) the one-particle energy, the self-energy, the eigenvalues of the diagonalized interaction operator Δ and the parameters α_S, B and Z_0, the energy for an exotic state can be calculated for $m_q \in [-10, ...10]$.

A final test was performed to check the consistency of the calculations. The exotic states $q^2\bar{q}^2$ were calculated using the software codes developed for the $q^3\bar{q}^3$ states (of course with the necessary changes $N_q = 4$). The spectrum obtained here for $q^2\bar{q}^2$ states fit almost exactly the spectrum calculated by Zimak and Viollier [16] for the case $m_q = 0$. It is said "almost exactly" because one should be reminded that in this work the self-energy of the quark is included.

A few observations can be made about these calculations.

The first refers to the Cavity QCD. It is known that models are often based on idealizations. They arise either from insufficient knowledge of the underlying physics or they are intended to make the theoretical description more transparent and more accessible to quantitative analysis. Cavity models, which occupy a prominent place among hadron models, furnish a typical example for such idealizations. The confinement of relativistic quarks inside hadrons is imposed in a region of modified vacuum by static boundary conditions at a cavity of radius R. Whereas the real vacuum is expected to return to its normal phase outside of the hadron gradually, however, this simple prescription leads to an infinitely thin bag boundary and thus to an abrupt transition between the two phases.

It is expected that such an approximation affects the features of the physics of the hadrons, in other words, the results will have a certain degree of inaccuracy.

An improvement of the boundaries of the model is therefore necessary. There are some attempts [40] to use the fuzzy set theory [41], [42] in order to implement an extended boundaries. The main motivation of using fuzzy sets is that their applications to the transition between the inside and outside regions of the bag suggests itself naturally, since fuzzy sets were specifically designed to implement smooth transition between unrealistically distinct domains in simplified models.

The fuzzy bag model should be useful for the investigation of observables with an enhanced sensitivity to the surface properties and for studying interactions among hadrons. Perhaps one of the next steps will be to integrate the fuzzy theory to the Cavity QCD.

A second observation to be made, is that it has not been possible to determine very accurately the absolute mass of the exotics. This is due to the fact that the quark self-energy was calculated in the $\overline{MS}$ scheme, thus the results are scheme dependant. Another factor which contributes to this inaccuracy is the Z_0 term in the mass-energy formula, the zero-point energy (which includes correction of the centre of mass and the Casimir energy) which is a parameter of the model and has been fit to the N, Δ^{++} and ρ states. It is not known how this parameter is behaving when the number of particles is increased and when the mass of the quark is changed.

Therefore, some caution should be taken when the spectra are fitted to the ex-

perimental data. The difference in energy among various states must be the same for experimental and theoretical cases because it is believed that the above mentioned factors shift the spectrum as a whole.

A possibility to circumvent the above problem is to fit a known exotic state to one of our states. The energy difference between these two states can be then substracted from all other calculated states. At this stage no exotic state is known with precision, hence the method is not applicable yet.

A third observation about the calculations is that a large number of exotics are found (figures 6.6-6.12). The spectra seem to approach the continuum in general. However, the spectra have a common structure, a few low-lying and well-separated states followed by states which lie very close. It is presumably not possible to observe the higher excited states in experiments because they are very broad and not well-separated from each other. They will be part of the background. Consequently, we will focus our attention on the low-lying exotic states.

An advantage of the multiquark states is the fact that pairs of $q - \bar{q}$ are allowed to reside in the colour octet representation. If the other quantum numbers are $J = 1$ and $I = 0$ then this particular pair is called ω^8 state. The pair can annihilate because it carries the quantum numbers of a gluon. Here the one-gluon annihilation diagram comes into the calculations. Since the interaction via virtual annihilation turns out to be repulsive, states with low isospin and large ω^8 components are heavier then states with high isospin. This common feature of all the multiquark states can be observed in the figures 4.1-4.5 and 6.6-6.12.

All the above remarks are generally valid, for any exotic state calculated here. Let us analyze in more details the terms which make up the mass-energy formula (4.11).

Figure 5.1 shows that the single-particle energy increases linearly with the mass of the quark and the momentum remains almost constant. For the negative mass region, the opposite is true, i.e. the energy remains constant and the momentum increases linearly.

In the first case ($m_q \geq 0$), the quark's kinetic energy remains constant and its rest energy is increasing. This means that the quarks move towards a nonrelativistic region. Analyzing the figure 5.1 in conjuction with figure 6.2, one could observe that the quark self-energy becomes negative which make the sum of one-particle energy

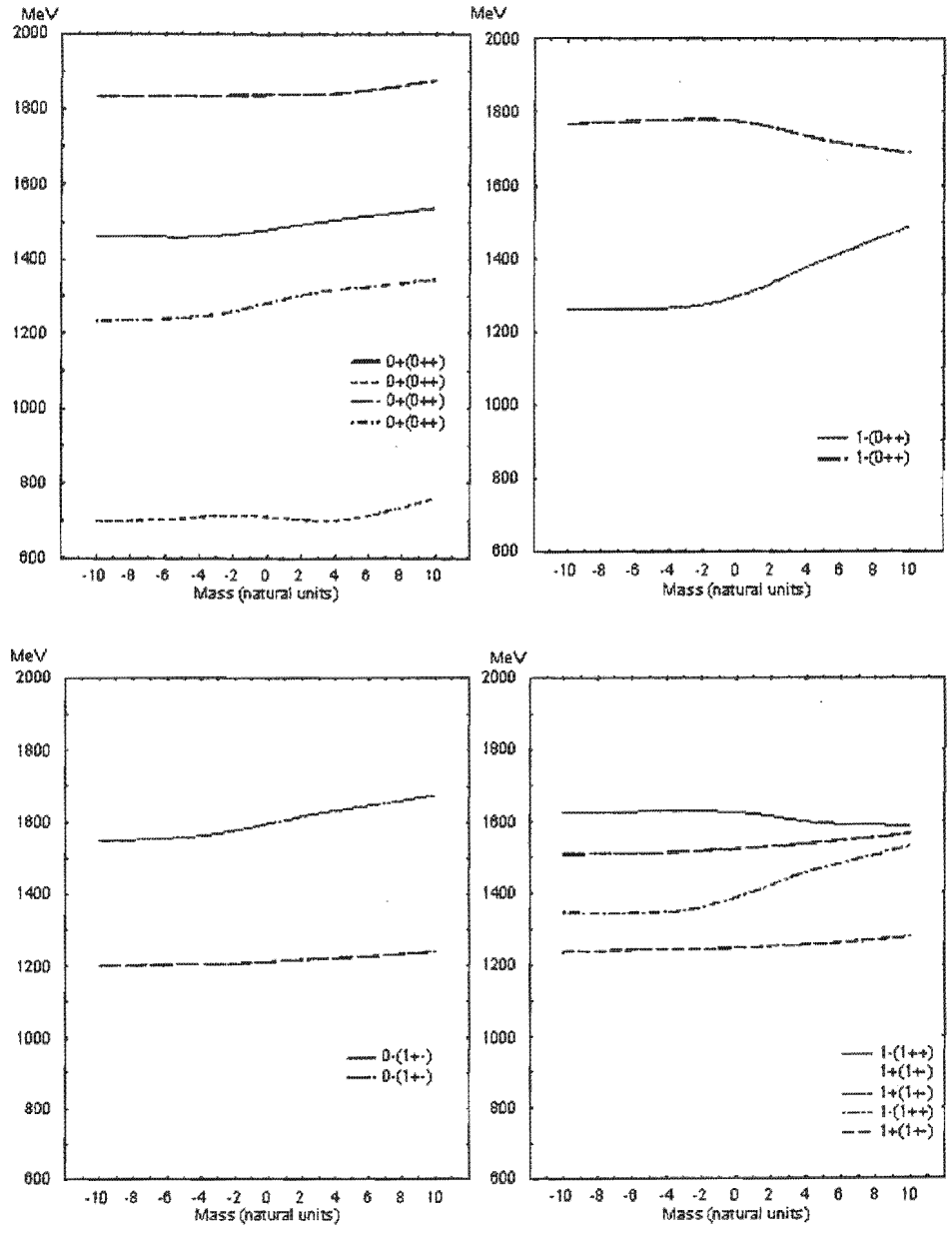

Figure 6.6: The mass spectrum for $q^2\bar{q}^2$ states. The notation is $I^G(J^{PC})$.

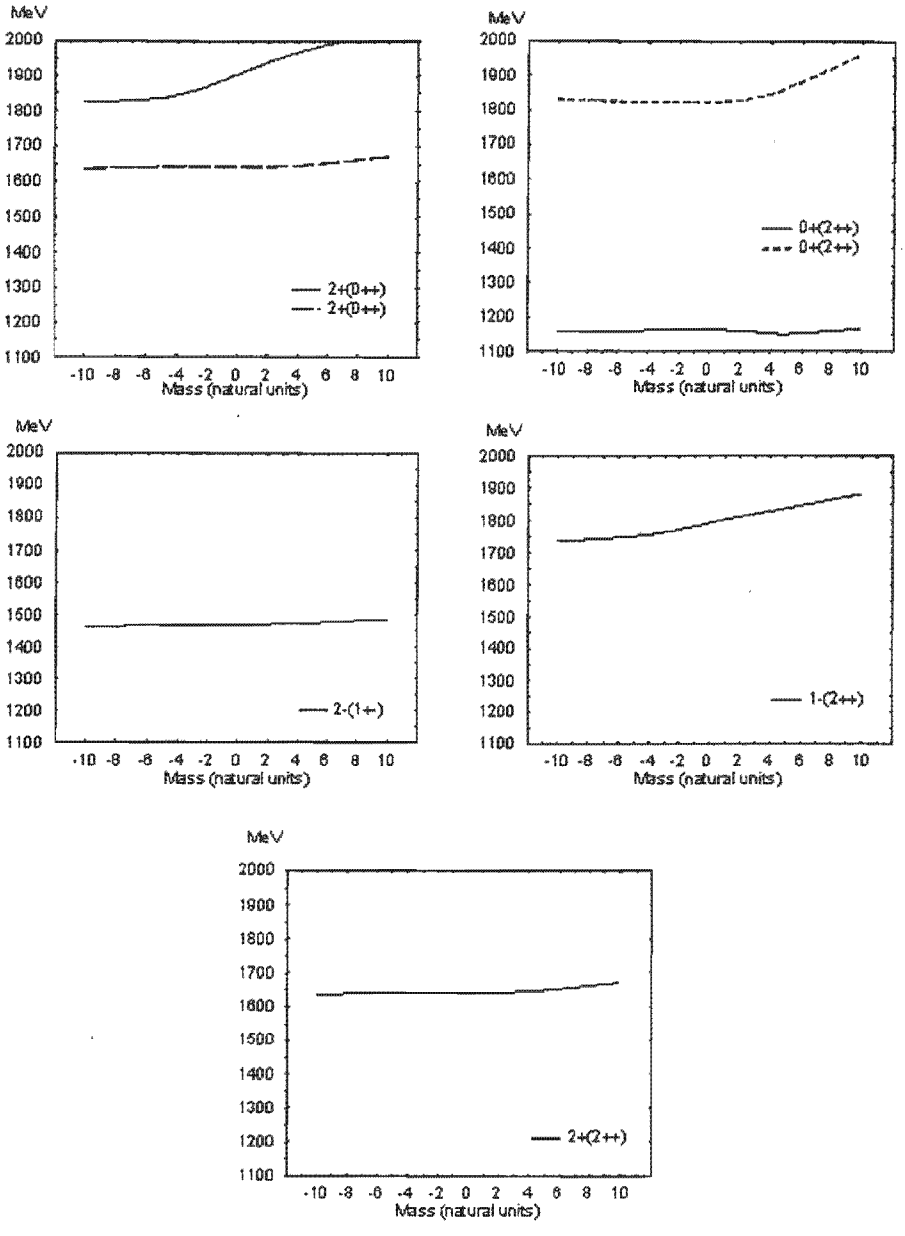

Figure 6.7: The mass spectrum for $q^2\bar{q}^2$ states. The notation is $I^G(J^{PC})$.

and the quark self-energy to be almost constant. This behaviour affects the spectrum of the exotic states as it can be seen in figure 6.6 and 6.7.

For negative values of m_q, the one-particle energy remains constant but the momentum increases, therefore the quark becomes more energetic and a relativistic treatment is absolutely necessary. The combination of one-particle energy with the quark self-energy is again constant as the quark self-energy is constant in the range of 0.4 - 0.9 MeV. This feature appears nicely in figures 6.6-6.12.

An important term in the mass-energy formula is the interaction term $\alpha_S\Delta$. The figures 6.1 and 6.2 show the dependence of the α_S and Δ on mass.

In the first graph, it can be seen that the one-gluon exchange contribution for both $J = 0$ and $J = 1$ is increasing for $m_q \geq 0$, not as in the one-gluon annihilation case, where the value of Δ is decreasing. In the same region of m_q, the strong coupling constant is increasing drastically. Hence, the product $\alpha_S\Delta$ is increasing for one-gluon exchange and it is decreasing for one-gluon annihilation.

Due to the negative sign of the $J = 1$ exchange contribution, the total energy of an exotic is smaller than the sum of the energies of the components, which prevents the fall-out phenomenon. These different combinations of increasing/decreasing values for α_S and two-particle interaction energy will result in an increase/constant mass spectrum for exotics.

There have been objections that the coupling constant is to high, even for $m_q = 0$ ($\alpha_S = 2.2$), and the use of perturbative QCD is not justified. As it has been argued in [7], the particles inside the cavity must occupy cavity modes of a certain energy. Thus, it is not possible for a quark to radiate off a gluon with arbitrary small energy in QCD cavity. A second reason supporting the use of perturbation approach is that the expression derived for QCD cavity appears to be very much similar to old-fashioned perturbation theory. Hence, a combination of α_S, energy denominator and vertex integral determine the convergence of the perturbation expansion. The energy denominator and the vertex integral usually decrease very rapidly for the higher cavity modes, therefore a perturbative QCD is appropriate for the bag model.

For negative values of m_q, the coupling constant approaches a constant value (0.65) and the two-particle interaction becomes constant for $J = 1$ in both exchange and annihilation cases and is increasing for $J = 0$ case. The almost constant behaviour of

the interaction energy and coupling constant for $m_q < 0$, coupled with the fact that the same behaviour is exhibited by the one-particle energy and self-energy, give rise to a constant energy value for an exotic state.

Qualitatively this expectation for the exotic spectrum is fulfilled. It can be seen in all the graphs (figures 6.6-6.12) that the energy is not sensitive to m_q for $m_q < 0$.

6.2 Comparison to the Experimental Data

As it was discussed and explained in the previous section, the absolute value of total energy for an exotic state has a degree of inaccuracy, therefore the evaluation of the energy difference between the states is the first step in comparing our results to the experimental data.

A common feature of the states plotted in the figures 6.6-6.12 is that the ground state is shifted upwards as the number of the quarks (antiquarks) is increased from 4 to 6. This is expected as the mass-energy formula's (4.11) main term is proportional to the number of the quarks.

A common feature for figures 6.8 and 6.9 is the shrinking of the relative energies among the states. It can be seen that the energy difference between two consecutive $q^3\bar{q}^3$ states (the lowest) vary from 240 MeV (η like state) to 366 MeV (π like state). For the $q^3\bar{q}^3$ states, the same difference varies from 50 MeV (ρ like state) to 170 (ω like state) and the spectrum approaches the continuum.

No pattern can be observed in the ordering (in terms of the energy) of the ground state energy levels. For the $q\bar{q}$ mesons the order is π, η, ρ and ω, for $q^2\bar{q}^2$ states the order is η, ω, ρ and π (note that the P, C and G parity numbers for a $q^2\bar{q}^2$ state are not the same as those of a meson, but for simplicity we use the same notation), and for the $q^3\bar{q}^3$ states the order is ρ, η, π and ω.

Comparing the $I^G(J^{PC})$ numbers of the multiquark states calculated here to those from the Particle Data Group, it is found that all the experimental quantum numbers but one are explained by our model. The only combination of parities, spin and isospin numbers which is not covered by our calculations is the f_1 state, $0^+(1^{++})$ with 1285, 1420, and 1510 MeV. This state is probable a hybrid or glueball [47].

As the non-$q\bar{q}$ mesons are difficult to distinguish from the many conventional $q\bar{q}$

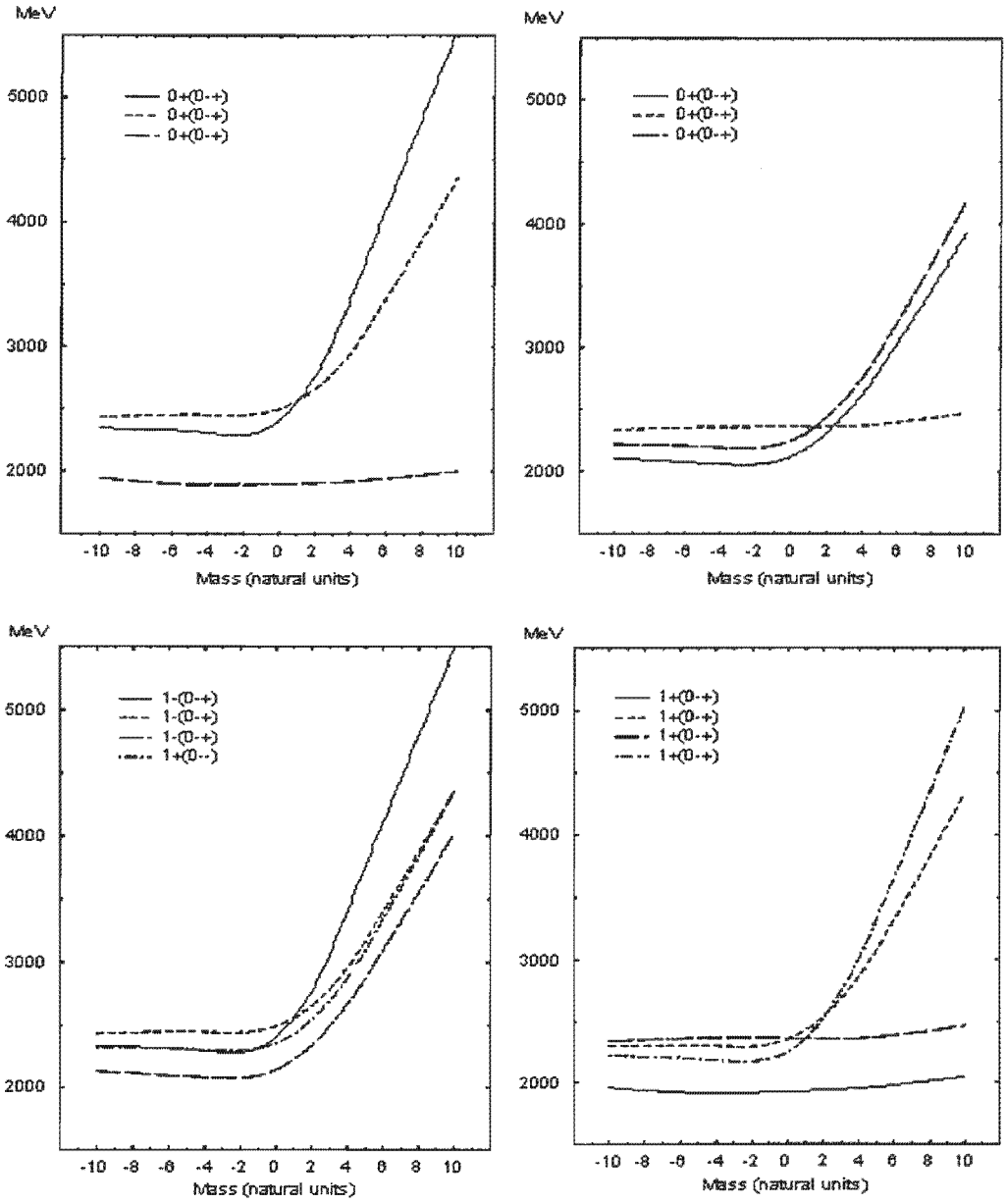

Figure 6.8: The mass spectrum for $q^3\bar{q}^3$ states. The notation is $I^G(J^{PC})$. The lowest states are probable to be observed experimentally.

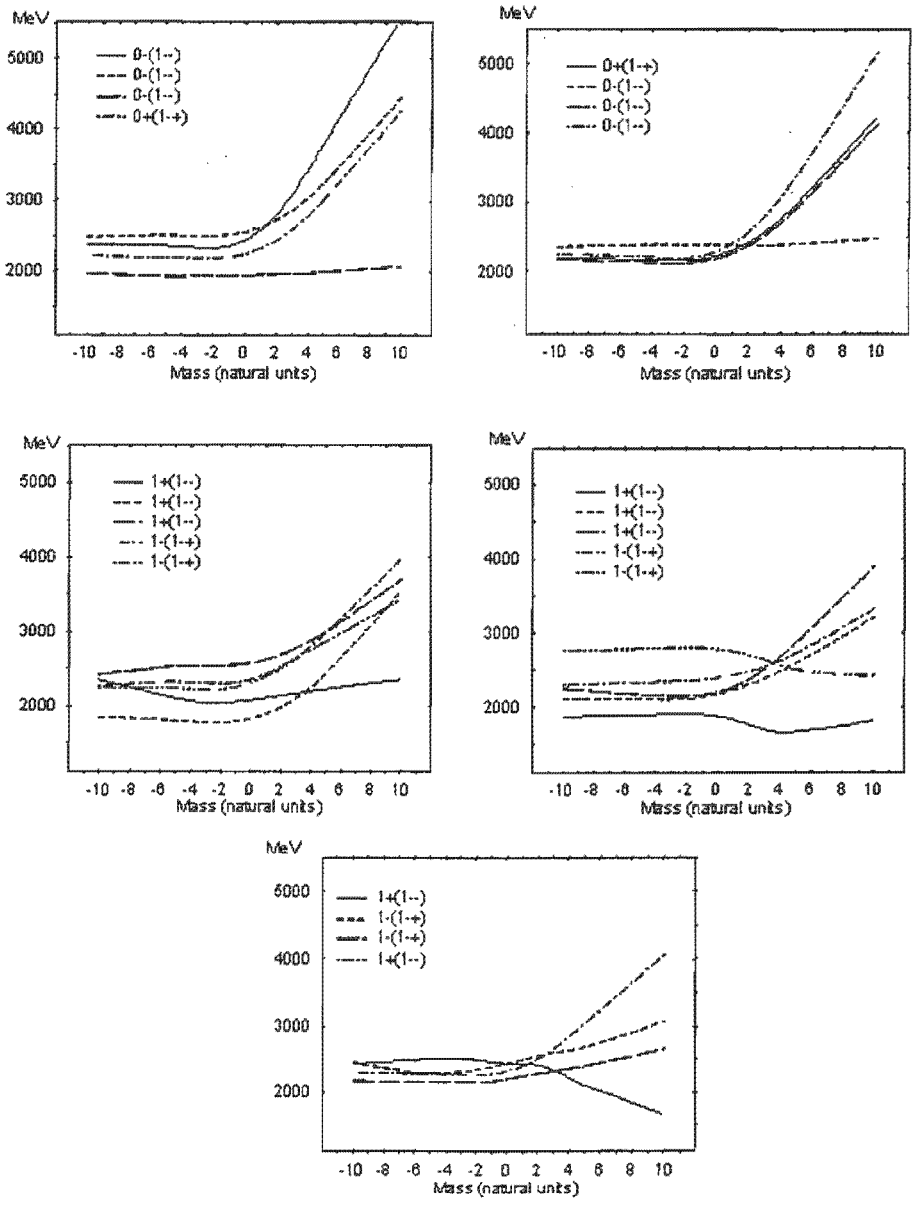

Figure 6.9: The mass spectrum for $q^3\bar{q}^3$ states. The notation is $I^G(J^{PC})$.

states which populate the meson spectrum, much effort has been put in the past years to produce mesons with manifestly exotic J^{PC} quantum numbers. It is known that a $q\bar{q}$ meson with orbital angular momentum l and total spin s must have $P = (-1)^{l+1}$ and $C = (-1)^{l+s}$. Thus, a state with $J^{PC} = 0^{--}, 0^{+-}, 1^{-+}$ and 2^{+-} must be exotic. It can be a glueball ($2g$, $3g$, ...), a hybrid ($q\bar{q}g^N$) or a multiquark state ($q^N\bar{q}^N$).

We note that all the identifications made in this work are based mainly on quantum numbers and secondly on the total energy. As the total energy can be shifted either ways by future model improvements, we proceed to identify experimental states from those calculated by us.

In a recent paper [40], the E852 Collaboration has shown that an exotic meson with $J^{PC} = 1^{-+}$ and having the mass 1370 ± 16 MeV is very probable to exist. Lattice calculations [43], [44] for 1^{-+} hybrid meson estimate its mass to be in the range of 1.7 to 2.1 GeV. Our calculations for the 1^{-+} $q^3\bar{q}^3$ multiquark state shows (figure 6.9) a mass range from 2.1 to 2.3 GeV.

The experimental results of the above exotic state appear to be inconsistent. Alde *et al.* [45], in an experiment at CERN (the GAMS experiment), claimed to observe a 1^{-+} state at 1.4 GeV. Aoyagi *et al.* [46], at KEK observed a 1^{-+} state at 1.3 GeV. A third experiment [51] Crystal Barrel reported a resonance with mass 1.4 GeV.

However, the observation of an exotic state is definitely a sign that the research in this direction is well justified and necessary.

Another sector where states beyond the predictions of the quark model have emerged in the past years is the π-family. There are two isovector 0^{-+} states in the mass region 1.4-1.9 GeV, [49]. The masses of the resonances are 1790 ± 6 MeV for $\pi(1800)$ and 1580 ± 42 MeV for the new resonance. All other known quark models [50] predict only one state in this mass region. Our model predicts for this quantum numbers two states with energy 1910 and 2050 MeV (figure 6.8) respectively. If we rely on the energy difference between states (as discussed) one sees that the experimental energy difference is 210 MeV and our energy difference is 140 MeV.

The experimental data for the f_0 family is marked by controversy. A clear unfamiliar peak in the $p\bar{p}$ annihilation at rest into 3π states has been reported by the ASTERIX Collaboration [52] and the Crystal Barrel Collaboration [53]. In the first analysis, they suggested that this new peak is caused by the production of a new ex-

otic meson AX(1565) or $X_2(1515)$ with $I^G(J^{PC}) = 0^+(2^{++})$. Later, the Crystal Barrel Collaboration [54] and Anisovich *et al.* [55], reanalyzed the data and reached quite a different conclusion. They suggested that the new peak is caused by the production of two fairly narrow resonating states $f_0(1335)$ and $f_0(1505)$. The too new resonances are assumed to be four-quark states. Our model predicts masses of 1250 and 1475 MeV (figure 6.6) for the quantum numbers $0^+(0^{++})$ required.

Anisovich *et al.* suggested in their analysis the possible existence of another f_0 resonance with mass around $1.7 - 1.8$ GeV. We remark that the fourth state $0^+(0^{++})$ in our spectrum (figure 6.6) has a mass of 1.8 GeV, and it could be assigned to this resonance. In fact even from theoretical point of view the scalar σ is very controversial [56], [57] and [58].

For the ρ-family ($1^+(1^{--})$) there are various experimental results suggesting exotic states responsible for the states with the mass in the range $1.3 - 1.8$ GeV. Two resonances $\rho(1420)$ and $\rho(1770)$ have been found by Bisello *et al.*[59], a low lying resonance $\rho(1300)$ has been founded by LASS [60], a $\rho(1780)$ resonance has been discovered by Killian *et al.*[61], and a broad resonance $\rho(1520)$ has been found by Aston *et al.*,[62]. If one tries to fit the experimental data to our states (figure 6.9), apparently there is a discrepancy between them. At a closer look, the separation of the states appears to be the same.

The energy separations among the experimental data are 120, 100 and 250 MeV respectively. If we consider that our 1800 and 1850 states, and 2175 and 2200 states (figure 6.9) are the components of a single state around 1800 and 2174, respectively, then the energy differences are 200, 150 and 250 MeV. However, it is difficult to make a clear identification as the separation of the events caused by the $q^3\bar{q}^3$, $q^2\bar{q}^2$ and $q\bar{q}$ states is not easy revealed in any experiment and the mass spectra of these states overlap each other. No attempt has been made to fit the states presented in figures 6.11 and 6.12 with the experimental data as their spin/isospin is high and they are very improbable to be clearly observed.

There are many other states [63], [39] which are believed to be exotics but unfortunately we can not even attempt to interpret them. For a reliable comparison we need at least two exotics from the same family in order to compare the energy difference with ours. Therefore, the states depicted in figures 6.10-6.12 need more

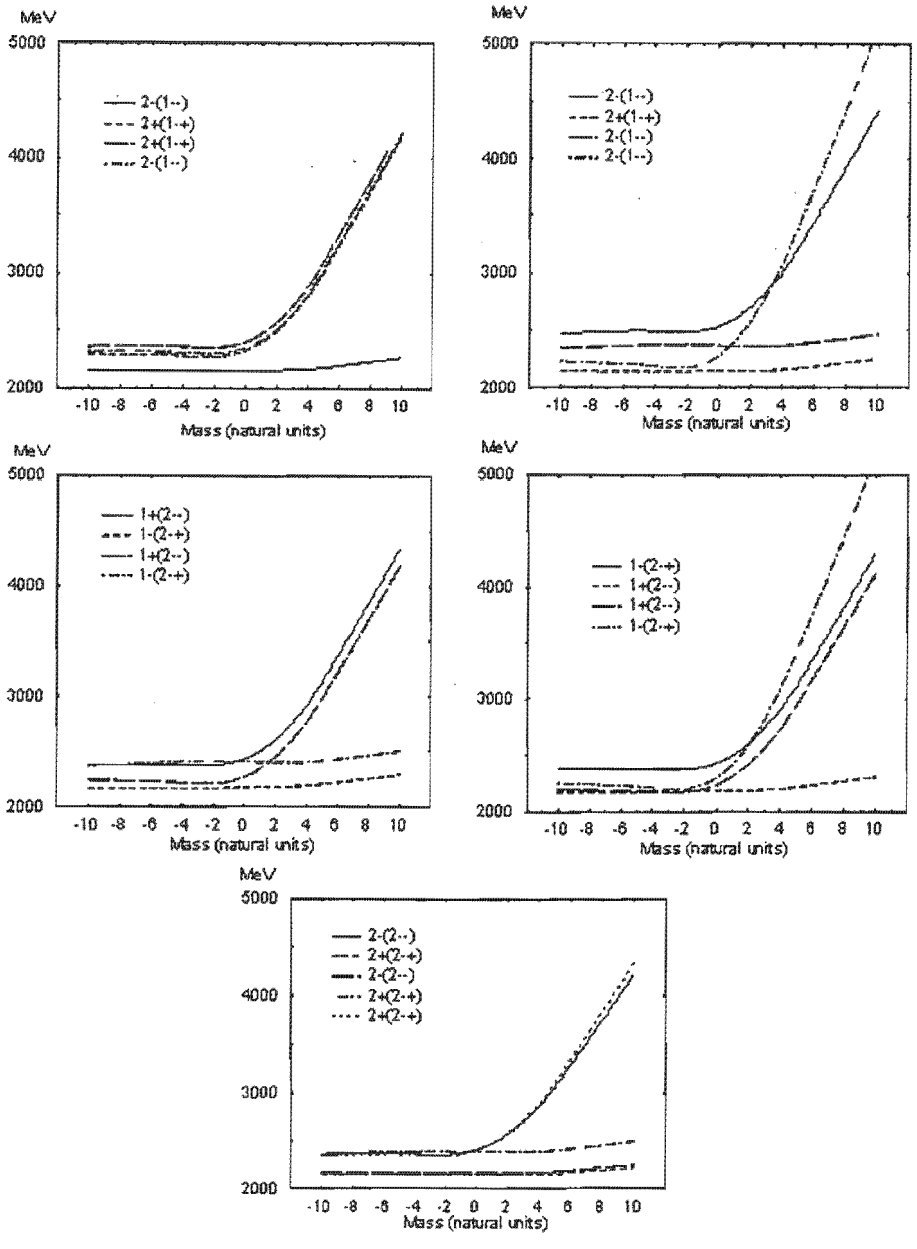

Figure 6.10: The mass spectrum for $q^3\bar{q}^3$ states. The notation is $I^G(J^{PC})$. These states appear to be less probable to be observed due to their high energy.

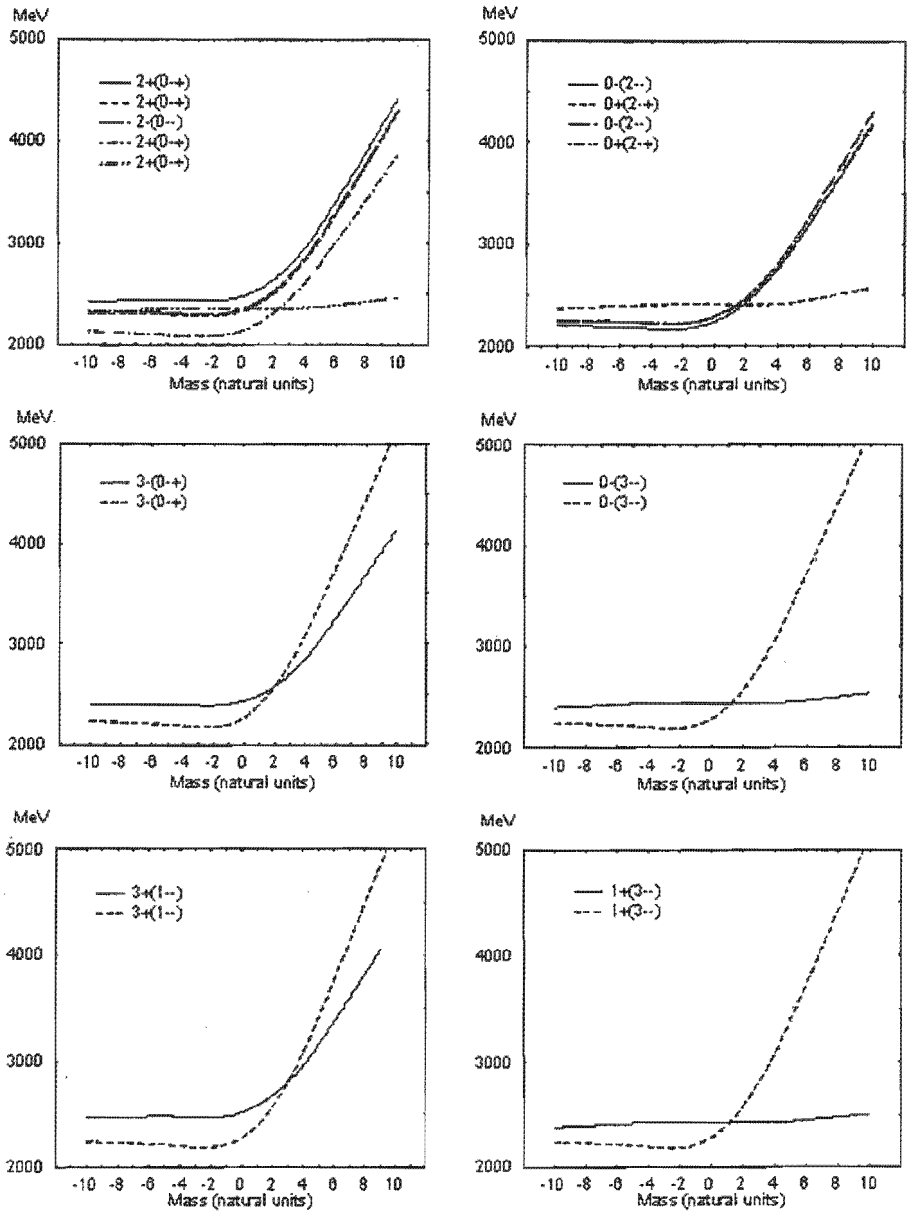

Figure 6.11: The mass spectrum for $q^3\bar{q}^3$ states. The notation used is $I^G(J^{PC})$. These states appear to be concentrated in the same energy band of 2000-2500 MeV.

experimental data in order to be analyzed. However it is believed that due to their high energy they contribute to the background and cannot be observed.

As a final observation to this section, we note that the $f_0(980)$ and $a_0(980)$ states are known to be inconsistent with $q\bar{q}$ mesons. An alternative assignment as $K\bar{K}$ molecules [64] is widely believed to be at least qualitatively correct.

6.3 Other Theoretical Models

There are many models available today which predict exotic states. In the following, we list a few of them, the most common ones, and we analyze briefly their predictions.

One of the first model which accommodated and predicted the possibility of exotics is the M.I.T. bag model [6]. Based on the M.I.T. bag model many calculations have been done. We mention here those of Chanowitz *et al.* [65], and Barnes *et al.* [66].

Chanowitz *et al.* [65] have calculated the spectrum of hybrids with $J^{PC} = (0,1,2)^{-+}$ and 1^{--}, by performing the calculations to first order in cavity perturbation theory. The incorporation of the self-energy effects, significantly improved the quality of the fit to the baryons and their static properties.

Barnes *et al.* [66] have been presented detailed calculations of the highest hybrids within the spherical cavity approximation to the M.I.T. bag. They concentrated on the $J^{PC} = (0,1,2)^{-+}$ states with their mass between 1 and 2 GeV and $\alpha_S = 2.2$. Their results are in good agreement to those of Chanowitz *et al.* [65].

An alternative to the M.I.T. bag model is the lattice gauge theory. Most effort has gone into the determination of the masses of states that can be constructed using quark and antiquark propagators. However, the extension of these studies to include states with excited orbital momentum l is important in order to gain a complete insight and better understanding of the QCD spectrum.

Perantonis *et al.* [72], have used a static potential in the SU(3) lattice gauge theory and they studied the spectrum of the low-lying hybrids. Lacock *et al.* [72], have used the same model to study excited $q\bar{q}$ mesons and hybrids mesons and to calculate their spectra. Predictions for masses of the spin-exotic mesons with $J^{PC} = 1^{-+}, 0^{+-}$ and 2^{+-} are given.

Another model which gained credibility has been developed in mid eighties by

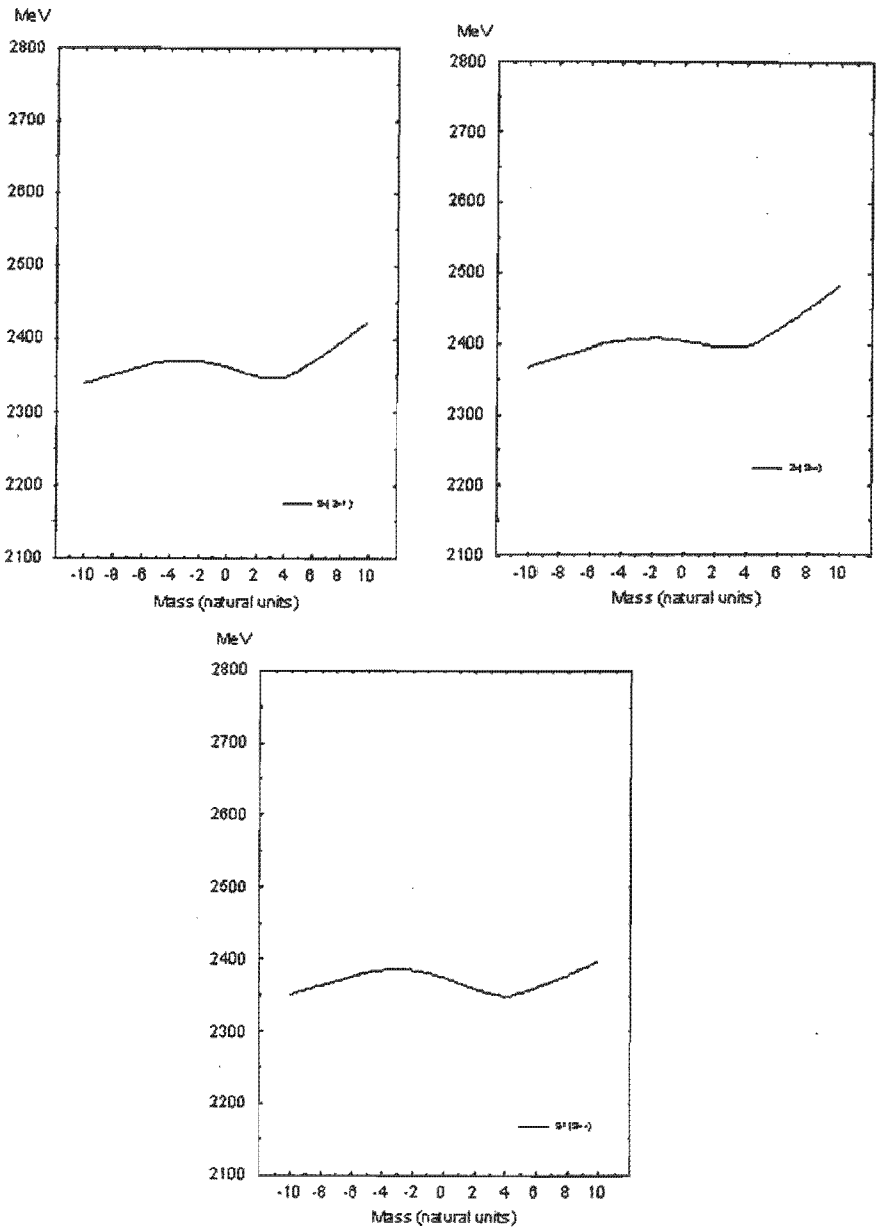

Figure 6.12: The mass spectrum for $q^3\bar{q}^3$ states. The notation is $I^G(J^{PC})$.

Isgur *et al.* [67], [68]. The flux tube model is based on the strong coupling Hamiltonian lattice formulation of QCD. In this picture, mesons consist of $q\bar{q}$ connected by a cylindrical bag of coloured fields the 'flux tube'. When the flux tube is in its ground state, the excitation of the $q\bar{q}$ degree of freedom yields the conventional meson spectrum. Excited modes of the flux tube lead to a set of states that have to be confirmed by experiments. The model has been applied with some success to the decays of the conventional mesons [69], and has also given some limited predictions of decays of a few hybrid states [70], specifically those with light flavours and exotic J^{PC} quantum numbers. It is the latter paper that has in part motivated the experimental search strategy for hybrids. They have found that the predictions of the decays of relatively light mesons (ordinary mesons) are very similar to the successful $^3P_0$ model. The authors have managed to reproduce with their model nearly a hundred well-known decay amplitudes.

Using the same model with an harmonic oscillator approximation, Close *et al.* [71], have been predicted the signature for a hybrid meson $J^{PC} = 1^{-+}$ in the mass region $1.6 - 2.2$ GeV. Other possible hybrid states calculated by them are 0^{-+} and 2^{-+}.

In a more recent paper [74], the multiquark $q^2\bar{q}^2$ states have been studied using the static $SU(2)$ lattice Monte Carlo method. Its main conclusion is that 'the lattice artefact are still large'.

A different approach in the line of lattice theory has been used in the work of Green *et al.*, [76]. They have constructed an interquark potential model that reproduces lattice results for the simplest multiquark systems. The model explains the energies of a series of four-quark systems.

The Nonrelativistic Potential Model is another strong candidate model which predicts and calculates hybrid and multiquark states. Weinstein *et al.* [76], have examined the $q^2\bar{q}^2$ states in the framework of nonrelativistic potential model with colour-dependant confinement forces and hyperfine interactions by solving the four-particle Schrödinger equation variationally. They found that the $q^2\bar{q}^2$ bound states are a model for the weak binding and colour-singlet clustering observed in nuclei.

There are many other models in literature which reproduce more or less the available experimental data. We list in the following a few more models without any

details of their methods or results.

An interesting analysis of the multiquark states is given by Uehara *et al.* [77], using the diquark cluster model. Gerasyuta *et al.* [78], were using a relativistic four-quark equation in the framework of dispersion relation technique, to analyze exotic mesons. Not on the last place, the QCD sum rules [79], [80] , [81] have came with interesting predictions for hybrids and glueballs.

Chapter 7

Conclusions

In this paper the spectra of the lowest $q^2\bar{q}^2$ and $q^3\bar{q}^3$ systems composed of light quarks were calculated in the framework of Cavity QCD. The main question for a conclusion is: what has been achieved with this work?

One of the aims of the thesis was to study the $q^3\bar{q}^3$ multiquark state. This state is often called in literature, but to our knowledge no one so far has tried to calculate its spectrum. Somehow, the reluctance is understandable because of the high energy of the states but we believe that is worthwhile knowing exactly where these states are lying in the meson spectrum.

Then, by calculating the states $q^3\bar{q}^3$, the model's possibility to predict more exotics has been tested. The results have shown that the number of states increases severely and the spectrum is becoming almost continuous. Some multiquark states have their energy very close to the $q\bar{q}$ mesons or other exotics in the range of $1.0 - 2.5$ GeV. This suggests that interference of states is possible.

The $q^3\bar{q}^3$ states offer a reach variety of exotic quantum numbers, $I^G(J^{PC})$, a few of them being observed in experiments.

Another aim of the thesis was to extend the study of the $q^2\bar{q}^2$ and $q^3\bar{q}^3$ exotic states using the new boundary condition. The suggestion of this new boundary condition has been made by Jaffe *et al.* [6]. It has been later developed by Lindebaum [28]. The consequences of the new boundary condition are a reduction of the strong coupling constant (to 0.9) and an interesting constant behaviour of the energy spectrum for various values of m_q.

The spectra of the exotics for $m_q = 0$ has been compared to the experimental data. Because the absolute value of the energy is not exactly known, the energy differences between states have been compared. Good results have been obtained for the isovectors 0^{-+} and for the ρ-family.

The absolute energy problem can be fixed in a few ways, as it was suggested in the previous chapter. The most attractive way is the softening of the present rigid boundary by using a fuzzy sets boundary condition. Another way to fix the absolute energy problem is to calculate more precisely the Casimir energy of the quarks in the bag. Some work is in progress in both directions.

As more and more research papers are predicting that the hybrids have a lower ground energy than the multiquark states, it will be useful to evaluate the spectrum for these exotics in this model. We should mention that the properties of the hybrids and glueballs have been studied [16] with this model for $m_q = 0$, up to the tree level. The spectra for the hybrids and glueballs can be calculated relatively easy in this model with new boundary condition and including the quark and gluon self energy.

An interesting issue is how the mass spectrum and self-energy of the gluon and quark would be affected by including the next order corrections. Our calculations have been performed at the tree-level approximation. Some preliminary results from an attempt to calculate the spectrum of hadrons to second order are encouraging [82].

One comment about the mass of the quark is necessary as the mass of the quark is the central issue in this thesis.

It is known that quarks' masses cannot be measured directly, but must be determined indirectly through their influence on hadron properties. As a result, the values of the quarks' masses depend on how precisely they are defined. There is no one definition that is the obvious choice. Therefore, the masses only make sense in the limited context of a particular quark model.

A final remark is that despite of having so many theoretical models, no one is making full predictions regarding the spectra of the mesons and exotic mesons, so that, at this stage, taking into account the controversy in the experimental sector, it is rather impossible to rule out any model or to fully confirm another.

It is hoped that the situation will soon be clarified by the new results. The relevant experiments, both on-going and planned throughout the world, should shed light on

the missing and uncertain members of the exotic states. New results are expected from the BNL-E852 data, IHEP data taken by the VES and the GAMS groups. Further new information should come from the massive statistics being accumulated by the Crystal Barrel and Obelix collaboration at LEAR.

Towards the end of this decade and at the beginning of the next millennium, one can look forward to getting new insights from the new experiments planned at CERN SPS, KEK, Beijing τ-charm factory and upgraded AGS and RHIC at BNL.

Acknowledgments

I received great amounts of encouragement, support and help from many people during my studies. I would never be able to respond back in the same way. The least I can do is to give all of them a big THANK YOU.

Along my professional path, I greatly appreciate and THANK Dr. Petru Dragos, my high school mathematics teacher, who was the first person who showed me the beauty of science. Thanks to him, I switched my career from a respectable possible wealthy medic to a modest scientist.

Then, during my undergraduate studies, when the future was not promising in a traumatic post-communist era, Dr. Ovidiu Lipan showed me that everything is possible. He is a model of strength and a big fighter. THANK YOU Ovidiu.

A big THANK YOU to my fellow undergraduate student, Mirela Nes, for her courage to tackle problems which looked impossible for me. Later she became my wife.

A THANK YOU goes to Dr. G.C. Paunescu, romanian business man, who offered to pay all my and my wife's expenses to go to South Africa without even knowing us. He has showed us what the meaning of a good samaritan is.

A big THANK YOU goes to Prof. R. D. Viollier, who offered me a Ph.D. bursary at UCT and gave me the chance to interact in an open environment and to enrich my knowledge about this world.

THANK YOU Prof. Viollier for your expert advice and patience in guiding me through this thesis.

I also express my gratitude for the Ph.D. bursary to the Foundation for Research and Development, for facilitating the development of this thesis.

Prof. A. Petroianu from Department of Electrical Engineering has offered me,

besides his friendship, the financial support for the last year by means of a research contract. A THANK YOU goes unreserved to him.

THANK YOU to Prof. C. Comrie, Dr. A. Buffler, Prof. D. Aschman and Dr. S. Allie for your trust and the privilege given to me to teach , as a Ph.D. student, a few undergraduate classes.

I also want to THANK Dr. R. Lindebaum for being always there when I needed help.

THANK YOU Joan Parson and Dulcie Hess for making the place much friendlier and not physics dominated.

THANK YOU to all the staff from the Physics Department for your warmness and friendliness.

Along my personal life there are some people who deserve special thanks. I would like to THANK my parents who gave me the opportunity to open my mind which finally came back like a boomerang against them. It hurts them because this openness took me across the planet, to South Africa, at the other 'corner' of the globe. But in the same time, they are proud of my achievements.

A second big THANK YOU to my wife, now Mirela Fetea, for everything that she has done for us. There are no words which can describe our seven years together.

THANK YOU once again to all friends and people who's names are or not in this acknowledgment. All of you have a place in my heart.

CAPE TOWN

26 Nov. 1998

Appendix A

Cavity QCD

The quarks are confined to a spherically symmetric and static cavity. The Dirac equation provides a solution for the wave function of the quarks. The boundary condition imposed on the wave function (in order to prevent the quarks from escaping) yields the one-particle energy ω of the quarks. The same is true for the gluons with the difference that the Dirac equation is substituted by the d'Alembert equation. Using the cavity modes of the particles, the vertex integrals are calculated. The radial and angular parts are separated as explained in section 2.2. With the expressions for the vertex integrals, it is a problem of computer programming to calculate the dimensionless interaction operator, to diagonalize it and to find the spectrum of the states.

A.1 Quarks inside the Cavity

The quarks are described by the time-independent Dirac equation

$$\left(-i\vec{\gamma}\vec{\nabla} + m_f\right) u_n(\vec{r}) = \varepsilon_n \gamma^0 u_n(\vec{r}), \tag{A.1}$$

where ε_n is the energy and m_f is the mass of quark with flavour f. One solution of the above equation in a spherical cavity [30] is the Dirac spinor

$$u_n(\vec{r}) = \begin{pmatrix} g_n(r)\chi_\kappa^\mu(\hat{r}) \\ i f_n(r)\,\chi_{-\kappa}^\mu(\hat{r}) \end{pmatrix}, \tag{A.2}$$

where $n = \{f, \nu, \kappa, \mu\}$ stands for flavour, radial, Dirac and magnetic quantum numbers and $\chi_\kappa^\mu(\hat{r})$ is the two-component spherical spinor. The radial functions $g_n(r)$ and $f_n(r)$

are given in terms of the spherical Bessel functions as

$$g_n(r) = \frac{\mathcal{N}_n}{R^{3/2}} j_l(p_n r) \tag{A.3}$$

$$f_n(r) = \frac{\mathcal{N}_n p_n \cdot \mathrm{sgn}\kappa}{R^{3/2}(\varepsilon_n + m_f)} j_{\bar{l}}(p_n r), \tag{A.4}$$

where R is the radius of the cavity, p_n is the momentum of the quark and $j(x)$ is a spherical Bessel function. The index of the spherical Bessel function are the orbital angular momenta l or $\bar{l}$ which are defined as

$$j(\kappa) = |\kappa| - \frac{1}{2} \tag{A.5}$$

$$l(\kappa) = j(\kappa) + \frac{1}{2}\mathrm{sgn}\kappa \tag{A.6}$$

$$\bar{l}(\kappa) = j(\kappa) - \frac{1}{2}\mathrm{sgn}\kappa. \tag{A.7}$$

The linear boundary condition of the M.I.T. bag model yields another equation for the Dirac spinor

$$\left(i\vec{\gamma}\,\hat{\vec{r}} + 1\right) u_n(\vec{r}) \mid_{r=R} = 0 \tag{A.8}$$

which can be re-expressed in terms of the spherical Bessel functions as

$$j_l(x_n) + \frac{x_n \mathrm{sgn}\kappa}{\omega_n + \zeta_f} j_{\bar{l}}(x_n) = 0, \tag{A.9}$$

where the dimensionless energy ω_n, momentum x_n, and mass ζ_n are given by

$$\omega_n = \varepsilon_n R = \mathrm{sgn}\nu \cdot \sqrt{x_n^2 + \zeta_n^2} \tag{A.10}$$

$$x_n = p_n R \tag{A.11}$$

$$\zeta_n = m_f R. \tag{A.12}$$

Substituting the eqs. (A.10), (A.11), and (A.12) in eq. (A.9), the energy of the quark can be calculated (see table below).

κ	j	l	$\bar{l}$	state	ω_n
-1	$\frac{1}{2}$	0	1	$s_{\frac{1}{2}}$	2.04
1	$\frac{1}{2}$	1	0	$p_{\frac{1}{2}}$	3.81
-2	$\frac{3}{2}$	1	2	$p_{\frac{3}{2}}$	3.20
2	$\frac{3}{2}$	2	1	$d_{\frac{3}{2}}$	5.12

(A.13)

The normalization constant $\mathcal{N}_n$ can be calculated from the condition that the norm of the Dirac spinor is unity

$$1 = \int d^3r \; u_n^\dagger(\vec{r})\, u_n(\vec{r}). \tag{A.14}$$

N_n is therefore given by

$$\mathcal{N}_n^2 = \frac{1}{2\omega_n(\omega_n+\kappa)+\zeta_f}\left(\frac{x_n}{j_l(x_n)}\right)^2. \tag{A.15}$$

A.2 Gluons inside the Cavity

In the Feynman gauge ($\lambda = 1$), the cavity modes of the gluon are solutions of the time-independent d'Alembert equation

$$\left[\Delta + \left(\Omega_m^\Sigma\right)^2\right] a_{m\Sigma}(\vec{r}) = 0 \tag{A.16}$$

subject to the linear M.I.T. bag model boundary conditions. The conditions, as in the case of the quarks, prevent the gluons from leaving the cavity, i.e.

$$n_k\left(\partial^k \hat{\mathbf{A}}^\nu - \partial^\nu \hat{\mathbf{A}}^k\right)\Big|_S = n_k \hat{\mathbf{A}}^k = n_k \partial^k\left(\partial_\nu \hat{\mathbf{A}}^\nu\right)\Big|_S = 0. \tag{A.17}$$

The cavity modes are labelled according to the gluon polarization $\Sigma = \mathcal{S}, \mathcal{L}, \mathcal{M}$ and $\mathcal{E}$ and $m = \{N, J, M\}$. The cavity modes can be expressed in terms of spherical Bessel functions and vector spherical harmonics as

$$\begin{aligned}
a_{m\mathcal{S}}(\vec{r}) &= \frac{\mathcal{N}_{m\mathcal{S}}}{R^{3/2}} i j_J\left(\Omega_m^{\mathcal{S}} r\right) Y_{JM}(\hat{r}) \\
\vec{a}_{m\mathcal{L}}(\vec{r}) &= \frac{\mathcal{N}_{m\mathcal{L}}}{\sqrt{R^3(2J+1)}}\left[\sqrt{J} j_{J-1}\left(\Omega_m^{\mathcal{L}} r\right)\vec{Y}_{JM}^{J-1}(\hat{r}) + \sqrt{J+1} j_{J+1}\left(\Omega_m^{\mathcal{L}} r\right)\vec{Y}_{JM}^{J+1}(\hat{r})\right] \\
\vec{a}_{m\mathcal{M}}(\vec{r}) &= \frac{\mathcal{N}_{m\mathcal{M}}}{R^{3/2}} j_J\left(\Omega_m^{\mathcal{S}} r\right)\vec{Y}_{JM}^{J}(\hat{r}) \\
\vec{a}_{m\mathcal{E}}(\vec{r}) &= \frac{\mathcal{N}_{m\mathcal{E}}}{\sqrt{R^3(2J+1)}}\left[\sqrt{J+1} j_{J-1}\left(\Omega_m^{\mathcal{E}} r\right)\vec{Y}_{JM}^{J-1}(\hat{r}) - \sqrt{J} j_{J+1}\left(\Omega_m^{\mathcal{E}} r\right)\vec{Y}_{JM}^{J+1}(\hat{r})\right].
\end{aligned} \tag{A.18}$$

The eigenvalues of the gluon energy Ω_m^Σ are found by imposing the linear M.I.T. bag model boundary conditions

$$J j_J\left(\Omega_m^\Sigma R\right) - \Omega_m^\pm R j_{J+1}\left(\Omega_m^\Sigma R\right) = 0 \text{ for } \Sigma = \mathcal{S}, \mathcal{L} \tag{A.19}$$

$$(J+1) j_J\left(\Omega_m^{\mathcal{M}} R\right) - \Omega_m^{\mathcal{M}} R j_{J+1}\left(\Omega_m^{\mathcal{M}} R\right) = 0 \tag{A.20}$$

$$j_J\left(\Omega_m^{\mathcal{E}} R\right) = 0. \tag{A.21}$$

The scalar and longitudinal modes obey the same equation and therefore have the same energy spectrum, except that there is a zero energy scalar mode and no corresponding longitudinal mode. The normalization constants are

$$N_{m\mathcal{S}}^{-2} = N_{m\mathcal{L}}^{-2} = \frac{1}{2} j_J^2 \left(\Omega_m^{\mathcal{S}} R\right) \left(1 - \frac{J(J+1)}{\left(\Omega_m^{\mathcal{S}} R\right)^2}\right) \tag{A.22}$$

$$N_{m\mathcal{M}}^{-2} = \frac{1}{2} j_J^2 \left(\Omega_m^{\mathcal{M}} R\right) \left(1 - \frac{J(J+1)}{\left(\Omega_m^{\mathcal{M}} R\right)^2}\right) \tag{A.23}$$

$$N_{m\mathcal{E}}^{-2} = \frac{1}{2} j_{J+1}^2 \left(\Omega_m^{\mathcal{E}} R\right) \tag{A.24}$$

for all the gluon modes with one exception. The zero energy scalar mode has the normalization constant

$$N_{m_0\mathcal{S}}^{-2} = \frac{1}{3}. \tag{A.25}$$

The quantum numbers of the zero energy mode are $m_0 = \{0, 0, 0\}$, and thus the mode is

$$a_{m_0\mathcal{S}} = i\sqrt{\frac{3}{4\pi}}. \tag{A.26}$$

The gluon modes are a complete and orthonormal set,

$$\begin{aligned} \sum_{m\Sigma} g^{\Sigma\Sigma} a_m^{\mu\Sigma}(\vec{r}) a_m^{\nu^*\Sigma}(\vec{r}') &= g^{\mu\nu}\delta^{(3)}(\vec{r} - \vec{r}') \\ \int d^3r \; g_{\mu\nu} a_m^{\mu\Sigma}(\vec{r}) a_{m'}^{\nu^*\Sigma'}(\vec{r}) &= g^{\Sigma\Sigma'}\delta_{mm'}, \end{aligned}$$

where $g^{\Sigma\Sigma'}$ is the diagonal metric tensor in polarization space, defined as

$$g^{\mathcal{S}\mathcal{S}} = -g^{\mathcal{L}\mathcal{L}} = -g^{\mathcal{M}\mathcal{M}} = -g^{\mathcal{E}\mathcal{E}} = 1 \qquad g^{\Sigma\Sigma'} = 0; \Sigma \neq \Sigma'. \tag{A.27}$$

Under complex conjugation, the gluon cavity modes transform according to

$$a_m^{\mu^*\Sigma}(\vec{r}') = \zeta_\Sigma (-1)^M a_{m^*}^{\mu\Sigma}(\vec{r}'), \tag{A.28}$$

where m^* is defined as $m^* = \{N, J, -M\}$ and the phase ζ_Σ is

$$\zeta_\Sigma = \begin{cases} +1 \text{ for } \Sigma = \mathcal{L}, \mathcal{E} \\ -1 \text{ for } \Sigma = \mathcal{S}, \mathcal{M} \end{cases} \tag{A.29}$$

A.3 The Vertex Integrals

The vertex integrals describe the absorption or emission of a gluon by a quark. They are defined as

$$Q^{\Sigma}_{nn'm} = i \int \bar{u}_n \left(\vec{r}\right) \gamma_\mu u_{n'} \left(\vec{r}\right) a^{\mu\Sigma}_m \left(\vec{r}\right) d^3r, \tag{A.30}$$

where n and m stand for quark and gluon quantum numbers, Σ for the polarization of the gluon $(\mathcal{S}, \mathcal{L}, \mathcal{M}, \mathcal{E})$, and $a^{\mu\Sigma}_m$ are the Hansen functions or solutions of the d'Alembert equation for the gluon.

The radial and angular parts can be separated yielding for the angular part

$$\begin{aligned} Q^{\Sigma}_{nn'm} &= R^{-3/2} R^{\Sigma}_{nn'm} \int \chi^{\mu^+}_{\kappa} \left(\hat{\vec{r}}\right) Y_{JM} \left(\hat{\vec{r}}\right) \chi^{\mu'}_{\kappa'} \left(\hat{\vec{r}}\right) d\Omega; \ \Sigma = \mathcal{S}, \mathcal{L}, \mathcal{E} \\ Q^{\mathcal{M}}_{nn'm} &= R^{-3/2} R^{\mathcal{M}}_{nn'm} \int \chi^{\mu^+}_{\kappa} \left(\hat{\vec{r}}\right) Y_{JM} \left(\hat{\vec{r}}\right) \chi^{\mu'}_{-\kappa'} \left(\hat{\vec{r}}\right) d\Omega, \end{aligned} \tag{A.31}$$

where Y_{JM} are the spherical functions.

The radial matrix elements turn out to be of the form

$$R^{\mathcal{S}}_{nn'm} = -\mathcal{N}^{\mathcal{S}}_m \int_0^R j_J \left(\Omega^{\mathcal{S}}_m r\right) S_{nn'} \left(r\right) r^2 dr \tag{A.32}$$

$$\begin{aligned} R^{\mathcal{L}}_{nn'm} &= \frac{-\mathcal{N}^{\mathcal{L}}_m}{\Omega^{\mathcal{S}}_m} \int_0^R \{[\Omega^{\mathcal{S}}_m r j_{J+1}(\Omega^{\mathcal{S}}_m r) - J j_J(\Omega^{\mathcal{S}}_m r)] U_{nn'} \\ &\quad + \left(\kappa - \kappa'\right) j_J(\Omega^{\mathcal{S}}_m r) T_{nn'} \left(r\right)\} \end{aligned} \tag{A.33}$$

$$R^{\mathcal{M}}_{nn'm} = \frac{\kappa' + \kappa}{\left[J\left(J+1\right)\right]^{1/2}} \mathcal{N}^{\mathcal{M}}_m \int_0^R j_J \left(\Omega^{\mathcal{M}}_m r\right) T_{nn'} \left(r\right) r^2 dr \tag{A.34}$$

$$\begin{aligned} R^{\mathcal{E}}_{nn'm} &= \frac{\mathcal{N}^{\mathcal{E}}_m}{\left[J\left(J+1\right)\right]^{1/2} \Omega^{\mathcal{E}}_m} \int_0^R \{J\left(J+1\right) j_J(\Omega^{\mathcal{E}}_m r) U_{nn'} \left(r\right) \\ &\quad + \left(\kappa - \kappa'\right) [J j_J(\Omega^{\mathcal{E}}_m r) - \Omega^{\mathcal{E}}_m r j_{J-1}(\Omega^{\mathcal{E}}_m r)] T_{nn'} \left(r\right)\} dr, \end{aligned} \tag{A.35}$$

where the notation

$$\begin{aligned} S_{nn'} &= g_n g_{n'} + f_n f_{n'} \\ T_{nn'} &= g_n f_{n'} + f_n g_{n'} \\ U_{nn'} &= g_n f_{n'} - f_n g_{n'} \end{aligned} \tag{A.36}$$

was used for the radial functions of the quark. These radial integrals are combined with a factor which governs the parity selection rules, and they are used in further calculations as

$$S^{\Sigma}_{nn'm} = \frac{1 - \eta_\Sigma g^{\Sigma\Sigma} (-1)^{l+J+l'}}{2} R^{\Sigma}_{nn'm}, \tag{A.37}$$

where η_Σ is $+1$ for $\mathcal{L}, \mathcal{E}$ and -1 for $\mathcal{S}, \mathcal{M}$ gluon modes.

Appendix B

Coefficients of Fractional Parentage

The coefficients of fractional parentage appear when a multiquark state is constructed in two different bases [15], [16]. Usually one base is well defined from the mathematical point of view, (i.e. all the states are linearly independent) while the second is overcomplete (i.e. the "basis" vectors are not linearly independent). However, this second base is very useful because it is a physical base (e.g. meson-meson base), and from the physics point of view it is more convenient to study a process in this base. The transformation between these two bases it is realized with the help of the coefficients of fractional parentage.

The quarks, antiquarks and gluons are carrying the colour, spin flavour and orbital quantum numbers. Considering only equal-mass up and down quarks, flavour degenerates to isospin symmetry. By combining the quarks, antiquarks and gluons to obtain the exotic states, care should be taken so that the quantum numbers couple in a correct way. It is worthwhile to separate the overall wave function of the exotic state in a colour $SU(3)_C$, spin $SU(2)$ and isospin $SU(2)$ part. The exotic state should be colourless and the constituents should obey the correct statistics (Fermi-Dirac for fermions and Bose-Einstein for bosons).

In general, one would also have to include an orbital wave function. However, due to the fact that we consider in this study only the lowest-energy cavity modes, the particles are all in the same orbital state and the corresponding wave function is just the symmetric product of one-particle functions. In the following this factor will be omitted.

B.1 The Three-Quark System

B.1.1 SU(3) Colour

The notations introduced in chapter 3 for quarks, antiquarks, gluons, two quarks and two antiquarks are used here. To construct the wave function of three quarks, we add a new quark to the already known two-quark system. The three-antiquark system will be derived from the three-quark system through a C transformation. The possible colour representations of the three quarks are

$$\{3\} \otimes \{3\} \otimes \{3\} = \{1\} \oplus \{8\}_a \oplus \{8\}_s \oplus \{10\}, \tag{B.1}$$

where a and s denote the symmetry property of the colour wave function with respect to the first and second quark. In terms of $SU(3)_C$ tensors, the three quarks can be written as

$$[qqq] \sim [qq]_i c^i = \varepsilon_{ijk} c^i c^j c^k \tag{B.2}$$

$$\begin{aligned} [qqq]^i_j &\sim [qq]_j c^i - \frac{1}{3}\delta^i_j [qq]_k c^k \\ &= \varepsilon_{jkl} c^k c^l c^i - \frac{1}{3}\delta^i_j \varepsilon_{klm} c^k c^l c^m \end{aligned} \tag{B.3}$$

in analogy with the quark-antiquark system described in section 2.1. The first expression describes the colour singlet representation (no indices, antisymmetric in all the quarks) and the second describes the octet representation of $SU(3)_C$ that is antisymmetric (with respect to two quarks). The symmetric octet and the decuplet (a symmetric combination in all the quarks) can be written as

$$\begin{aligned} \{qqq\}^i_j &\sim \varepsilon_{jkl} \{qq\}^{ik} c^l \\ &= \varepsilon_{jkl} \left(c^i c^k + c^k c^i \right) c^l, \end{aligned} \tag{B.4}$$

and

$$\begin{aligned} \{qqq\}^{ijk} &\sim \{qq\}^{ij} c^k + \{qq\}^{ki} c^j + \{qq\}^{jk} c^i \\ &= (c^i c^j + c^j c^i) c^k + (c^k c^i + c^i c^k) c^j + (c^j c^k + c^k c^j) c^i, \end{aligned} \tag{B.5}$$

respectively. The norms can be calculated as

$$\langle [qqq], [qqq] \rangle = 2\delta_{ij}\delta^{ij} = 6$$

$$
\begin{aligned}
\langle [qqq]^i_j, [qqq]^{i'}_{j'} \rangle &= 2(\delta^{ii'}\delta_{jj'} - \frac{1}{3}\delta^i_j\delta^{i'}_{j'}) \\
\langle \{qqq\}^i_j, \{qqq\}^{i'}_{j'} \rangle &= 6(\delta^{ii'}\delta_{jj'} - \frac{1}{3}\delta^i_j\delta^{i'}_{j'}) \\
\langle \{qqq\}^{ijk}, \{qqq\}^{i'j'k'} \rangle &= 6(\delta^{ii'}\delta^{jj'}\delta^{kk'} + \delta^{ij'}\delta^{ji'}\delta^{kk'} + \delta^{ii'}\delta^{jk'}\delta^{kj'} + \delta^{ik'}\delta^{ji'}\delta^{kj'} \\
&\quad + \delta^{ij'}\delta^{jk'}\delta^{ki'} + \delta^{ik'}\delta^{jj'}\delta^{ki'}).
\end{aligned} \tag{B.6}
$$

Note that the scalar products among different representations vanish.

In order to keep the notation as simple as possible we use the symbolism

$$
\begin{aligned}
|1\rangle &\sim \frac{1}{\sqrt{6}}[qqq] \\
|8_a\rangle &\sim \frac{1}{\sqrt{2}}[qqq]^i_j \\
|8_s\rangle &\sim \frac{1}{\sqrt{6}}\{qqq\}^i_j \\
|10\rangle &\sim \frac{1}{\sqrt{6}}\{qqq\}^{ijk}.
\end{aligned} \tag{B.7}
$$

The reason for which the curly bracket was dropped from the notation (usually the colour representations are in a curly bracket) is to distinguish the exotic state $q^3\bar{q}^3$ from the q^2 and the q^3 systems.

We now determine how the colour wave functions behave under permutations of two quarks. Because the final wave function should obey the Pauli principle, it is useful to know how each component of the wave function (colour, spin and isospin) responds to a permutation.

Therefore, permuting the quarks 1 and 2, the colour wave functions are (anti-) symmetric by construction

$$
\begin{aligned}
P_{12}|1\rangle &= -|1\rangle \\
P_{12}|8_a\rangle &= -|8_a\rangle \\
P_{12}|8_s\rangle &= +|8_s\rangle \\
P_{12}|10\rangle &= +|10\rangle .
\end{aligned} \tag{B.8}
$$

We need to know another permutation, in order to be able to calculate all the perturbations. For example, by knowing the P_{23} permutation, the P_{13} can be calculated as

$$
P_{13} = P_{12}P_{23}P_{12}. \tag{B.9}
$$

By transposing the particles 2 and 3 in the eqs. B.2-B.5 and calculating the scalar product with the original functions, we obtain for the P_{23} permutation

$$\begin{aligned} P_{23}\,|1\rangle &= -\,|1\rangle \\ P_{23}\,|8_a\rangle &= \frac{1}{2}\,|8_a\rangle + \frac{\sqrt{3}}{2}\,|8_s\rangle \\ P_{23}\,|8_s\rangle &= \frac{\sqrt{3}}{2}\,|8_a\rangle - \frac{1}{2}\,|8_s\rangle \\ P_{23}\,|10\rangle &= +\,|10\rangle\,. \end{aligned} \tag{B.10}$$

B.1.2 SU(2) Spin and Isospin

For the spin and isospin wave functions, we follow the same procedure used to construct the colour wave function. Only the spin is considered here, as the formalism for isospin is identical.

As in the colour case, the spin 1/2 of a quark is added to the q^2 system. The group $SU(2)$ is well known and it does not require a detailed tensorial treatment to get the wave functions [12]. The vectors describing the q^3 system are

$$|0;1/2\rangle\,,\,|1;1/2\rangle\,,\text{and}\,|1;3/2\rangle\,, \tag{B.11}$$

where the first number represents the spin of two quarks and the second number is the total spin. The total spin of the three quarks system can be either $\frac{1}{2}$ or $\frac{3}{2}$. Again the permutation operators are required to check the Pauli principle. The effect of P_{12} is easily obtained as the two quarks can couple to a 0 antisymmetric total spin or to a 1 symmetric total spin

$$\begin{aligned} P_{12}\,|0;1/2\rangle &= -\,|0;1/2\rangle \\ P_{12}\,|1;1/2\rangle &= +\,|1;1/2\rangle \\ P_{12}\,|1;1/2\rangle &= +\,|1;1/2\rangle\,. \end{aligned} \tag{B.12}$$

For the calculation of P_{23} a base where the spins 2 and 3 couple directly is necessary. With the help of the 6-j symbols, we can write

$$|(j_1j_2)j_{12},j_3;jm\rangle = \sum_{j_{23}} \sqrt{\hat{j}_{12}\hat{j}_{23}}(-1)^{j_1+j_2+j_3+j} \left\{ \begin{array}{ccc} j_1 & j_2 & j_{12} \\ j_3 & j & j_{23} \end{array} \right\} |j_1,(j_2j_3)j_{23};jm\rangle\,. \tag{B.13}$$

Acting with the operator P_{23} on the elements (B.13) and taking their scalar product with the original elements (B.11) we arrive at

$$\begin{aligned} P_{23}\,|0;1/2\rangle &= \frac{1}{2}\,|0;1/2\rangle + \frac{\sqrt{3}}{2}\,|1;1/2\rangle \\ P_{23}\,|1;1/2\rangle &= \frac{\sqrt{3}}{2}\,|0;1/2\rangle - \frac{1}{2}\,|1;1/2\rangle \\ P_{23}\,|1;1/2\rangle &= +\,|1;1/2\rangle\,. \end{aligned} \tag{B.14}$$

B.1.3 The Antisymmetric Wave Function

The colour wave function of the three-quark system is known, as well as the spin and isospin wave functions. We also know, how the transposition operators act on these wave functions, so the final wave function can be assembled and its antisymmetry checked. In principle, all the possible combinations among the colour (eq. (B.7)), spin (eq. (B.11)) and isospin (eq. (B.11)) wave functions will be taken into account. Then, we require the wave function to be antisymmetric under the transposition of any two particles. This is equivalent to demanding that $P_{12} = -1$ and $P_{23} = -1$ since $P_{13} = P_{12}P_{23}P_{12} = -1$.

To illustrate the method, we calculate the nucleon-like state. This means that we are looking for a wave function with the quantum numbers $N = \{1\}$, $J = 1/2$ and $I = 1/2$. The wave functions which can contribute to the antisymmetric wave function are

$$\begin{array}{ll} |1\rangle\,|0;1/2\rangle\,|0;1/2\rangle & |1\rangle\,|0;1/2\rangle\,|1;1/2\rangle \\ |1\rangle\,|1;1/2\rangle\,|1;1/2\rangle & |1\rangle\,|1;1/2\rangle\,|0;1/2\rangle\,, \end{array} \tag{B.15}$$

where the first vector represents the colour, the second spin and the last isospin.

We see that the wave functions in the second row are symmetric under P_{12}. Therefore these functions do not contribute to the final wave function. The functions of the first column probably mix up to form the antisymmetric wave function. Considering a linear combination of them, the action of P_{23} on it is required to be

$$P_{23}[a\,|1\rangle\,|0;1/2\rangle\,|0;1/2\rangle + b\,|1\rangle\,|1;1/2\rangle\,|1;1/2\rangle] = -1, \tag{B.16}$$

where a and b are coefficients of the linear combination which need to be determined and the products of kets refer to colour, spin and isospin in this order. Substituting

the expressions (B.10) and (B.14) for the action of P_{23} on colour, spin and isospin, we obtain

$$\begin{aligned} & P_{23}[a\,|1\rangle\,|0;1/2\rangle\,|0;1/2\rangle + b\,|1\rangle\,|1;1/2\rangle\,|1;1/2\rangle] \\ = & -\frac{a+3b}{4}\,|1\rangle\,|0;1/2\rangle\,|0;1/2\rangle - \frac{3a+b}{4}\,|1\rangle\,|1;1/2\rangle\,|1;1/2\rangle \\ & -\frac{\sqrt{3}}{4}(a-b)\,|1\rangle\,|0;1/2\rangle\,|0;1/2\rangle - \frac{\sqrt{3}}{4}(a-b)\,|1\rangle\,|1;1/2\rangle\,|1;1/2\rangle\,. \end{aligned} \quad \text{(B.17)}$$

Equations (B.16) and (B.17) are satisfied for $a = b$. Demanding that the wave function is normalized, we arrive at the antisymmetric wave function

$$|\{1\},1/2,1/2\rangle = \frac{1}{\sqrt{2}}\,|1\rangle\,|0;1/2\rangle\,|0;1/2\rangle + \frac{1}{\sqrt{2}}\,|1\rangle\,|1;1/2\rangle\,|1;1/2\rangle\,. \quad \text{(B.18)}$$

In a similar way all the other combinations which obey the Pauli principle can be found. They are listed in the table below

q^2	$N^1_{\frac{1}{2}}$	$\Delta^1_{\frac{3}{2}}$	$N^8_{\frac{1}{2}}$	$\Delta^8_{\frac{1}{2}}$	$N^8_{\frac{3}{2}}$	$N^{10}_{\frac{1}{2}}$
$\|\{\bar{3}\},0,0\rangle$	$\frac{1}{\sqrt{2}}$	0	$\frac{1}{2}$	0	0	0
$\|\{\bar{3}\},1,1\rangle$	$\frac{1}{\sqrt{2}}$	1	$-\frac{1}{2}$	$\frac{1}{\sqrt{2}}$	$\frac{1}{\sqrt{2}}$	0
$\|\{6\},0,1\rangle$	0	0	$-\frac{1}{2}$	$-\frac{1}{\sqrt{2}}$	0	$\frac{1}{\sqrt{2}}$
$\|\{6\},1,0\rangle$	0	0	$-\frac{1}{2}$	0	$-\frac{1}{\sqrt{2}}$	$-\frac{1}{\sqrt{2}}$

, (B.19)

where in the first column, the two-quark content is indicated, in the first line the three-quark states are listed, N or Δ denote the total isospin (N stands for $I = 1/2$ and Δ stands for $I = 3/2$), the upper index indicates the colour representation and the lower index stands for the spin. The other positions in the table indicate the coefficients of the linear combination and together with the two-quark column can be used to reconstruct the full wave function for any three-quark system.

Of course not all the states listed above can be identified with physical baryons, due to their colour ($\{8\}$ or $\{10\}$) but the reason why all these states were calculated is that for $q^3\bar{q}^3$ system all of them are playing an important role.

B.2 The Three-Quark Three-Antiquark System

For the $q^3\bar{q}^3$ system, the colour wave functions are presented in section 3.1.4. In this section, we discuss the spin wave functions for the two bases $(q^3)(\bar{q}^3)$ and $(q^2\bar{q}^2)(q\bar{q})$.

The isospin wave functions are identical to those for spin.

The state vector $|(j_{q^2}), j_{q^3}, (j_{\bar{q}^2}), j_{\bar{q}^3}; J\rangle$ describes a state in which the spin of two quarks is coupled with the third quark, the total spin of two antiquarks is coupled with a third antiquark, and finally, the spins of three quarks and three antiquarks are coupled to the total spin J. For the second base, the notation $|(j_{q^2}), (j_{\bar{q}^2}), j_{q^2\bar{q}^2}, j_{q\bar{q}}; J\rangle$ is used, where two quarks are coupled to two antiquarks and then they are coupled to a pair of quark-antiquark. To establish the transformation matrix from one base to the other, the four spin are recoupled as

$$|(j_{q^2}), j_{q^3}, (j_{\bar{q}^2}), j_{\bar{q}^3}; J\rangle = \sum_{j_{q^2\bar{q}^2}, j_{q\bar{q}}} \hat{j}_{q^3} \hat{j}_{\bar{q}^3} \hat{j}_{q^2\bar{q}^2} \hat{j}_{q\bar{q}} \begin{Bmatrix} j_{q^2} & j_q & j_{q^3} \\ j_{\bar{q}^2} & j_{\bar{q}} & j_{\bar{q}^3} \\ j_{q^2\bar{q}^2} & j_{q\bar{q}} & J \end{Bmatrix} \times |(j_{q^2}), (j_{\bar{q}^2}), j_{q^2\bar{q}^2}, j_{q\bar{q}}; J\rangle . \tag{B.20}$$

One thus obtains the following states

$$|(j_{q^2}), j_{q^3}, (j_{\bar{q}^2}), j_{\bar{q}^3}; J\rangle \begin{cases} \left|(0), \frac{1}{2}, (0), \frac{1}{2}; 0\right\rangle & \left|(1), \frac{1}{2}, (1), \frac{1}{2}; 1\right\rangle \\ \left|(1), \frac{1}{2}, (0), \frac{1}{2}; 0\right\rangle & \left|(1), \frac{3}{2}, (1), \frac{1}{2}; 1\right\rangle \\ \left|(1), \frac{1}{2}, (1), \frac{1}{2}; 0\right\rangle & \left|(1), \frac{1}{2}, (1), \frac{3}{2}; 1\right\rangle \\ \left|(1), \frac{3}{2}, (1), \frac{3}{2}; 0\right\rangle & \left|(1), \frac{3}{2}, (1), \frac{3}{2}; 1\right\rangle \\ \left|(0), \frac{1}{2}, (1), \frac{1}{2}; 0\right\rangle & \left|(1), \frac{3}{2}, (0), \frac{1}{2}; 2\right\rangle \\ \left|(0), \frac{1}{2}, (0), \frac{1}{2}; 1\right\rangle & \left|(1), \frac{3}{2}, (1), \frac{1}{2}; 2\right\rangle \\ \left|(0), \frac{1}{2}, (1), \frac{1}{2}; 1\right\rangle & \left|(1), \frac{1}{2}, (1), \frac{3}{2}; 2\right\rangle \\ \left|(0), \frac{1}{2}, (1), \frac{3}{2}; 1\right\rangle & \left|(1), \frac{3}{2}, (1), \frac{3}{2}; 2\right\rangle \\ \left|(1), \frac{1}{2}, (0), \frac{1}{2}; 1\right\rangle & \left|(0), \frac{1}{2}, (1), \frac{3}{2}; 2\right\rangle \\ \left|(1), \frac{3}{2}, (0), \frac{1}{2}; 1\right\rangle & \left|(1), \frac{3}{2}, (1), \frac{3}{2}; 3\right\rangle \end{cases} \tag{B.21}$$

for the $(q^3)(\bar{q}^3)$ base and

$$|(j_{q^2}),(j_{\bar{q}^2}),j_{q^2\bar{q}^2},j_{q\bar{q}};J\rangle \begin{cases} |(0),(0),0,0;0\rangle & |(1),(0),1,1;1\rangle \\ |(1),(1),0,0;0\rangle & |(1),(1),1,1;1\rangle \\ |(0),(1),1,1;0\rangle & |(1),(1),0,1;1\rangle \\ |(1),(1),0,0;0\rangle & |(1),(1),2,1;1\rangle \\ |(1),(0),1,1;0\rangle & |(1),(1),2,0;2\rangle \\ |(1),(0),1,0;1\rangle & |(0),(1),1,1;2\rangle \\ |(0),(1),1,0;1\rangle & |(1),(0),1,1;2\rangle \\ |(1),(1),1,0;1\rangle & |(1),(1),1,1;2\rangle \\ |(0),(0),0,1;1\rangle & |(1),(1),2,1;2\rangle \\ |(0),(1),1,1;1\rangle & |(1),(1),2,1;3\rangle \end{cases} \tag{B.22}$$

for the $(q^2\bar{q}^2)(q\bar{q})$ base. The transformation matrices between the two bases are given by

$$\begin{pmatrix} +1 & 0 & 0 & 0 & 0 \\ 0 & 0 & 0 & +1 & 0 \\ 0 & \frac{1}{\sqrt{3}} & 0 & 0 & \frac{\sqrt{6}}{3} \\ 0 & \frac{\sqrt{6}}{3} & 0 & 0 & -\frac{1}{\sqrt{3}} \\ 0 & 0 & -1 & 0 & 0 \end{pmatrix} \tag{B.23}$$

for $J=0$,

$$\begin{pmatrix} 0 & 0 & 0 & +1 & 0 & 0 & 0 & 0 & 0 \\ 0 & \frac{\sqrt{3}}{3} & 0 & 0 & \frac{\sqrt{6}}{3} & 0 & 0 & 0 & 0 \\ 0 & \frac{\sqrt{6}}{3} & 0 & 0 & -\frac{\sqrt{3}}{3} & 0 & 0 & 0 & 0 \\ -\frac{\sqrt{3}}{3} & 0 & 0 & 0 & 0 & \frac{\sqrt{6}}{3} & 0 & 0 & 0 \\ \frac{\sqrt{6}}{3} & 0 & 0 & 0 & 0 & \frac{\sqrt{3}}{3} & 0 & 0 & 0 \\ 0 & 0 & \frac{\sqrt{2}}{3} & 0 & 0 & 0 & 0 & -\frac{1}{3\sqrt{3}} & \frac{2\sqrt{15}}{9} \\ 0 & 0 & \frac{1}{3} & 0 & 0 & 0 & \frac{\sqrt{2}}{2} & -\frac{2\sqrt{6}}{9} & -\frac{\sqrt{30}}{18} \\ 0 & 0 & -\frac{1}{3} & 0 & 0 & 0 & \frac{\sqrt{2}}{2} & \frac{2\sqrt{6}}{9} & \frac{\sqrt{30}}{18} \\ 0 & 0 & \frac{\sqrt{5}}{3} & 0 & 0 & 0 & 0 & \frac{\sqrt{30}}{9} & \frac{\sqrt{6}}{9} \end{pmatrix} \tag{B.24}$$

for $J = 1$ and

$$\begin{pmatrix} 0 & 0 & +1 & 0 & 0 \\ \frac{1}{\sqrt{3}} & 0 & 0 & -\frac{\sqrt{6}}{6} & \frac{\sqrt{2}}{2} \\ -\frac{1}{\sqrt{3}} & 0 & 0 & \frac{1}{\sqrt{6}} & \frac{\sqrt{2}}{2} \\ \frac{\sqrt{3}}{3} & 0 & 0 & \frac{\sqrt{6}}{3} & 0 \\ 0 & +1 & 0 & 0 & 0 \end{pmatrix} \tag{B.25}$$

for $J = 2$. For $J = 3$ there is only one element in each base and the transformation "matrix" is $+1$.

Appendix C

Examples

In this appendix, two examples are presented for calculating the coefficients of fractional parentage. The first example is chosen to be very simple, in order to get used to the notations.

The $q^3\bar{q}^3$ state described by $C = \{1\}$, $J = 3$ and $I = 0$ is illustrative for our purpose. This state can be obtained either from the $\Delta^1_{3/2}\bar{\Delta}^1_{3/2}$ combination or from $N^8_{3/2}\bar{N}^8_{3/2}$, where the notation has been introduced and explained in chapter 3. Any other combinations of three-quark or three-antiquark states that are allowed by the Pauli principle cannot be coupled to $C = \{1\}$, $J = 3$ and $I = 0$. We now concentrate on the $\Delta^1_{3/2}\bar{\Delta}^1_{3/2}$ combination. This state vector can be written as a product of the colour, spin and isospin parts of the wave function, i.e.

$$\begin{aligned} \Delta^1_{3/2}\bar{\Delta}^1_{3/2} &= |\{1\},3/2,3/2;\{1\},3/2,3/2\rangle \\ &= |\{1\},\{1\};\{1\}\rangle^C \, |3/2,3/2;3\rangle^J \, |3/2,3/2;0\rangle^I . \end{aligned} \tag{C.1}$$

The colour, spin and isospin parts of the total wave function refer to the partitions $|q^3,\bar{q}^3;q^3\bar{q}^3\rangle$. In (C.1) we have made use of table B.19 to express the three-quark system as a product of $|q^2\rangle\,|q\rangle$. Using the colour matrix (3.19) transformations introduced in chapter three and the spin and isospin matrix transformations defined in the previous appendix B.23 we arrive at

$$\begin{aligned} |\{1\},\{1\};\{1\}\rangle^C \, |3/2,3/2;3\rangle^J \, |3/2,3/2;0\rangle^I = \left[\frac{1}{3}\,|\{1\},\{1\};\{1\}\rangle + \frac{2\sqrt{2}}{3}\,|\{8\},\{8\};\{1\}\rangle\right]^C \\ \times\, |2,1;3\rangle^J \left[\frac{\sqrt{6}}{3}\,|0,0;0\rangle - \frac{\sqrt{3}}{3}\,|0,0;0\rangle\right]^I , \end{aligned} \tag{C.2}$$

where the coupling of the quarks is now $q^2\bar{q}^2 - q\bar{q} - q^3\bar{q}^3$. After rearranging the terms, the final result is

$$\begin{aligned}\Delta^1_{3/2}\bar{\Delta}^1_{3/2} &= \frac{\sqrt{6}}{9}\,|\{1\},2,0\rangle\,|\{1\},1,0\rangle - \frac{\sqrt{3}}{9}\,|\{1\},2,1\rangle\,|\{1\},1,1\rangle \\ &\quad + \frac{2\sqrt{12}}{9}\,|\{8\},2,0\rangle\,|\{8\},1,0\rangle - \frac{2\sqrt{2}}{3}\,|\{8\},2,1\rangle\,|\{8\},1,1\rangle\,,\end{aligned} \tag{C.3}$$

where the quark order is $q^2\bar{q}^2(C,J,I) - q\bar{q}(C,J,I)$.

For a more complex transformation from $(q^3)(\bar{q}^3)$ states to $(q^2\bar{q}^2)\,(q\bar{q})$ states, we analyze the $C = \{1\}$, $J = 0$ and $I = 0$ state. A colour singlet with zero spin and isospin can be written as $N^1_{1/2}\bar{N}^1_{1/2}$, $N^8_{1/2}\bar{N}^8_{1/2}$, $N^8_{3/2}\bar{N}^8_{3/2}$, $N^{10}_{1/2}\bar{N}^{10}_{1/2}$, $\Delta^1_{3/2}\bar{\Delta}^1_{3/2}$, or $\Delta^8_{1/2}\bar{\Delta}^8_{1/2}$. We calculate in detail only the term $N^8_{3/2}\bar{N}^8_{3/2}$. As before, we separate the colour, spin and isospin

$$\begin{aligned}N^8_{3/2}\bar{N}^8_{3/2} &= |\{8\},3/2,1/2;\{8\},3/2,1/2\rangle \\ &= |\{8\},\{8\};\{1\}\rangle^C\,|3/2,3/2,0\rangle^J\,|1/2,1/2;0\rangle^I\,,\end{aligned} \tag{C.4}$$

where the order is as in the previous example. Next, we use the table B.19 to write the three-quark (three-antiquark) system as a product of $(q^2)(q)$ and $(\bar{q}^2)(\bar{q})$,

$$\begin{aligned}N^8_{3/2}\bar{N}^8_{3/2} &= \left[\frac{\sqrt{2}}{2}\,|\{\bar{3}\};\{8\}\rangle^C\,|1;3/2\rangle^J\,|1;1/2\rangle^I - \frac{\sqrt{2}}{2}\,|\{6\};\{8\}\rangle^C\,|1;3/2\rangle^J\,|0;1/2\rangle^I\right] \\ &\quad \times\left[\frac{\sqrt{2}}{2}\,|\{3\};\{8\}\rangle^C\,|1;3/2\rangle^J\,|1;1/2\rangle^I - \frac{\sqrt{2}}{2}\,|\{\bar{6}\};\{8\}\rangle^C\,|1;3/2\rangle^J\,|0;1/2\rangle^I\right],\end{aligned}$$

where the first quantum number inside the ket stands for the q^2 ($\bar{q}^2$), while the second denotes q^3 ($\bar{q}^3$) wave functions. By working out the products, we get

$$\begin{aligned}N^8_{3/2}\bar{N}^8_{3/2} &= \frac{1}{2}\,|\{\bar{3}\}\{8\},\{3\}\{8\};\{1\}\rangle^C\,|(1)3/2,(1)3/2;0\rangle^J\,|(1)1/2,(1)1/2;0\rangle^I \\ &\quad -\frac{1}{2}\,|\{\bar{3}\}\{8\},\{\bar{6}\}\{8\};\{1\}\rangle^C\,|(1)3/2,(1)3/2;0\rangle^J\,|(1)1/2,(0)1/2;0\rangle^I \\ &\quad -\frac{1}{2}\,|\{6\}\{8\},\{3\}\{8\};\{1\}\rangle^C\,|(1)3/2,(1)3/2;0\rangle^J\,|(0)1/2,(1)1/2;0\rangle^I \\ &\quad +\frac{1}{2}\,|\{6\}\{8\},\{\bar{6}\}\{8\};\{1\}\rangle^C\,|(1)3/2,(1)3/2;0\rangle^J\,|(0)1/2,(0)1/2;0\rangle^I\,.\end{aligned}$$

The notation used here is $|q^2,q^3,\bar{q}^2,\bar{q}^3;q^3\bar{q}^3\rangle$. Using the transformation matrices for colour (3.19), spin and isospin (B.23), to express the $(q^2)(q)(\bar{q}^2)(\bar{q})$ vector in terms of

$(q^2\bar{q}^2)(q\bar{q})$ vectors, yields

$$
\begin{aligned}
N^8_{3/2}\bar{N}^8_{3/2} \;=\; & \frac{1}{2}\left[\frac{2\sqrt{2}}{2}\,|\{1\},\{1\};\{1\}\rangle - \frac{1}{3}\,|\{8\},\{8\};\{1\}\rangle\right]^C \\
& \times\left[\frac{\sqrt{6}}{3}\,|0,0;0\rangle - \frac{\sqrt{3}}{3}\,|1,1;0\rangle\right]^J \left[\frac{\sqrt{3}}{3}\,|0,0;0\rangle + \frac{\sqrt{6}}{3}\,|1,1;0\rangle\right]^I \\
& -\frac{1}{2}\,|\{8\},\{8\};\{1\}\rangle^C \left[\frac{\sqrt{6}}{3}\,|0,0;0\rangle - \frac{\sqrt{3}}{3}\,|1,1;0\rangle\right]^J (-1)\,|1,1;0\rangle^I \\
& -\frac{1}{2}(-1)\,|\{8\},\{8\};\{1\}\rangle^C \left[\frac{\sqrt{6}}{3}\,|0,0;0\rangle - \frac{\sqrt{3}}{3}\,|1,1;0\rangle\right]^J (-1)\,|1,1;0\rangle^I \\
& +\frac{1}{2}\left[-\frac{\sqrt{5}}{3}\,|\{8\},\{8\};\{1\}\rangle + \frac{2}{3}\,|\{1\},\{1\};\{1\}\rangle\right]^C \\
& \times\left[\frac{\sqrt{6}}{3}\,|0,0;0\rangle - \frac{\sqrt{3}}{3}\,|1,1;0\rangle\right]^J |0,0;0\rangle^I\,, \qquad \text{(C.5)}
\end{aligned}
$$

where the notation is $|(q^2\bar{q}^2),(q\bar{q});q^3\bar{q}^3\rangle$. After all the products are calculated, the final state has 16 terms.

All the other elements of the $(q^3)(\bar{q}^3)$ base follow the same pattern as the two example presented here with the difference that the number of $(q^2\bar{q}^2)(q\bar{q})$ terms is becoming large (up to 96 terms).

Appendix D

Units and Conventions

The flat Minkowski space is used with the metric

$$g^{\mu\nu} = g_{\mu\nu} = \mathrm{diag}(1,-1,-1,-1), \qquad g^{\mu}_{\nu} = \delta^{\mu}_{\nu}. \tag{D.1}$$

The Greek indices (μ, ν, ...) can take the values $0, 1, 2$ and 3, Latin indices ($k, l, ...$) the values $1, 2$ and 3 when they refer to space-time. The Dirac matrices that satisfy the Clifford algebra

$$\{\gamma^{\mu}, \gamma^{\nu}\} = 2g^{\mu\nu}, \tag{D.2}$$

may be represented as

$$\gamma^0 = \begin{pmatrix} I & 0 \\ 0 & -I \end{pmatrix}, \qquad \gamma^k = \begin{pmatrix} 0 & \sigma^k \\ -\sigma^k & 0 \end{pmatrix}, \tag{D.3}$$

where the σ^k are the 2×2 Pauli matrices

$$\sigma^1 = \begin{pmatrix} 0 & 1 \\ 1 & 0 \end{pmatrix}, \qquad \sigma^2 = \begin{pmatrix} 0 & -i \\ i & 0 \end{pmatrix}, \qquad \sigma^3 = \begin{pmatrix} 1 & 0 \\ 0 & -1 \end{pmatrix}. \tag{D.4}$$

The usual 3j-, 6j- and 9j-symbols, vector spherical harmonics and spherical spinors as defined by Edmonds [12] are used.

Throughout this thesis, natural units with $\hbar = c = 1$ have been used. These factors may be restored in the final results of the calculation using simple dimensional analysis. Some useful numerical values are

$$\begin{aligned} \hbar c &= 197.327053 \text{ MeV fm} \\ 1 \text{ GeV} &= 5.06768963\ \hbar c \text{ fm}^{-1} \end{aligned} \tag{D.5}$$

The cavity radius has been set to 1 fm and is the natural unit of length in the cavity. To convert the mass and energy into dimensional units,

$$m_f = \frac{\zeta_f \hbar}{Rc} \tag{D.6}$$

and

$$\varepsilon = \frac{\omega R}{\hbar c} = \frac{\omega}{0.197327} \text{ GeV} \tag{D.7}$$

have been used.

Bibliography

[1] H.Fritzsch, M. Gell-Mann and H. Leutwyler, Phys. Lett. **B47** (1973) 365.

[2] H. D. Politzer, Phys. Rev. Lett. **30** (1973) 1346.

[3] D. J. Gross and F. Wilczek, Phys. Rev. Lett.**30** (1973) 1323;
Phys. Rev. **D8** (1973) 3635;
Phys. Rev. **D9** (1974) 980.

[4] N. Cason (E852 Collab.), Proc. of CIPANP97 (Big Sky, 1997);
D.P. Weygand and A.I. Ostrovidov (E852 Collab.), Proc. of HADRON '97 (BNL, 1997).

[5] Yu.P. Gouz *et al.* (VES Collab.), Proc. of the 26^{th} ICHEP (Dallas, 1992), ed. J.R. Sanford, p. 572.

[6] A. Chodos, R.C. Jaffe, K. Johnson, C.B. Thorn, V.F. Weisskopf, Phys. Rev. **D9** (1974) 3471;
A. Chodos, R.L. Jaffe, K. Johnson, C.B. Thorn, Phys. Rev. **D10** (1974) 2599;
A. Chodos, C.B. Thorn, V.F. Weisskopf, Phys. Rev. **D12** (1975) 2733.

[7] R. F. Buser, R. D. Viollier and P.Zimak, International Journal of Theoretical Physics **27** (1988) 925.

[8] A. J. Stoddart, R. D. Viollier, Phys. Lett. **236B** (1990) 387.

[9] G. U. Schreiber and R. D. Viollier, Phys. Lett. **B279** (1992) 131;
G. U. Schreiber and R. D. Viollier, Ann. Phys. **215** (1992) 277.

[10] A. J. Stoddart, R. D. Viollier, Nucl. Phys. **A532** (1991) 657;
A. J. Stoddart, R. D. Viollier, Nucl. Phys. **A541** (1992) 413.

[11] P.R. Page,R.J. Lindebaum and R.D. Viollier, Nucl. Phys. **A506** (1993) 1003.

[12] A. R. Edmonds, *Angular Momentum in Quantum Mechanics*, Princeton University Press, 1957, p. 31.

[13] L. H. Ryder, *Elementary Particles and Symmetries*, Gordon and Breach Science Publishers, 1984, p. 39.

[14] B. P. Roe, *Particle Physics at the New Millenium*, Springer-Verlag, 1996, p. 57.

[15] P. Zimak, Das $q^2\overline{q}^2$ System im Rahmen des M.I.T. Bagmodells, Masters Thesis, University of Basel (1983), unpublished.

[16] P. Zimak and R. D. Viollier, Prog. Part. Nucl. Phys. **27** (1991) 273.

[17] L. D. Fadeev and V. N. Popov, Phys. Lett. **B25** (1967) 29.

[18] C. Becchi, A. Rouet and R. Stora, Phys. Lett. **52B** (1974) 344.

[19] C. Becchi, A. Rouet and R. Stora, Ann. Phys. (N.Y.) **98** (1976) 287.

[20] F. E. Close, *An Introduction to Quarks and Partons*, Academic Press (1979), p.17.

[21] P. Zimak, *Exotic Hadrons*, Ph.D. Thesis, University of Cape Town (1988).

[22] M. Gell-Mann and F. Low, Phys. Rev. **84** (1951) 350.

[23] A. L. Fetter and J. D. Walecka, *Quantum Theory of Many Particle Systems*, McGraw-Hill, NewYork, 1971, p. 45.

[24] J. Sucher, Phys. Rev. **107** (1949) 1448.

[25] A. J. Stoddart, R. D. Viollier, Phys. Lett. **208B** (1988) 65.

[26] S. N. Goldhaber, T. H. Hansson, R. L. Jaffe, Phys. Lett. **131B** (1983) 445.

[27] S. N. Goldhaber, T. H. Hansson, R. L. Jaffe, Nucl. Phys. **B277** (1986) 674.

[28] R. J. Lindebaum, *The Quark boundary Condition and the Electroweak Properties of the Nucleon in Cavity QCD*, Ph.D. Thesis, University of Cape Town (1997).

[29] G. Plunien, B. Müller, and W. Greiner, Phys. Rep. **134** (1986) 87.

[30] M. E. Rose, *Relativistic Electron Theory*, John Wiley & Sons, 1961, p. 157.

[31] Particle Data Group, Phys. Rev. **D54** (1996) 1.

[32] R. Bhaduri, *Models of the Nucleon*, Addison-Wesley Publishing Company, 1989, p. 95.

[33] W. Greiner, B. Müller, *Gauge Theory of Weak Interactions*, Springer, 1996, p. 154.

[34] T. DeGrand, R. L. Jaffe, K. Johnson, J. Kiskis, Phys. Rev. **D12** (1975) 2060.

[35] M. Abramowitz and I.A. Stegun, *Handbook of Mathematical Functions*, Dover, New York, 1965.

[36] U. Gastaldi, R. Klapisch and F. Close, *Spectroscopy of Light and Heavy Quarks*, Physical Sciences, 1989, p. 1.

[37] W. A. Bardeen, M.S. Chanowitz, S.D. Drell, M. Weinstein and T.M. Yan, Phys. Rev. **D11** (1974) 1094.

[38] W.H. Press, B. Flannery, S.A. Teukolsky and W. T. Vetterling, Numerical Recipes, *The Art of Scientific Computing*, Cambridge University Press, 1989, p. 23.

[39] S. U. Chung, Nucl. Phys. B (Proc. Suppl.) **56** (1997) 234.

[40] H. Forkel, *et al.*, hep-ph/9809407, Preprint 1998.

[41] L.A.Zadeh, Information and Control **8** (1965) 338.

[42] D. Dubois and H. Prade, *Fuzzy Sets, Theory and Applications*, Academic Press, Orlando, 1980, p. 23.

[43] P. Lacock *et al.*, Phys. Rev. **D54** (1996) 6997.

[44] C. Berbard *et al.*, Nucl. Phys. (Proc. Suppl.) **B53** (1997) 228.

[45] D. Alde *et al.*, Phys. Lett. **B205** (1988) 397.

[46] H. Aoyagi *et al.*, Phys. Lett. **B314** (1993) 246.

[47] T. Huang *et al.*, hep-ph/9809331, Preprint 1998.

[48] F. Close and C. Amsler, Phys. Rev. **D53** (1996) 295.

[49] D. V. Amelin (VES Collab.) Proc. of HADRON'97 (Brookhaven, Aug 1997)

[50] P.R. Page, hep-ph/9806233, Preprint 1998.

[51] A. Abele *et al.*, (Crystal Barrel Collab.), Phys.Lett. **B** (1998), accepted for publication.

[52] B. May *et al.*, Z. Phys. **C46** (1990) 191.

[53] E. Aker *et al.*, Phys. Lett. **B 260** (1991) 249.

[54] V.V. Anisovich *et al.*, Phys. Lett. **B323** (1994) 233.

[55] V.V. Anisovich *et al.*, Phys, Rev. **D50** (1994) 1972.

[56] S. Ishida *et al.*, Prog. Theor. Phys. **95** (1996) 745;
Prog. Theor. Phys. **98** (1997) 1005.

[57] M. R. Pennington, hep-ph/9905241, Preprint 1999.

[58] N. A. Törnqvist, hep-ph/9904346, Preprint 1999.

[59] D. Bisello *et al.*, Phys. Lett. **B220** (1989) 321.

[60] D. Aston *et al.*, SLAC-PUB-5657 (1990).

[61] T.J. Killian, Phys. Rev. **D21** (1980) 3005.

[62] D. Aston *et al.*, Nucl. Phys. **B189** (1981) 205.

[63] J. P. Stroot, Nucl. Phys. (Proc. Suppl.) **39B** (1995) 284.

[64] J. Westein *et al.*, Phys. Rev. **D41** (1990) 2236.

[65] M. Chanowitz and S. Sharpe, Nucl. Phys. **B222** (1983) 211.

[66] T. Barnes *et al.*, Nucl. Phys. **B224** (1983) 241.

[67] N. Isgur and J. Paton, Phys. Lett. **B124** (1983) 247.

[68] N. Isgur and J. Paton, Phys. Rev. **D31** (1985) 2910.

[69] R. Kokashi and N. Isgur, Phys. Rev. **D35** (1987) 907.

[70] N. Isgur *et al.*, Phys. Rev. Lett. **54** (1985) 869.

[71] F. Close and P. Page, Nucl. Phys. **B443** (1995) 233.

[72] S. Peratonius and C. Michael, Nucl. Phys. **B347** (1990) 854.

[73] P. Lacock *et al.*, Phys. Rev. **D54** (1996) 6997.

[74] A. Furui *et al.*, hep-lat/9809079, Preprint 1998.

[75] J. Weinstein and N. Isgur, Phys. Rev. **D27** (1983) 588.

[76] A. Green *et al.*, Phys. Rev. **C57** (1998) 3384.

[77] Y. Uehara *et al.*, Nucl. Phys. **A606** (1996) 357.

[78] G. Gerasyuta and V. Kochkin, Z. Phys. **C74** (1997) 325.

[79] I. Balitsky *et al.*, Phys. Lett. **B112** (1982) 71.

[80] J.I. Latorre *et al.*, Phys. Lett. **B147** (1984) 169.

[81] J. Govaerts *et al.*, Phys. Lett. **B128** (1983) 262.

[82] M. Schumann, MSc. Thesis, University of Cape Town (1998), unpublished.